DOTTORATO DI RICERCA IN

INGEGNERIA DELL'INFORMAZIONE

XII CICLO

Sede amministrativa

Università degli Studi di MODENA e REGGIO EMILIA

TESI PER IL CONSEGUIMENTO DEL TITOLO DI
DOTTORE DI RICERCA

MODEL-BASED FAULT DIAGNOSIS IN DYNAMIC SYSTEMS USING IDENTIFICATION TECHNIQUES

CANDIDATO Silvio Simani

SUPERVISORE Prof. Sergio Beghelli

CORRELATORE Prof. Ron J. Patton

Abstract

The control devices which are nowadays exploited to improve the overall performance of industrial processes involve both sophisticated digital system design techniques and complex hardware (input-output sensors, actuators, components and processing units). In such a way, the probability of failure occurrence on such equipment may result significant and an automatic supervision control should be used to detect and isolate anomalous working conditions as early as possible.

Since the early 1970's, the problem of fault detection and isolation in dynamic processes has received great attention and a wide variety of model-based approaches has been proposed and developed.

Model-based techniques have been widely recognized as powerful approaches for fault diagnosis and require a realistic mathematical model of the monitored system. An effective model-based fault diagnosis system should manage noises and modeling uncertainties, always present in real situation.

On the other hand, for the diagnosis of faults, mathematical models of the process under investigation are required, either in state space or input-output

A state space description of the system provides general and mathematically rigorous tools for system modeling and residual generation, which may be used in fault diagnosis of industrial systems, for both the deterministic and the stochastic case.

Residuals should then be processed to detect an actual fault condition, rejecting any false alarms caused by noise, spurious signals and modeling uncertainties.

This thesis aims to define a comprehensive methodology for actuator, component and sensor fault detection and isolation by using an output estimation approach, in conjunction with residual processing schemes, which include a simple threshold detection, in deterministic case, as well as statistical analysis when data are affected by noise.

The final result consists in a fault detection and isolation strategy based on diagnostic methods to analytically generate redundant residuals. A number of strategies for the design of residual generators are then proposed.

The suggested methods do not require any physical knowledge of the processes under observation since the mathematical description of the monitored system is obtained by means of a system identification scheme based on equation error and errors–in–variables models. The latter identification approach gives a reliable model of the plant under investigation, as well as the variances of the input–output noises affecting the data.

It is worthy to note how this work presents a novel point of view of the model-based fault diagnosis. The new aspect consists in exploiting linear system identification procedures in connection with the model-based residual generation problem.

The diagnostic tools presented in this thesis are well illustrated using practical application examples and the results show the effectiveness of the developed techniques.

Finally, even if industrial processes are nonlinear, instead of exploiting complicated nonlinear models obtained by modeling techniques in connection with nonlinear observers, this work concerns mainly the development of linear identified prototypes for the design of linear output estimators. Moreover, if the number of studies addressing nonlinear fault diagnosis theory clearly increases over the years, unfortunately it is important to note the lack of nonlinear process applications using these nonlinear models.

Contents

1 Introduction **17**
- 1.1 Background . . . 17
- 1.2 Nomenclature . . . 18
- 1.3 Fault Detection and Diagnosis Methods . . . 20
- 1.4 Model-Based Fault Detection Methods . . . 21
- 1.5 Fault Diagnosis Methods . . . 22
- 1.6 Summary of FDI Applications . . . 23
- 1.7 Model Uncertainty and Fault Detection . . . 26
- 1.8 Outline of the Thesis . . . 26
- 1.9 Conclusions . . . 28

2 Model-Based Fault Diagnosis Techniques **29**
- 2.1 Introduction . . . 29
- 2.2 Model-Based FDI Techniques . . . 30
- 2.3 Mathematical Description of the System . . . 31
- 2.4 Residual Generator Structure . . . 34
- 2.5 Fault Detectability and Isolability . . . 36
- 2.6 Residual Generation Techniques . . . 36
  - 2.6.1 Residual Generation via Parameter Estimation . . . 36
  - 2.6.2 Residual Generation with Dynamic Observers . . . 39
  - 2.6.3 Fault Detection with Parity Equations . . . 42
- 2.7 Change Detection and Symptom Evaluation . . . 44
- 2.8 Residual Generation Problem . . . 44
- 2.9 Fuzzy Logic and Neural Networks in FDI . . . 45
- 2.10 Summary . . . 46

3 System Identification for Fault Diagnosis **47**
- 3.1 Introduction . . . 47
- 3.2 The Frisch Scheme in the Algebraic Case . . . 47
- 3.3 The Frisch Scheme in the Dynamic Case . . . 49
- 3.4 The Frisch Scheme in the MIMO Case . . . 52
- 3.5 Identification of Nonlinear Dynamic Systems . . . 53
- 3.6 Multiple Model Structure . . . 54
- 3.7 Multiple Model Identification . . . 55
- 3.8 Simplifying the Optimization Problem . . . 58

3.9 Fuzzy Modeling from Noisy Data . . . 60
3.10 Fuzzy Multiple Inference Identification . . . 61
3.11 Fuzzy Model Structure . . . 61
3.12 Conclusions . . . 62

4 Residual Generation **63**
4.1 Introduction . . . 63
4.2 Unknown Input Observer . . . 64
4.3 UIO Mathematical Description . . . 65
4.4 UIO Design Procedure . . . 66
4.5 FDI Schemes Based on UIO . . . 67
4.6 Kalman Filtering and FDI from Noisy Measurements . . . 71
4.7 Residual Robustness to Disturbances . . . 72
4.8 Residual Generation via Parameter Estimation . . . 74
4.9 Residual Generation via Fuzzy Models . . . 75
4.10 Fault Identification Using Neural Networks . . . 75
4.11 Summary . . . 77

5 Fault Diagnosis Applications **79**
5.1 Introduction . . . 79
5.2 FDI of an Industrial Gas Turbine using Dynamic Observers . . . 80
5.3 FDI of the Gas Turbine using Kalman Filters . . . 87
5.4 Sensor Fault Identification Using Neural Networks . . . 92
5.5 Power Plant of Pont sur Sambre Identification and FDI . . . 96
5.6 Disturbance Decoupled Observers for Sensor FDD . . . 101
5.7 Fuzzy Models and Fault Diagnosis of an Industrial Process . . . 103
5.8 Actuator, Process and Sensor FDD of a Turbine Prototype . . . 106
5.9 Conclusion . . . 118

6 Conclusions and Further Research **121**
6.1 Introduction . . . 121
6.2 Suggestion for Future Research . . . 123
6.3 Frequency Domain Residual Generation . . . 123
6.4 Adaptive Residual Generators . . . 124
6.5 Integration of Identification, FDD and Control . . . 126
6.6 Fault Identification . . . 126
6.7 Fault Diagnosis of Nonlinear Dynamic Systems . . . 126
6.8 Conclusion . . . 128

List of Figures

1.1 Comparison between hardware and analytical redundancy schemes. 21
1.2 Scheme for the model-based fault detection. 22

2.1 Structure of model-based FDI system. 30
2.2 Fault diagnosis and control loop. 31
2.3 The monitored system and fault topology. 32
2.4 The structure of the plant sensors. 33
2.5 Fault topology with actuator input signal measurement. 33
2.6 Residual generator general structure. 35
2.7 Residual generatior via system simulator. 35
2.8 Parameter estimation equation error. 37
2.9 Parameter estimation output error. 38
2.10 Process and state observer. 39
2.11 MIMO process with faults and noises. 40
2.12 Process and output observer. 42
2.13 Parity equation methods. 43
2.14 Parity equation methods for a MIMO model. 44

3.1 Singularity surfaces in the noisy space. 52
3.2 An example of , $^{(i')}$ and , $^{(i'')}$ surfaces 56
3.3 An example of singularity surfaces in two regions R_i and R_j. 57
3.4 Singularity surfaces in two regions R_i and R_j with non-stationary noise. 58

4.1 The UIO structure. 65
4.2 Bank of estimators for output residual generation. 68
4.3 Scheme for system inputs FDI. 68
4.4 The monitored system. 73
4.5 The structure of the equation error model. 73
4.6 The structure of the monitored system. 75
4.7 The residual generation scheme. 76

5.1 Layout of the single-shaft industrial gas turbine with highlighted the monitored sensors. 80
5.2 Fault-free residual function of the UIO driven by the M_f signal with minimum positive ('+') and negative ('-') thresholds. 84
5.3 Residual function of the UIO driven by the M_f signal in the presence of positive failure. 84

5.4 Residual function of the UIO driven by the M_f signal in the presence of negative failure. . . . 85
5.5 Fault-free residual function of output observer driven by p_{ot} signal with minimum positive ('+') and negative ('-') thresholds. . . . 85
5.6 Residual function of output observer driven by p_{ot} signal with positive failure. . . 86
5.7 Residual function of output observer driven by p_{ot} signal with negative failure. . 86
5.8 Residual function of the UIO driven by the α signal in the presence of a drift in the α measurement. . . . 87
5.9 Residual function of the output observer regarding the T_{oc} signal in the presence of a drift in the T_{oc} measurement. . . . 87
5.10 Mean value of the residual computed by using KF with unknown input in a growing window. . . . 90
5.11 Standard deviation of the residual computed by using a KF with unknown input in a growing window. . . . 90
5.12 Whiteness of the residual computed by using a KF with unknown input in a growing window. . . . 91
5.13 Mean value of p_{ic} residual computed by using a growing window. . . . 91
5.14 Standard deviation of p_{ic} residual computed by using a growing window. . . . 92
5.15 Whiteness of p_{ic} residual computed by using a growing window. . . . 92
5.16 NN input pattern . . . 94
5.17 Output pattern of the NN. . . . 94
5.18 The structure of the power plant. . . . 96
5.19 First four input of the power plant. . . . 97
5.20 Last input and three output of the power plant. . . . 98
5.21 Fault-free residual function $r_1(t)$ of the UIO driven by the O_s signal with minimum positive ('+') and negative ('-') thresholds. . . . 99
5.22 Residual function $r_1(t)$ of the UIO driven by the O_s signal in the presence of a failure. . . . 99
5.23 Fault-free residual function $r_3(t)$ of output observer driven by T_{rs} signal with minimum positive ('+') and negative ('-') thresholds. . . . 100
5.24 Residual function $r_3(t)$ of output observer driven by T_{rs} signal with a failure. . . 100
5.25 Predicted and measured $P_v(t)$ output. . . . 104
5.26 Predicted and measured $T_s(t)$ output. . . . 104
5.27 Predicted and measured $T_{rs}(t)$ output. . . . 105
5.28 The residual generation scheme. . . . 105
5.29 Turbine Simulink prototype. . . . 107
5.30 Turbine closed-loop scheme. . . . 107
5.31 Logic diagram of the residual generator. . . . 107
5.32 First input for the turbine. . . . 108
5.33 Second input for the turbine. . . . 109
5.34 Compressor air flow rate. . . . 109
5.35 Dynamics of the compressor fault. . . . 110
5.36 Fault-free and faulty residual. . . . 110
5.37 Fault on the temperature sensor. . . . 111
5.38 Output signal from the temperature sensor. . . . 111
5.39 Residuals from the temperature sensor. . . . 112

5.40 Turbine fault signal. 112
5.41 Turbine output signal. 113
5.42 Turbine output signal. 113
5.43 Turbine actuator fault. 114
5.44 Turbine output measurement. 114
5.45 Fault free and faulty residuals concerning the turbine actuator. 115
5.46 Parameter variations. 115
5.47 Parameter variations in case of actuator fault occurrence. 116
5.48 KF residuals when a fault $f_s(t)$ *case 1* occurs. 116
5.49 KF residuals in case of output *case 2* sensor fault $f_y(t)$ occurrence. 117
5.50 Component *case 3* fault $f_s(t)$ and KF residuals. 117
5.51 Actuator fault $f_u(t)$ and KF residuals *case 4*. 118
5.52 Detection delay definition. 118

6.1 Residual generator with adaptive observer. 125
6.2 Fault estimation scheme. 127

List of Tables

1.1 FDI applications and number of contributions. 24
1.2 Fault type and number of contributions. 24
1.3 FDI methods and number of contributions. 24
1.4 Residual evaluation methods and number of contributions. 24
1.5 Reasoning strategies and number of contributions. 24
1.6 Applications of model-based fault detection. 25

4.1 Fault signatures. 69

5.1 Gas turbine main cycle parameters (ISO design conditions). 81
5.2 Parameter variation of the p_{ic} ARX model versus measurement noise. 82
5.3 Fault detectability thresholds. 83
5.4 Minimal detectable step faults. 86
5.5 Minimal detectable ramp faults. 88
5.6 Measurement noise standard deviation. 88
5.7 Minimum detectable faults by monitoring residual mean value 91
5.8 Minimum detectable faults by monitoring residual whiteness. 91
5.9 Training results concerning the M_f sensor. 95
5.10 Training results concerning the IGV sensor. 95
5.11 Minimal detectable step faults. 95
5.12 Minimal detectable step and ramp faults with classical observers and UIO. . . . 101
5.13 The three output estimation errors with equation error models. 101
5.14 Minimal detectable step and ramp faults with classical KF and UIKF. 101
5.15 The three output estimation errors with EIV models. 101
5.16 The three output estimation errors without disturbance decoupling. 102
5.17 The three output estimation errors with KF. 102
5.18 Minimal detectable step and ramp faults with UIO. 102
5.19 The three output estimation errors with disturbance decoupling. 103
5.20 The three output estimation errors with fuzzy multiple model. 103
5.21 Minimal detectable step and ramp faults with multiple model. 106
5.22 Minimum detectable faults by monitoring residual and innovation values. 117

Acknowledgments

At the end of this thesis, I wish to express my gratitude to my supervisor, Prof. Sergio Beghelli, for valuable suggestions and for having always been an ideal Ph.D. tutor and to Dr. Cesare Fantuzzi, for the constant encouragement during these three years. I would also like to thank them for their friendship and suggestions at the beginning of my experience.

I am grateful to all the staff of the Department of Electronics of the University of Ferrara for supporting my work in these three years.

Part of this work has been developed while I was visiting the Electronic Engineering Department of the University of Hull (UK). I want to express my sincere thanks to Prof. Ron J. Patton who, with his strong scientific personality, discussed and collaborate with me in many aspects. I wish also to thank, beside the staff of the Department, all the guys of the Control Systems Engineering Group who made my stay there pleasant and profitable.

Special thanks to my parents and relatives for their continuous support and stimulation in persevering in my research activity. They saw myself often absent or absent-minded and without whom this work would have been much harder to carry out.

Symbols and Abbreviations

The symbols and abbreviations listed here are used unless otherwise stated.

ARMAX	AutoRegressive Moving Average eXogenous
ARX	AutoRegressive eXogenous
BFDF	Beard Fault Detection Filter
DOS	Dedicated Observer Scheme
EE	Equation Error
EIV	Errors-In-Variables
FDD	Fault Detection and Diagnosis
FDI	Fault Detection and Isolation
FFT	Fast Fourier Transform
GK	Gustafson-Kessel
GOS	Generalized Observer Scheme
IGV	Inlet Guided Vane
KF	Kalman Filter
LS	Least Squares
MIMO	Multi-Input Multi-Output
MISO	Multi-Input Single-Output
MLP	MultiLayer Perceptron
NN	Neural Network
OO	Output Observer
OLS	Ordinary Least Squares
RBF	Radial Basis Function
RLS	Recursive Least Squares
SISO	Single-Input Single-Output
TS	Takagi-Sugeno
UIKF	Unknown Input Kalman Filter
UIO	Unknown Input Observer

Chapter 1

Introduction

1.1 Background

There is an increasing interest in the development of model-based fault detection and fault diagnosis methods, as can be seen in the many papers submitted to the IFAC (International Federation of Automatic Control) Congress and IFAC Symposium SAFEPROCESS [1, 2, 3].

The development began at various places in the early 1970's. Beard [4] and Jones [5] reported on observer-based fault detection in linear systems.

A summary of this development is given by Willsky [6]. Then Rault and his staff [7] have considered the application of identification methods to the fault detection of jet engines. Correlation methods were applied to leak detection [8].

A first book appeared on model-based methods for fault detection and diagnosis in chemical processes [9]. Sensor failure detection based on the inherent analytical redundancy of multiple observers was shown by Clark [10].

The use of parameter estimation techniques for fault detection of technical systems was proved by Hohmann [11], Bakiotis [12], Geiger [13], Filbert and Metzger [14].

The development of process fault detection methods based on modeling, parameter and state estimation was then summarized by Isermann [15].

Parity equation-based methods were treated early [16], and then further developed by Patton and Chen [17], Gertler [18], Höfling and Pfeufer [19].

Frequency domain methods are typically applied when the effects of faults as well as the disturbances have frequency characteristics which differ from each other and thus the frequency spectra serve as criterion to distinguish the faults [20, 21].

The development of fault detection methods up to the corresponding times is summarized in the books of Pau [22], Patton *et al.* [23], Chen and Patton [24], Gertler [25], Isermann [26] and in survey papers by Gertler [27], Frank [28] and Isermann [29].

Within IFAC, the increasing interest in this field was taken into account by creating first in 1991 a SAFEPROCESS (fault detection supervision and safety for technical processes) Steering Committee which then became a Technical Committee in 1993.

A first IFAC SAFEPROCESS Symposium was organized in Baden-Baden, Germany in 1991, and a second one in Espo, Finland in 1994. The third symposium was scheduled for Hull, UK in 1997 and the next one will be held in Budapest, Hungary in 2000.

Another series of IFAC Workshop exist for "Fault detection and supervision in the chemical

process industries". Meetings have been held in Newark, Delaware and Newcastle, UK between 1992 and 1995.

This first chapter of the thesis tries to propose a common terminology in the fault diagnosis framework and to comment on some developments in the field of fault detection and diagnosis based on papers selected during 1991-1999.

1.2 Nomenclature

By going through the literature, one recognize immediately that the terminology in this field is not consistent. This makes it difficult to understand the goals of the contributions and to compare the different approaches.

The SAFEPROCESS Technical Committee therefore discussed this matter and tried to find commonly accepted definitions. Some basic definitions can be found, for example, in the RAM (Reliability, Availability and Maintainability) dictionary [30], in contributions to IFIP [31].

Below, some definitions used through this thesis are suggested. They are based on the discussion within the Committee. However, these proposal are preliminary, because the discussions are still going on.

1. ***States and Signals***

   Fault
   An unpermitted deviation of at least one characteristic property or parameter of the system from the acceptable, usual or standard condition.

   Failure
   A permanent interruption of a system's ability to perform a required function under specified operating conditions.

   Malfunction
   An intermittent irregularity in the fulfillment of a system's desired function.

   Error
   A deviation between a measured or computed value of an output variable and its true or theoretically correct one.

   Disturbance
   An unknown and uncontrolled input acting on a system.

   Residual
   A fault indicator, based on a deviation between measurements and model-equation-based computations.

   Symptom
   A change of an observable quantity from normal behavior.

2. ***Functions***

   Fault detection
   Determination of faults present in a system and the time of detection.

Fault isolation
Determination of the kind, location and time of detection of a fault. Follows fault detection.

Fault identification
Determination of the size and time-variant behavior of a fault. Follows fault isolation.

Fault diagnosis
Determination of the kind, size, location and time of detection of a fault. Follows fault detection. Includes fault detection and identification.

Monitoring
A continuous real-time task of determining the conditions of a physical system, by recording information, recognizing and indication anomalies in the behavior.

Supervision
Monitoring a physical and taking appropriate actions to maintain the operation in the case of fault.

3. ***Models***

Quantitative model
Use of static and dynamic relations among system variables and parameters in order to describe a system's behavior in quantitative mathematical terms.

Qualitative model
Use of static and dynamic relations among system variables in order to describe a system's behavior in qualitative terms such as causalities and if-then rules.

Diagnostic model
A set of static or dynamic relations which link specific input variables, *the symptoms*, to specific output variables, the faults.

Analytical redundancy
Use of more (not necessarily identical) ways to determine a variable, where one way uses a mathematical process model in analytical form.

4. ***System properties***

Reliability
Ability of a system to perform a required function under stated conditions, within a given scope, during a given period of time.

Safety
Ability of a system not to cause danger to persons or equipment or the environment.

Availability
Probability that a system or equipment will operate satisfactorily and effectively at any point of time.

5. ***Time dependency of faults***

   Abrupt fault
   Fault modeled as stepwise function. It represents bias in the monitored signal.

   Incipient fault
   Fault modeled by using ramp signals. It represents drift of the monitored signal.

   Intermittent fault
   Combination of impulses with different amplitudes.

6. ***Fault typology***

   Additive fault
   Influences a variable by an addition of the fault itself. They may represent, e.g., offsets of sensors.

   Multiplicative fault
   Are represented by the product of a variable with the fault itself. They can appear as parameter changes within a process.

1.3 Fault Detection and Diagnosis Methods

A traditional approach to fault diagnosis in the wider application context is based on *hardware or physical redundancy* methods which use multiple sensors, actuators, components to measure and control a particular variable. Typically, a voting technique is applied to the hardware redundant system to decide if a fault has occurred and its location among all the redundant system components. The major problems encountered with hardware redundancy are the extra equipment and maintenance cost, as well as the additional space required to accommodate the equipment.

In view of the conflict between reliability and the cost of adding more hardware, it is possible to use the dissimilar measured values together to cross-compare each other, rather than replicating each hardware individually. This is the meaning of *analytical or functional redundancy*. It exploits redundant analytical relationships among various measured variables of the monitored process.

In analytical redundancy scheme the resulting differences generated from the comparison of different variables is called a *residual or symptom signal*. The residual should be zero when the system is in normal operating condition and should be different from zero in case of fault occurrence. This property of the residual is used to determine whether or not faults have occurred.

Consistency checking in analytical redundancy is normally achieved through a comparison between a measured signal with its estimation. The estimation is generated by a mathematical model of the considered plant. The comparison is done using the residual quantities which are computed as differences between the measured signals and the corresponding signals generated by the mathematical model.

In Figure (1.1) the hardware and analytical redundancy concept in illustrated.

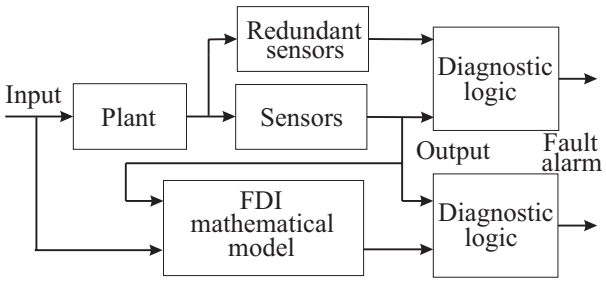

Figure 1.1: Comparison between hardware and analytical redundancy schemes.

In practice, the most frequently used diagnosis method is to monitor the level (or trend) of the residual and taking action when the signal reached a given threshold. This method of *geometrical analysis*, whilst is simple to implement, has few drawbacks. The most serious is that, in case of noises, input variations and change of operating point of the monitored process, false alarms are possible.

The major advantage of the model-based approach is that no additional hardware components are required in order to realize a Fault Detection and Identification (FDI) algorithm. A model-based FDI algorithm can be implemented via software on a process control computer. In many cases, the measurements necessary to control the process are also sufficient for the FDI algorithm so that no additional sensors have to be installed.

Analytical redundancy makes use of a mathematical model of the system under investigation and it is therefore often referred to as the *model-based approach* to fault diagnosis.

1.4 Model-Based Fault Detection Methods

The task consists of the detection of faults on the technical process including actuators, components and sensors by measuring the available input and output variables $\mathbf{u}(t)$ and $\mathbf{y}(t)$. The principle of the model-based fault detection is depicted in Figure (1.2).
Basic process model-based FDI methods are:

(1) Output observers (OO, estimators, filters),

(2) Parity equations,

(3) Identification and parameter estimation.

They generate residuals for output variables with fixed parametric models for method (1), fixed parametric or nonparametric models for method (2) and adaptive nonparametric or parametric models for method (3).

An important aspect of these methods is the kind of fault to be detected. As noted above, one can distinguish between *additive faults* which influence the variables of the process by a summation and *multiplicative faults* which are products with the process variables. The basic methods show different results, depending on these types of faults.

If only output signals $y(t)$ can be measured, *signal model-based methods* can be applied. E.g. vibrations can be detected, which are related to rotating machinery or electrical circuits. Typical signal model-based methods of fault detection are:

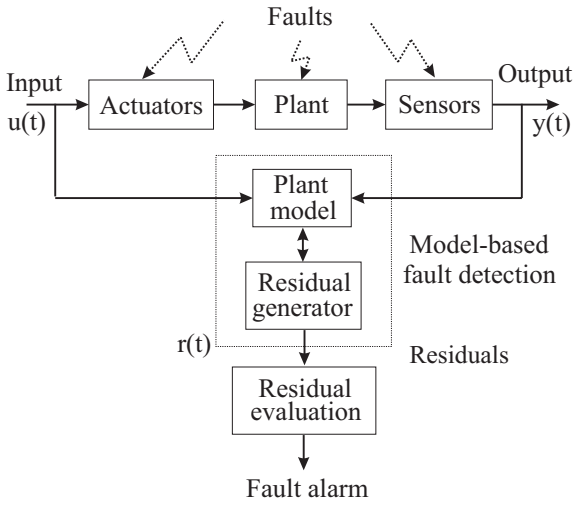

Figure 1.2: Scheme for the model-based fault detection.

(4) Bandpass filters,

(5) Spectral analysis (FFT),

(6) Maximum-entropy estimation.

The characteristic quantities or features from fault detection methods show stochastic behavior with mean values and variances. Deviations from the normal behavior have then to be detected by methods of *change detection* (residual analysis, Figure (1.2)) like:

(7) Mean and variance estimation,

(8) Likelihood-ratio test, Bayes decision,

(9) Run-sum test.

1.5 Fault Diagnosis Methods

If several symptoms change differently for certain faults, a first way of determining them is to use classification methods which indicate changes of symptom vectors.

Some classification methods are:

(10) Geometrical distance and probabilistic methods,

(11) Artificial neural networks,

(12) Fuzzy clustering.

When more information about the relations between symptoms and faults is available in form of diagnostic models, methods of reasoning can be applied. Diagnostic models then exist in the

form of symptom-fault causalities, e.g. in the form of symptom-fault tree. The causalities can be expressed as IF-THEN rules. Then analytical as well as heuristic symptom (from operators) can be processed. By considering them as vague facts, probabilistic or fuzzy set descriptions lead to a unified symptom representation. By forward and backward reasoning, probabilities or possibilities of faults are obtained as a result of diagnosis. Typical approximate reasoning methods are:

(13) Probabilistic reasoning,

(14) Possibilistic reasoning with fuzzy logic,

(15) Reasoning with artificial neural networks.

This very short consideration shows that many different methods have been developed during the last 20 years. It is obvious that many combinations of them are possible.

Based on more than 100 publications during the last 5 years, it can be stated that parameter estimation and observer-based methods are the most frequently applied techniques for fault detection, especially for the detection of sensor and process faults. Nevertheless, the importance of neural network-based and combined methods for fault detection is steadily growing. In most applications, fault detection is supported by simple threshold logic or hypothesis testing. Fault isolation is often carried out using classification methods. For this task, neural networks are being more and more widely used.

The number of applications using nonlinear models is growing, while the trend of using linearized models is diminishing. It seems that analytical redundancy-based methods have their best application areas in mechanical systems where the models of the processes are relatively precise. Most nonlinear processes under investigation belong to the group of thermal and fluid dynamic processes. The field of applications on chemical processes is only slightly developed, but the number of applications is growing. The favorite linear process under investigation is the DC motor. In general, the trend is changing from applications to safety-related processes with many measurements, as in nuclear reactors or aerospace, to applications in common technical processes with only a few sensors. For diagnosis, classification and rule-based reasoning methods are the most important and the use of neural network classification as well as fuzzy logic-based reasoning is growing.

1.6 Summary of FDI Applications

Because of the many publications and increasing number of applications, it is of interest to show some trends. Therefore, a literature study of IFAC FDI-related Conferences was performed.

Contributions taking into account the applications reported in Table (1.1) were considered.

The type of faults considered are distinguished according to Table (1.2).

Among all contributions, the fault detection methods were classified as in Table (1.3).

The change detection and fault classification methods are indicated by Table (1.4).

The reasoning strategies for fault diagnosis are reported in Table 1.5.

The contributions considered are summarized in Table (1.6). The evaluation has been limited to the Fault Detection and Diagnosis (FDD) of laboratory, pilot and industrial processes.

Table (1.6) shows that among mechanical and electrical processes, DC motor applications are mostly investigated. Parameter estimation and observer-based methods are used in the

Application	Number of contributions
Simulation of real processes	55
Large-scale pilot processes	44
Small-scale laboratory processes	18
Full-scale industrial processes	48

Table 1.1: FDI applications and number of contributions.

Fault type	Number of contributions
Sensor faults	69
Actuator faults	51
Process faults	83
Control loop or controller faults	8

Table 1.2: Fault type and number of contributions.

Method type	Number of contributions
Observer	53
Parity space	14
Parameter estimation	51
Frequency spectral analysis	7
Neural networks	9

Table 1.3: FDI methods and number of contributions.

Evaluation method	Number of contributions
Neural networks	19
Fuzzy logic	5
Bayes classification	4
Hypothesis testing	8

Table 1.4: Residual evaluation methods and number of contributions.

Reasoning strategy	Number of contributions
Rule based	10
Sign directed graph	3
Fault symptom tree	2
Fuzzy logic	6

Table 1.5: Reasoning strategies and number of contributions.

majority of applications on these kind of processes, followed by parity space and combined methods. Thermal and chemical processes are investigated less frequently.

FDD	Number of contributions
Milling and grinding processes	41
Power plants and thermal processes	46
Fluid dynamic processes	17
Combustion engine and turbines	36
Automotive	8
Inverted pendulum	33
Miscellaneous	42
DC motors	61
Stirred tank reactor	27
Navigation system	25
Nuclear process	10

Table 1.6: Applications of model-based fault detection.

Table (1.3) shows that parameter estimation and observer-based methods are used in nearly 70% of all application considered. Neural networks, parity space and combined methods are significantly less often applied.

More than 50% of sensor faults are detected using observer-based methods, while parameter estimation and parity space and combined methods play a less important role. For the detection of actuator faults, observer-based methods are mostly used, followed by parameter estimation and neural networks methods.

Parity space and combined methods are rarely applied. In general, there are fewer applications for actuator faults than for sensor or process faults. The detection of process faults is mostly carried out with parameter estimation methods. Nearly 50% of all the applications considered use parameter estimation-based methods for detection of process faults. Observer-based, parity space and neural networks-based methods are used less often for this class of faults.

Among all the described processes, linear models have been used much more than nonlinear ones. On processes with nonlinear models, observer-based methods are applied most, but parity equations and neural networks do also play an important role. Parity space and combined methods are only used to a minor extent. On processes with a linear or linearized models, parameter estimation and observer-based methods are mostly used. Parity space and combined methods are also used in several applications, but not to the same extent as observer-based and parameter estimation methods.

Taking into account the considered systems, the number of nonlinear process applications using nonlinear models are decreasing. For linear processes, no significant change can be stated.

The applications of fault-detection methods for nonlinear processes, used mostly observer-based and parameter estimation, more than parity space methods. The use of neural networks and combinations seems to be increasing.

Concerning the fault diagnosis methods, in recent years, the field of classification approaches, especially with neural networks and fuzzy logic has steadily been growing. Also, rule-based reasoning methods are increasingly being used in fault diagnosis. A growing application of fuzzy rule-based reasoning can be stated. Applications using neural networks for classification are increasing and the trends are analogous to the increasing number of nonlinear process investiga-

tions. Nevertheless, the classification of generated residuals seems to remain the most important application area for neural networks.

1.7 Model Uncertainty and Fault Detection

Model-based FDI makes use of mathematical models of the system. However, a perfectly accurate mathematical model of a physical system is never available. Usually, the parameters of the system may vary with time and the characteristics of the disturbances and noises are unknown so that they cannot be modeled accurately. Hence, there is always a mismatch between the actual process and its mathematical model even under no fault conditions. Such discrepancies cause difficulties in FDI applications, in particular, since they act as sources of false alarms and missed alarms. The effect of modeling uncertainties, disturbances and noises is therefore the most crucial point in the model-based FDI concept and the solution to this problem is the key for its practical applicability [24].

To overcome these problems, a model-based FDI has to be insensitive to modeling uncertainty. Sometimes, a reduction of the sensitivity to modeling uncertainty does not solve the problem since the sensitivity reduction may be associated with a reduction of the sensitivity to faults [24, 25]. A more meaningful formulation of the FDI problem is to increase insensitivity to modeling uncertainty in order to provide increasing fault sensitivity.

The difficulties introduced by model uncertainties, disturbances and noises in model-based FDI have been widely considered during the last 10 years by both academia and industry [25]. A number of methods have been proposed to tackle this problem, for example the Unknown Input Observer (UIO), eigenstructure assignment and parity relation methods.

An important task of the model-based FDI scheme is to be able to diagnose *incipient faults* in a system. With respect to *abrupt faults*, incipient faults may have a small effect on residuals and they can be hidden by disturbances. On the other hand, hard faults can be easier detected because their effects are usually larger than modeling uncertainties and a simple fixed threshold is usually enough to diagnose their occurrence analyzing residuals.

The presence of incipient faults may not necessarily degrade the performance of the plant, however, they may indicate that component should be replaced before the probability of more serious malfunctions increases. The successful detection and diagnosis of incipient faults can therefore be considered a challenge for the design and evaluation of FDI algorithms.

1.8 Outline of the Thesis

To detect and isolate faults in a dynamic system, based on the use of an analytical model, a residual signal has to be used. It is derived from a comparison between real measurements and the relative estimates (generated by the model). The modeling uncertainty problem can be tackled by designing a FDI scheme, whose residuals are insensitive to uncertainties whilst sensitive to faults. On the other hand, a model with satisfactory accuracy can be estimated using identification procedures [32, 33, 34].

The aim of the design of a FDI scheme is to reduce the effects of uncertainties on the residuals and to enhance the effects of faults acting on the residuals. The *main aim of this thesis* is to develop a residual generator for model-based fault diagnosis of a process by means of input and output signals. An accurate model of the process under investigation will be estimated

using identification procedures from data affected by noises and acquired from simulated and/or actual plants. The thesis consists of 6 chapters and the main contributions are presented in Chapters 3, 4 and 5. Chapters are devoted to the particular problem in residual generation and the are organized as follows.

Chapter 2 reviews the state of the art of the model-based FDI. The FDI problem is formalized in an uniform framework by presenting the mathematical description and definitions. The fundamental issue of model-based methods is the generation of residuals using the mathematical model of the monitored system. By analyzing residuals, fault diagnosis can be performed. Some structures of the residual generator are presented in this chapter in order to give ideas how to implement the residual generation. A residual generator can be designed for achieving the required diagnosis performances, e.g. fault isolation and disturbance decoupling.

In order to design the residual generator, some assumptions about the modeling uncertainties need to be made. The most frequently used hypothesis is that the modeling uncertainty is expressed as a disturbance term in the system dynamic equation. The disturbance vector is unknown whilst its distribution matrix can be estimated by using identification procedures. Based on this assumption, the disturbance decoupling residual generator can be design by using unknown input observer [24, 35].

Chapter 3 demonstrates how to apply dynamic system identification methods in order to estimate an accurate model of the monitored system.

The presented FDI methods require, in fact, a linear mathematical model of the process under investigation, either in state space or input-output form.

In particular, since state–space descriptions provide general and mathematically rigorous tools for system modeling, they may be used in the residual generator design, both for the deterministic case (UIO and OO) [24, 28, 36, 37] and the stochastic case (Kalman filters (KF) and unknown input Kalman filters (UIKF)) [38, 39, 40].

In such a manner, the suggested FDI tool does not require any physical knowledge of the process under observation since the linear models are obtained by means of an identification scheme which exploits equation error (EE) and errors–in–variables (EIV) models. In this situation, the identification technique is based on the rules of the Frisch scheme [41], traditionally exploited to analyze economic systems. This approach, modified to be applied to dynamic system identification [42, 43, 44], gives a reliable model of the plant under investigation, as well as the variances of the input–output noises affecting the data.

For the nonlinear case, piecewise affine and fuzzy models will be used as prototypes for the identification. In particular, the multiple model approach, using several local affine submodels each describing a different operating condition of the process, is exploited.

Chapter 4 aims to define a comprehensive methodology for actuator, process component and sensor fault detection. It is based on an output estimation approach, in conjunction with residual processing schemes, which include a simple threshold detection, in deterministic case, as well as statistical analysis when data are affected by noise. The final result consists in a strategy based on fault diagnosis methods well–known in literature to generate redundant residuals.

In particular, this chapter studies the approach to residual generator with the aid of OO, UIO, KF and UIKF. The residual is defined as the *output estimation error*, obtained by difference

between the measurement of one output and the relative estimate. This chapter presents also the design of such estimators both in the deterministic and stochastic environment.

The diagnosis procedure may be further specialized for actuators, input or output sensors and process components. In fact, the fault diagnosis of input sensors and actuators uses a bank of UIO in high signal to noise ratio conditions or a bank of UIKF, otherwise. The i–th UIO or UIKF is designed to be insensitive to the i–th input of the system. On the other side, output sensor and process component faults affecting a single residual can be detected by means of a OO or a classical KF, driven by a single output and all the inputs of the system.

Chapter 5 shows how the proposed algorithms can be applied to the FDI of actuators, process components and input-output sensors of industrial plants.

In particular, the FDI techniques presented in this thesis have been tested on time series of data acquired from different simulated and real industrial gas turbine working in parallel with electrical mains, whose linear mathematical description is obtained by using identification procedures.

Results from simulation show that minimum detectable faults are perfectly compatible with the industrial target of this application.

Chapter 6 summarizes the contributions and achievements of the thesis providing some suggestions for possible further research topics as an extension of this work.

1.9 Conclusions

The first chapter of the thesis tried to suggest a common terminology in the fault diagnosis framework in order to comment on some developments in the field of fault detection and diagnosis based on papers selected during the last 10 years.

The structure of the 6 chapters composing this thesis and the main contributions presented were briefly outlined.

Chapter 2

Model-Based Fault Diagnosis Techniques

2.1 Introduction

The model-based approach to fault detection in dynamic systems has been received more and more attention over the last two decades, both in a research context and also in the domain of application studies on real plants. There is a great variety of techniques in the literature, based on the use of mathematical models of the process under investigation and exploiting modern control theory [24].

The most important issue in model-based fault detection concerns the accuracy of the model describing the behavior of the monitored system. This issue has become a central research theme over recent years. Modeling uncertainty arises from the impossibility of obtaining complete knowledge and understanding of the monitored process, in connection with the presence of noises on process measurements.

Since this thesis focuses on the development and the design of model-based FDI algorithms, this chapter studies basic principles of model-based fault detection. As shown in Chapter 3, a linear model for the monitored process will be obtained by means of linear dynamic system identification methods.

Attention in first turned to the modelling of the process with fault typology reported in Section 1.2. Residual generation is then identified as an essential problem in model-based FDI, since, if it is not performed correctly, some fault information could be lost. A general framework for the residual generation is also recalled.

Residual generators based on different methods, such as (state) output observers, parity relations and parameter estimations, are just special cases in this general framework. Some commonly used residual generation methods are discussed and their mathematical formulation summarized in the following sections.

The chapter introduces and analyses some basic problems and methods in FDI. The main task of FDI are considered and a description of model-based FDI methods is given.

2.2 Model-Based FDI Techniques

According to definitions given in Section 1.2, model-based FDI can be defined as the detection, isolation and characterization of faults on a system by means of methods which extract features from measured signals and use process mathematical models.

Faults are thus detected by setting fixed or variable thresholds on residual signals generated from the difference between actual measurements and their estimates obtained by using the process model.

A number of residuals can be designed with each having sensitivity to individual faults occurring in different locations of the system. The analysis of each residual, once the threshold is exceeded, then leads to fault isolation.

Figure (2.1) shows the general and logic block diagram of model-based FDI system. It comprises two main stages of residual generation and residual evaluation. This structure was first suggested by Chow in [45] and now is accepted by the fault diagnosis community.

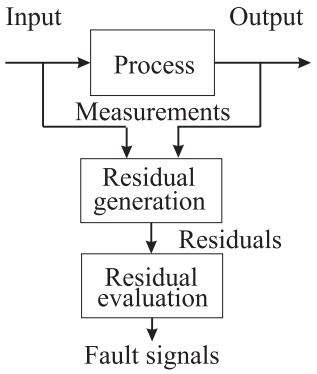

Figure 2.1: Structure of model-based FDI system.

The two main block are described as follows:

1. **Residual generation:** this block using available inputs and outputs from the monitored system has to generate residual signals. This residual (or fault symptom) should indicate any fault occurrence. It should be normally zero or close to zero under no fault condition, whilst is distinguishably different from zero when a fault occurs. This means that the residual is characteristically independent of process inputs and outputs, in ideal conditions.

   The procedure used to compute residuals is called a *residual generation*, as depicted in Figure (2.1).

   Such a procedure is thus exploited to extract fault symptoms from the system, with the fault symptom represented by the residual signal.

2. **Residual evaluation:** This block examines residuals for the likelihood of faults and a decision rule is then applied to determine if any faults have occurred. The *residual evaluation* block, shown in Figure (2.1), may perform a simple threshold test on the instantaneous values or moving averages of the residuals, or it may consist of statistical methods, e.g., generalized likelihood ratio testing or sequential probability ratio testing [2, 6, 46, 47].

Most of the contribution in the field of quantitative model-based FDI focuses on the residual generation problem, since the decision-making becomes relatively easy if residuals are well-designed.

The thesis will present a number of strategies for the quantitative residual generation problem for FDI of industrial processes. These model-based procedures do not require a deep insight into the monitored plant, since a process model is obtained by identification procedures.

2.3 Mathematical Description of the System

This thesis is concerned with the FDI of Multi-Input Single-Output (MISO) and Multi-Input Multi-Output (MIMO) dynamic systems. The first step in the model-based approach consists in describing the system under investigation from a mathematical point of view.

The FDI technique presented in this thesis considers open-loop system model. In fact, as depicted in Figure (2.2) the system model required in model based FDI can be seen as open-loop system although the system can be considered in the control loop.

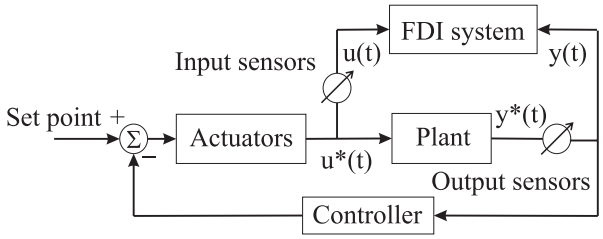

Figure 2.2: Fault diagnosis and control loop.

The information required by the FDI system is related to the open-loop system, hence it is not necessary to consider the controller in the design of a FDI scheme. Once the actual process inputs and outputs $\mathbf{u}^*(t)$ and $\mathbf{y}^*(t)$ (not available) are measured by the input and output sensors, FDI theory can be treated as an observation problem of $\mathbf{u}(t)$ and $\mathbf{y}(t)$.

In particular, the open-loop subsystem considered for FDI design is illustrated in Figure (2.3). It is separated into four different parts: actuators, process, input and output sensors.
The dynamics of the monitored system, shown in Figure (2.3), can be described by the following discrete-time, time-invariant, linear dynamic system in the state-space form

$$\begin{cases} \mathbf{x}(t+1) &= \mathrm{A}\mathbf{x}(t) + \mathrm{B}\mathbf{u}^*(t) \\ \mathbf{y}^*(t) &= \mathrm{C}\mathbf{x}(t) \end{cases} \tag{2.1}$$

where $\mathbf{x}(t) \in \Re^n$ is the system state vector, $\mathbf{u}^*(t) \in \Re^r$ is the actuation signal vector from the actuators and $\mathbf{y}^*(t) \in \Re^m$ is the actual (not available) system output vector. A, B, and C are system matrices with appropriate dimension obtained by identification procedure.

With reference to Figure (2.3), when a component fault $\mathbf{f}_c(t)$ occurs in the system, its dynamics can be described as

$$\mathbf{x}(t+1) = \mathrm{A}\mathbf{x}(t) + \mathrm{B}\mathbf{u}^*(t) + \mathbf{f}_c(t) \tag{2.2}$$

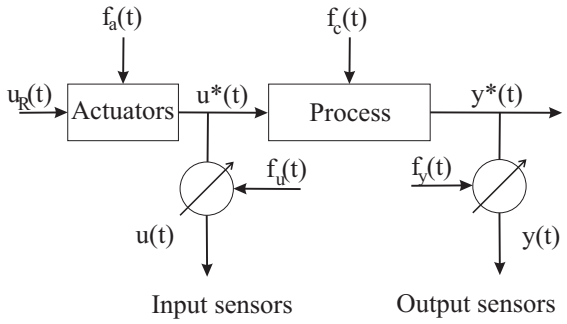

Figure 2.3: The monitored system and fault topology.

The component fault represents the situation in which expression (2.1) is invalid, since some condition changes. In some cases, it can represent a change in the system parameters, e.g. a change in entries of the A matrix. Under this assumption, with reference to the i-th row and the j-th column of the A matrix, the vector $\mathbf{f}_c(t)$ can be expressed as

$$\mathbf{f}_c(t) = I_i \Delta a_{ij} x_j(t) \tag{2.3}$$

where $x_j(t)$ in the j-th element of the vector $\mathbf{x}(t)$ and I_i is a n-dimensional vector with all zero except a '1' in the i-th element.

Under the assumption that actuators are fault free, the actual inputs and outputs of the process $\mathbf{u}^*(t) = \mathbf{u}_R(t)$ and $\mathbf{y}^*(t)$ are usually not directly accessible. Sensors have to be used to measure the system inputs and outputs. As it is shown in Figure (2.3), by neglecting sensor dynamics, they can be described mathematically as

$$\begin{cases} \mathbf{u}(t) &= \mathbf{u}^*(t) + \mathbf{f}_u(t) \\ \mathbf{y}(t) &= \mathbf{y}^*(t) + \mathbf{f}_y(t) \end{cases} \tag{2.4}$$

In real applications variables $\mathbf{u}^*(t)$ and $\mathbf{y}^*(t)$ are measured by means of sensors whose outputs, due to technological reasons, are affected by noise.

The measured signals $\mathbf{u}(t)$ and $\mathbf{y}(t)$, without faults, are thus modeled as

$$\begin{cases} \mathbf{u}(t) &= \mathbf{u}^*(t) + \tilde{\mathbf{u}}(t) \\ \mathbf{y}(t) &= \mathbf{y}^*(t) + \tilde{\mathbf{y}}(t) \end{cases} \tag{2.5}$$

in which the sequences $\tilde{\mathbf{u}}(t)$ and $\tilde{\mathbf{y}}(t)$ are usually described as white, zero–mean, uncorrelated Gaussian noises.

In this case Eq. (2.4) must be replaced by

$$\begin{cases} \mathbf{u}(t) &= \mathbf{u}^*(t) + \tilde{\mathbf{u}}(t) + \mathbf{f}_u(t) \\ \mathbf{y}(t) &= \mathbf{y}^*(t) + \tilde{\mathbf{y}}(t) + \mathbf{f}_y(t) \end{cases} \tag{2.6}$$

where the vectors $\mathbf{f}_u(t) = [f_{u_1}(t) \dots f_{u_r}(t)]^T$ and $\mathbf{f}_y(t) = [f_{y_1}(t) \dots f_{y_m}(t)]^T$ are additive signals which assume values different from zero only in the presence of faults. Usually these signals are described by step and ramp functions representing abrupt and incipient faults (bias or drift), respectively. By neglecting actuator block, Figure (2.4) shows the structure of the measurement process.

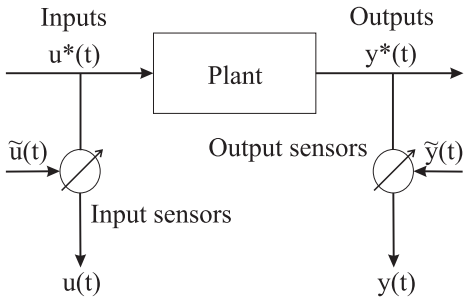

Figure 2.4: The structure of the plant sensors.

When $\mathbf{u}_R(t) = \mathbf{u}^*(t)$ descriptions of types (2.1) and (2.5) are known as EIV models [42, 43].

It is also true that the actual actuation $\mathbf{u}^*(t)$ of the system is not directly accessible. For a controlled system, according to Figure (2.3), $\mathbf{u}_R(t)$ is the input signal of the actuator, corresponding to a $\mathbf{u}^*(t)$ signal. By neglecting actuator dynamics, it can thus be described as

$$\mathbf{u}^*(t) = \mathbf{u}_R(t) + \mathbf{f}_a(t) \tag{2.7}$$

where, similar to input-output sensor fault situation, $\mathbf{f}_a(t) \in \Re^r$ is the actuator fault vector and $\mathbf{u}^*(t)$ is the control command (not available).

When the system has all possible faults, by neglecting sensor noises and under the assumption that the actuation signal $\mathbf{u}^*(t)$ can be measured, the process model is described as

$$\begin{cases} \mathbf{x}(t+1) &= \mathrm{A}\mathbf{x}(t) + \mathbf{f}_c(t) + B\mathbf{f}_u(t) + B\mathbf{u}(t) \\ \mathbf{y}(t) &= \mathrm{C}\mathbf{x}(t) + \mathbf{f}_y(t) \end{cases} \tag{2.8}$$

On the other hand, Figure (2.5) represents the case in which the $\mathbf{u}_R$ signal can be measured only by the input sensors.

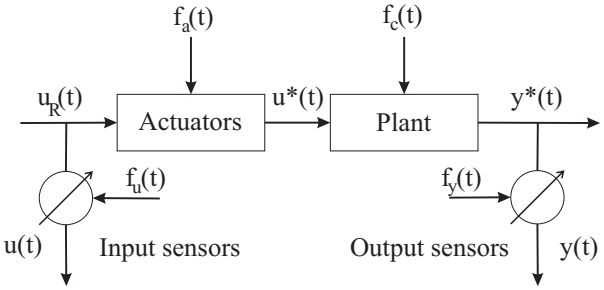

Figure 2.5: Fault topology with actuator input signal measurement.

In such a situation, system faults are related to the process by the following system

$$\begin{cases} \mathbf{x}(t+1) &= \mathrm{A}\mathbf{x}(t) + \mathrm{B}\mathbf{f}_a(t) + \mathbf{f}_c(t) + \mathrm{B}\mathbf{f}_u(t) + \mathrm{B}\mathbf{u}(t) \\ \mathbf{y}(t) &= \mathrm{C}\mathbf{x}(t) + \mathbf{f}_y(t) \end{cases} \tag{2.9}$$

Considering the general case, a system affected by all possible faults can be described by the the following state-space model

$$\begin{cases} \mathbf{x}(t+1) &= \mathrm{A}\mathbf{x}(t) + \mathrm{B}\mathbf{u}(t) + \mathrm{L}_1\mathbf{f}(t) \\ \mathbf{y}(t) &= \mathrm{C}\mathbf{x}(t) + \mathrm{L}_2\mathbf{f}(t) \end{cases} \tag{2.10}$$

where entries of the vector $\mathbf{f}(t) \in \Re^k$ correspond to a specific fault. L_1 and L_2 are matrices with appropriate dimension representing the effects of faults in the system. L_1 and L_2 can be obtained by modelling or identification procedure.

The vectors $\mathbf{u}(t)$ and $\mathbf{y}(t)$ are the measured inputs and outputs, respectively. Both vectors are known for FDI purpose.

The distribution of the fault in the system depicted in Figure (2.3) can be described an input-output transfer matrix representation in the following form

$$\mathbf{y}(s) = \mathrm{G}_{yu}(s)\mathbf{u}(s) + \mathrm{G}_{yf}(s)\mathbf{f}(s) \tag{2.11}$$

where

$$\begin{cases} \mathbf{G}_{yu}(s) &= \mathrm{C}(s\mathrm{I} - \mathrm{A})^{-1}\mathrm{B} \\ \mathbf{G}_{yf}(s) &= \mathrm{C}(s\mathrm{I} - \mathrm{A})^{-1}\mathrm{L}_1 + \mathrm{L}_2 \end{cases} \tag{2.12}$$

Both the general models for FDI described by Equations (2.10) and (2.11) in the time and frequency domain, respectively, have been widely accepted in the fault diagnosis literature [23, 24, 25, 47].

The problem treated in this work regards the detection and isolation of the actuator, process, input and output faults on the basis of the knowledge of the measured sequences $\mathbf{u}(t)$ and $\mathbf{y}(t)$.

Since the system matrices A, B and C, (2.10), in canonical forms can be obtained by multivariable identification procedures [48], state space descriptions provide general and mathematically rigorous tools for system modeling and robust residual generation, for both the deterministic (noise free measurements) and the stochastic case (measurements affected by noises).

In case of a MIMO system, the choice of state space representations in canonical form [48] instead of parity space methods [49] may avoid unexpected false alarm problems [50].

2.4 Residual Generator Structure

The most frequently used FDI methods exploit the a priori knowledge of characteristics of certain signals. As an example, the spectrum, the dynamic range of the signal and its variations may be checked. However, the necessity of a priori information concerning the monitored signals and the dependence of the signal characteristics on unknown working conditions of the system under diagnosis are main drawbacks of such a class of methods.

The most significant contribution in modern model-based approaches is the introduction of the symptom or residual signals, which depend on faults and are independent of system operating states. They represent the inconsistency between the actual system measurements and the corresponding signals of the mathematical model.

The residual generator block introduced in Figure (2.1) can be interpreted as illustrated in Figure (2.6) [24].

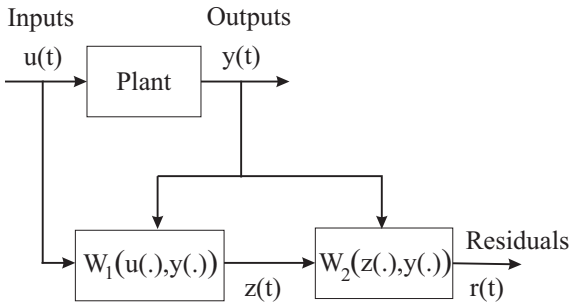

Figure 2.6: Residual generator general structure.

In the structure above, the auxiliary redundant signal $\mathbf{z}(t)$ is generated by the function $W_1\big(\mathbf{u}(\cdot),\mathbf{y}(\cdot)\big)$ and, together with the measurement $\mathbf{y}(t)$, the symptom signal $\mathbf{r}(t)$ is computed by means of $W_2\big(\mathbf{z}(\cdot),\mathbf{y}(\cdot)\big)$. The following relations are satisfied

$$\left\{\begin{array}{lcl} \mathbf{z}(t) &=& W_1\big(\mathbf{u}(\cdot),\mathbf{y}(\cdot)\big) \\ \mathbf{r}(t) &=& W_2\big(\mathbf{z}(\cdot),\mathbf{y}(\cdot)\big) \end{array}\right. = \mathbf{0} \tag{2.13}$$

for the fault free case. When a fault occurs in the plant, the residual $\mathbf{r}(t)$ will be different from zero.

The simplest residual generator is depicted in Figure (2.7) and it is obtained when the system W_1 is a model identical to the original plant $\mathbf{y}(t) = W_1\big(\mathbf{u}(\cdot)\big)$ or it is an identified input-output description for the actual process (e.g. an ARX model, see Chapter 3). In the former case, the measurement $\mathbf{y}(t)$ is not required in W_1 because it is a *system simulator*. The signal $\mathbf{z}(t)$ represents the simulated output and the residual is computed as $\mathbf{r}(t) = \mathbf{z}(t) - \mathbf{y}(t)$. Since it is an open-loop system, the disadvantage is the stability of the process simulator.

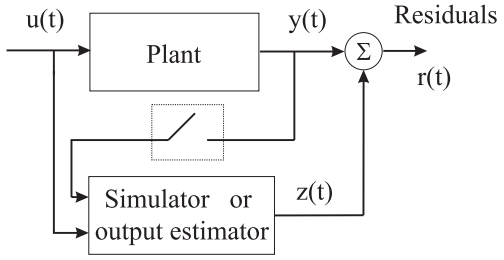

Figure 2.7: Residual generatior via system simulator.

An extension to the model-based residual generation is to replace $W_1\big(\mathbf{u}(\cdot)\big)$ by $W_1\big(\mathbf{u}(\cdot),\mathbf{y}(\cdot)\big)$, i.e. an *output estimator* fed by both system input and output. In such a case, function W_1 generates an estimation of a linear function of the output $W_1\big(\mathbf{z}(\cdot),\mathbf{y}(\cdot)\big) = \mathrm{M}\mathbf{y}(t)$ whilst function W_2 can be defined as $W_2\big(\mathbf{z}(\cdot),\mathbf{y}(\cdot)\big) = \mathrm{W}\big(\mathbf{z}(t) - \mathrm{M}\mathbf{y}(t)\big)$, with W a weighting matrix.

The parity space general structure for all residual generators using the input-output transfer matrix description was presented by Patton and Chen in [17].

The simplest and the most frequently used fault detection is obtained by performing a residual limit value checking. It consists in comparing the signal $\mathbf{r}(t)$ with a threshold function

ϵ as follows

$$\begin{cases} \mathbf{r}(t) \leq \epsilon & \text{for} \quad \mathbf{f}(t) = \mathbf{0} \\ \mathbf{r}(t) > \epsilon & \text{for} \quad \mathbf{f}(t) \neq \mathbf{0} \end{cases} \tag{2.14}$$

where $\mathbf{f}(t)$ is the general fault vector defined in Eq. (2.10). If the residual exceeds the threshold, a fault may be occurred.

This test works especially well if the process operates approximately in a steady state and it reacts after relatively large feature, i.e. after either a large sudden or a long-lasting gradually increasing fault.

2.5 Fault Detectability and Isolability

A successful detection of a fault is obtained if a residual has the maximal sensitivity to its occurrence. Fault *detectability* conditions were stated in [24]. Such a stage is followed by the fault isolation procedure which allows to distinguish a particular fault from others. Whilst a single residual signal is sufficient to detect faults, a vector of residuals is usually required for fault isolation. Faults are distinguishable or *isolable* using the residual set if each residual is sensitive to a subset of faults, whilst remaining insensitive to the remaining faults.

The design technique to obtain the so-called *structured residual set* will be briefly shown in the following Sections.

2.6 Residual Generation Techniques

The generation of symptoms is the main issue in model-based fault diagnosis. A variety of methods are available in literature for residual generation and this section presents briefly some of the most common methods. Most of the residual generation techniques are based on both continuous and discrete system models, however, in this thesis, the attention is focused only on discrete linear models.

2.6.1 Residual Generation via Parameter Estimation

In most practical cases, the process parameters are not known at all, or they are not known exactly enough. Then, they can be determined with parameter estimation methods, by measuring input and output signals, $\mathbf{u}(t)$ and $\mathbf{y}(t)$, if the basic structure of the model is known [2, 47].

a) *Equation error methods*

The SISO process model of order n is written in the vector form

$$y(t) = \Psi^T \Theta \tag{2.15}$$

where

$$\Theta^T = [a_1 \dots a_n,\ b_1 \dots b_n] \tag{2.16}$$

is the parameter vector and

$$\Psi^T = [y(t-1)\dots y(t-n) \;\; u(t-1)\dots u(t-n)] \tag{2.17}$$

the discrete-time data vector.

For parameter estimation, the equation error $e(t)$ is introduced (see Figure (2.8))

$$e(t) = y(t) - \Psi^T\Theta \tag{2.18}$$

or, if

$$\frac{y(s)}{u(s)} = \frac{B(s)}{A(s)} \tag{2.19}$$

is the transfer function of the process, the equation error via Laplace transformation becomes

$$e(s) = \hat{B}(s)u(s) - \hat{A}(s)y(s). \tag{2.20}$$

in which $\hat{A}(s)$ and $\hat{B}(s)$ correspond to the estimates of $A(s)$ and $B(s)$.

The least square (LS) estimate

$$\hat{\Theta} = [\Psi^T \; \Psi]^{-1}\Psi^T y \tag{2.21}$$

is obtained if the minimization of the sum of least squares is computed

$$J(\Theta) = \sum\nolimits_k e^2(k) = \mathbf{e}^T\mathbf{e} \tag{2.22}$$

$$\frac{d\,J(\Theta)}{d\,\Theta} = \mathbf{0}. \tag{2.23}$$

The least square estimate can be also expressed in recursive form (RLS) (see e.g. [47, 51]). For the improvement of the estimates, filtering methods can be exploited. When measurements are affected by noises, a Kalman filter for the parameter estimation can be used [38].

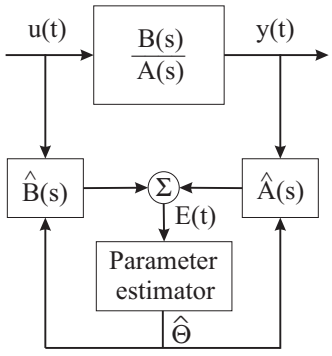

Figure 2.8: Parameter estimation equation error.

b) *Output error methods*

Instead of equation error computed in Eq. (2.18), the output error

$$e(t) = y(t) - \hat{y}(\Theta, t) \tag{2.24}$$

where

$$\hat{y}(\Theta, s) = \frac{\hat{B}(s)}{\hat{A}(s)} u(s) \tag{2.25}$$

is the model output, can also be used (see Figure 2.9).

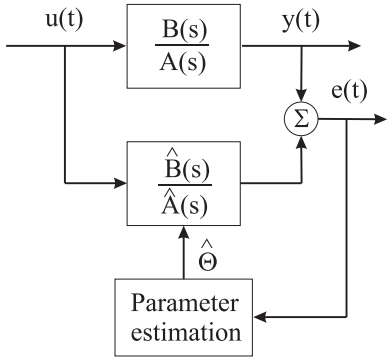

Figure 2.9: Parameter estimation output error.

Unfortunately, direct calculation of the parameter estimate Θ is not possible, because $e(t)$ is nonlinear in the parameters. Therefore, the loss function (2.24) as Eq. (2.18) has to be minimized by numerical optimization methods. The computational effort is then much larger and on-line real-time application is in general impossible. However, relatively precise parameter estimates may be obtained.

If a fault within the process changes one or several parameters by $\Delta\Theta$, the output signal changes for small deviations according to

$$\Delta y(t) = \Psi^T(t)\Delta\Theta(t) + \Delta\Psi^T(t)\Theta(t) + \Delta\Psi^T(t)\Delta\Theta(t) \tag{2.26}$$

and the parameter estimator indicates a change $\Delta\Theta$.

Generally, the process parameters Θ depend on physical process coefficients $\mathbf{p}$ (like stiffness, damping factor, resistance, ...)

$$\Theta = f(\mathbf{p}) \tag{2.27}$$

via nonlinear algebraic equations. If the inversion of the relationship

$$\mathbf{p} = f^{-1}(\Theta) \tag{2.28}$$

exists [47, 51], changes $\Delta\mathbf{p}$ of the process coefficients can be calculated. These changes in the coefficients are in many cases directly related to faults. Therefore, the knowledge of $\Delta\mathbf{p}$ facilitates fault diagnosis, but is not necessary for fault detection only. Parameter estimation can also be applied for nonlinear static process models [52].

2.6.2 Residual Generation with Dynamic Observers

A discrete-time, time-invariant, linear dynamic model for the process under consideration is described in state-space form

$$\begin{cases} \mathbf{x}(t+1) &= \mathrm{A}\mathbf{x}(t) + \mathrm{B}\mathbf{u}(t) \\ \mathbf{y}(t) &= \mathrm{C}\mathbf{x}(t). \end{cases} \tag{2.29}$$

Here, r input signals $\mathbf{u}(t)$ and m output signals $\mathbf{y}(t)$ are assumed, as the method described is especially suitable for multivariable process. Assuming that, as well as the structure, all process matrices A, B and C are known, an observer is used to reconstruct the system variables based on the measured inputs and outputs $\mathbf{u}(t)$ and $\mathbf{y}(t)$

$$\begin{cases} \hat{\mathbf{x}}(t+1) &= \mathrm{A}\hat{\mathbf{x}}(t) + \mathrm{B}\mathbf{u}(t) + \mathrm{H}\mathbf{e}(t) \\ \mathbf{e}(t) &= \mathbf{y}(t) - \mathrm{C}\hat{\mathbf{x}}(t). \end{cases} \tag{2.30}$$

In Figure (2.10), the vector $\mathbf{e}(t)$ is the output error.

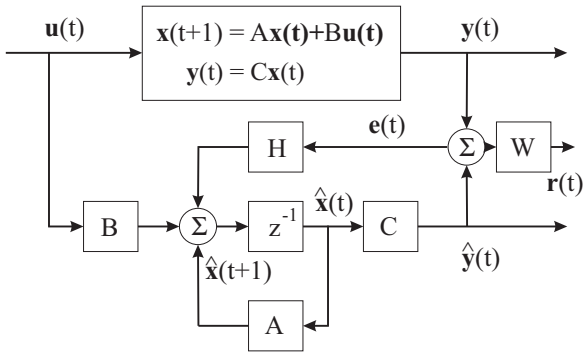

Figure 2.10: Process and state observer.

For the state estimation error, it follows from Equations (2.30) that

$$\begin{cases} \mathbf{e}_x(t) &= \mathbf{x}(t) - \hat{\mathbf{x}}(t) \\ \mathbf{e}_x(t+1) &= (\mathrm{A} - \mathrm{HC})\mathbf{e}_x(t). \end{cases} \tag{2.31}$$

The state error $\mathbf{e}_x(t)$ vanishes asymptotically

$$\lim_{t\to\infty} \mathbf{e}_x(t) = \mathbf{0} \tag{2.32}$$

if the observer is stable, which can be achieved by proper design of the observer feedback H.

If the process is influenced by disturbance and faults, by comparing Figure (2.11) and Equations (2.10), it is described by the following system

$$\begin{cases} \mathbf{x}(t+1) &= \mathrm{A}\mathbf{x}(t) + \mathrm{B}\mathbf{u}(t) + \mathrm{Q}\mathbf{v}(t) + \mathrm{L}_1\mathbf{f}(t) \\ \mathbf{y}(t) &= \mathrm{C}\mathbf{x}(t) + \mathrm{R}\mathbf{w}(t) + \mathrm{L}_2\mathbf{f}(t) \end{cases} \tag{2.33}$$

where $\mathbf{v}(t)$ is the nonmisurable disturbance vector at the input, $\mathbf{w}(t)$ the nonmisurable disturbance vector at the output, $\mathbf{f}(t)$ fault signals at the input and output acting through L_1 and L_2, respectively. They can represent actuator, process, input and output sensor additive faults.

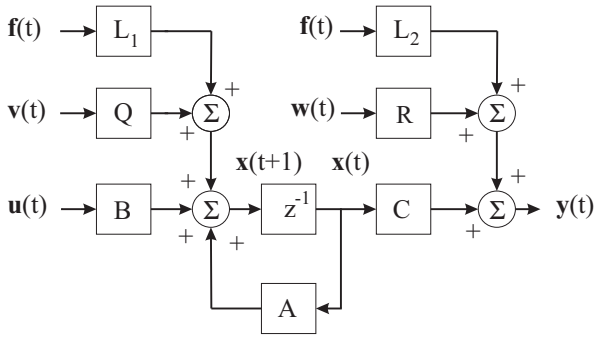

Figure 2.11: MIMO process with faults and noises.

For the state estimation error, the following equations hold if the disturbances $\mathbf{v}(t) = \mathbf{0}$ and $\mathbf{w}(t) = \mathbf{0}$

$$\mathbf{x}(t+1) = (\mathrm{A} - \mathrm{HC})\mathbf{x}(t) + \mathrm{L}_1\mathbf{f}(t) - \mathrm{HL}_2\mathbf{f}(t) \tag{2.34}$$

and the output error becomes

$$\mathbf{e}(t) = \mathrm{C}\mathbf{e}_x(t) + \mathrm{L}_2\mathbf{f}(t). \tag{2.35}$$

The vector $\mathbf{f}(t)$ represents *additive faults* because they influence $\mathbf{e}(t)$ and $\mathbf{x}(t)$ by a summation.

In case of suddenly appearing and permanent fault signals $\mathbf{f}(t)$, the state estimation error will deviate from zero. $\mathbf{e}_x(t)$ as well as $\mathbf{e}(t)$ show dynamic behaviors which are different for $\mathrm{L}_1\mathbf{f}(t)$ and $\mathrm{L}_2\mathbf{f}(t)$. Both $\mathbf{e}_x(t)$ or $\mathbf{e}(t)$ can be taken as residuals. In particular, the residual $\mathbf{e}(t)$ is the basis for different fault detection methods based on output estimation. For the generation of residual with special properties, the design of the observer feedback matrix H is of interest [24, 35]. Limiting conditions are the stability and the sensitivity against disturbances $\mathbf{v}(t)$ and $\mathbf{w}(t)$. If the signals are affected by noises, KFs have to be applied instead of classical observers [38].

If faults appear as changes ΔA or ΔB of the parameters, the process behavior becomes

$$\left\{ \begin{array}{lcl} \mathbf{x}(t+1) & = & (\mathrm{A} + \Delta\mathrm{A})\mathbf{x}(t) + (\mathrm{B} + \Delta\mathrm{B})\mathbf{u}(t) \\ \mathbf{y}(t) & = & \mathrm{C}\mathbf{x}(t) \end{array} \right. \tag{2.36}$$

while the state $\mathbf{e}_x(t)$ and the output estimation $\mathbf{e}(t)$ errors

$$\left\{ \begin{array}{lcl} \mathbf{e}_x(t+1) & = & (\mathrm{A} - \mathrm{HC})\mathbf{e}_x(t) + \Delta\mathrm{A}\mathbf{x}(t) + \Delta\mathrm{B}\mathbf{u}(t) \\ \mathbf{e}(t) & = & \mathrm{C}\mathbf{e}_x(t). \end{array} \right. \tag{2.37}$$

The changes ΔA and ΔB are then *multiplicative faults* [1]. In this case, the changes in the residuals depend on the parameter changes, input and state variable changes. Hence, the influence of parameter changes on the residuals is not as straightforward as in the case of the additive faults $\mathbf{f}(t)$.

The following detection methods are briefly summarized [1, 6, 23, 24, 47].

a) **Dedicated observers for MIMO processes**

- *Observer excited by one output*: one observer is driven by one sensor output. The other outputs $\hat{\mathbf{y}}(t)$ are reconstructed and compared with measured outputs $\mathbf{y}(t)$. This allows the detection of single output sensor faults.
- *Kalman filter, excited by all outputs*: the innovation (symptom) $\mathbf{e}(t)$ changes the characteristics of zero mean white noise with known covariance if a fault appears. This is detected by a hypothesis test.
- *Bank of observers, excited by all outputs*: several observers are designed for a definite fault signal and detected by hypothesis test.
- *Bank of observers, excited by single outputs*: several observers for single sensors outputs are used. The estimated outputs $\hat{\mathbf{y}}(t)$ are compared with the measured outputs $\mathbf{y}(t)$. This allows the detection of multiple sensor fault (dedicated observer scheme).
- *Bank of observers, excited by all outputs except one*: as before, but each observer is excited by all outputs except one sensor output, which is supervised.

b) **Fault detection filters for MIMO processes**

The feedback H of the state observer in Equation (2.30) is chosen so that particular fault signals $\mathrm{L}_1\mathbf{f}(t)$ change in a definite direction and fault signals $\mathrm{L}_2\mathbf{f}(t)$ in a definite plane [4, 5].

With directional residual vectors, the fault isolation problem consists in determining which of the known fault signature directions the residual vector lies the closest to. The most effective way to generate directional residual vectors is the use of the Beard Fault Detection Filters (BFDF) [4, 5].

Fault detection filters are a class of Luenberger observers with a specially designed feedback gain matrix. It allows to obtain output estimation errors having directional characteristics associated with some known fault directions.

These fault detection methods mostly require several measurable output signals and make use of internal analytical redundancy of multivariable systems. Recently it was proposed to improve their robustness with respect to process parameter changes and unknown input signals $\mathbf{v}(t)$ and $\mathbf{w}(t)$ [53, 54].

This can be reached, for example, through filtering the output error of the observer by

$$\mathbf{r}(t) = \mathrm{W}\mathbf{e}(t) \tag{2.38}$$

together with a special design of the observer feedback H.

c) **Output observers**

Another possibility is the use of output observers (or UIO) in the reconstruction of the output signals, if the estimate of the state variable $\hat{\mathbf{x}}(t)$ is not of primary interest [24]. Through a linear transformation

$$\mathbf{z}(t) = \mathrm{T}\mathbf{x}(t) \tag{2.39}$$

the state-space representation of the observer becomes

$$\hat{\mathbf{z}}(t+1) = \mathrm{F}\hat{\mathbf{z}}(t) + \mathrm{J}\mathbf{u}(t) + \mathrm{G}\mathbf{y}(t) \tag{2.40}$$

and the residual is determined by

$$\mathbf{r}(t) = \mathrm{W}_z\hat{\mathbf{z}}(t) + \mathrm{W}_y\mathbf{y}(t). \tag{2.41}$$

This situation is depicted in Figure (2.12).

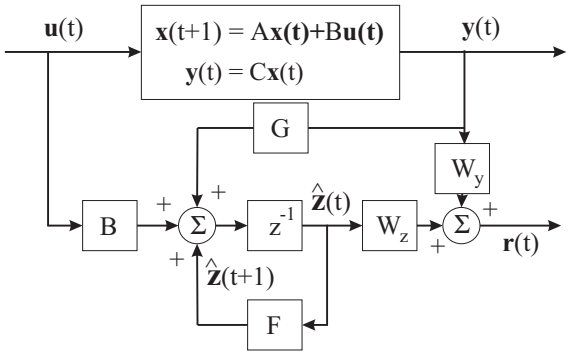

Figure 2.12: Process and output observer.

The state estimation error

$$\mathbf{e}_x(t) = \hat{\mathbf{z}}(t) - \mathbf{z}(t) = \hat{\mathbf{z}}(t) - \mathrm{T}\mathbf{x}(t) \tag{2.42}$$

and the residuals $\mathbf{r}(t)$ are then designed, such that they are independent of the process states $\mathbf{x}(t)$, the known input $\mathbf{u}(t)$ and the unknown inputs $\mathbf{v}(t)$ and $\mathbf{w}(t)$ (see Figure (2.11)). In this way, the residuals are dependent only on additive faults $\mathbf{f}(t)$ [24, 25, 47].

2.6.3 Fault Detection with Parity Equations

A straightforward model-based method of fault detection is to take a model $\frac{\hat{\mathrm{A}}(s)}{\hat{\mathrm{B}}(s)}$ and to run it in parallel to the process described by $\frac{\mathrm{A}(s)}{\mathrm{B}(s)}$, thereby forming an output error

$$\mathbf{r}(s) = \left(\frac{\mathrm{A}(s)}{\mathrm{B}(s)} - \frac{\hat{\mathrm{A}}(s)}{\hat{\mathrm{B}}(s)}\right)\mathbf{u}(s). \tag{2.43}$$

The methodology described is depicted in Figure (2.13(a)).
However, as for observers, the process model parameters have to be known a priori. With reference to Figure (2.3), if $\frac{\hat{\mathrm{A}}(s)}{\hat{\mathrm{B}}(s)} = \frac{\mathrm{A}(s)}{\mathrm{B}(s)}$, for additive input and output faults, the output error then becomes

$$\mathbf{r}(s) = \frac{\mathrm{A}(s)}{\mathrm{B}(s)}\mathbf{f}_u(s) + \mathbf{f}_y(s). \tag{2.44}$$

Another possibility is to generate a polynomial error (Figure (2.13(b)))

$$\begin{aligned} \mathbf{r}(s) &= \hat{\mathrm{A}}(s)\mathbf{y}(s) - \hat{\mathrm{B}}(s)\mathbf{u}(s) \\ &= \mathrm{B}(s)\mathbf{f}_u(s) + \mathrm{A}(s)\mathbf{f}_y(s). \end{aligned} \tag{2.45}$$

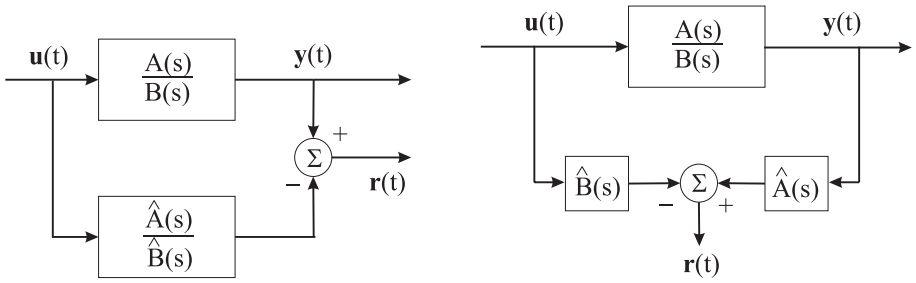

(a) Output error (b) Equation error

Figure 2.13: Parity equation methods.

In both cases, different time responses are obtained for an additive input or output fault. Moreover, $\mathbf{r}(s)$ computed by Equation (2.44) corresponds to the output error of parameter estimation method (see Eq. (2.24)), while $\mathbf{r}(s)$ in Eq. (2.45) concerns the equation error of Eq. (2.18).

Equations (2.44) and (2.45) generate residuals and are called *parity equations* [18]. To generate specific properties, the residuals can be filtered [18, 24, 47]

$$\mathbf{r}_f(s) = G_f \mathbf{r}(s). \tag{2.46}$$

However, for SISO processes only one residual can be generated and it is therefore not easy to distinguish between different faults.

More freedom in the design of parity equations can be obtained if for SISO processes intermediate signals can be measured (2.3), or for MIMO systems. Then a state-space model is appropriate, as shown in [25] for discrete-time models. Given the system

$$\left\{ \begin{array}{lcl} \mathbf{x}(t+1) & = & \mathrm{A}\mathbf{x}(t) + \mathrm{B}\mathbf{u}(t) \\ \mathbf{y}(t) & = & \mathrm{C}\mathbf{x}(t) \end{array} \right. \tag{2.47}$$

by substituting the second of Eqs. (2.47) in the first one and delaying several times, the following system is obtained

$$\begin{bmatrix} \mathbf{y}(t) \\ \mathbf{y}(t+1) \\ \mathbf{y}(t+2) \\ \vdots \end{bmatrix} = \begin{bmatrix} \mathrm{C} \\ \mathrm{CA} \\ \mathrm{CA}^2 \\ \vdots \end{bmatrix} \mathbf{x}(t) + \begin{bmatrix} 0 & 0 & 0 & \dots \\ \mathrm{CB} & 0 & 0 & \dots \\ \mathrm{CAB} & \mathrm{CB} & 0 & \dots \\ \vdots & \vdots & \vdots & \ddots \end{bmatrix} \begin{bmatrix} \mathbf{u}(t) \\ \mathbf{u}(t+1) \\ \mathbf{u}(t+2) \\ \vdots \end{bmatrix} \tag{2.48}$$

$$\mathbf{Y}_f(t) = \mathrm{T}\mathbf{x}(t) + \mathrm{Q}\mathbf{U}_f. \tag{2.49}$$

In order to remove the nonmeasurable states $\mathbf{x}(t)$, Eq. (2.48) is multiplied by W, such that

$$\mathrm{WT} = 0. \tag{2.50}$$

This leads to residuals

$$\mathbf{r}(t) = \mathrm{W}\mathbf{Y}_f - \mathrm{WQ}\mathbf{U}_f(t) \tag{2.51}$$

as shown in Figure (2.14).

The filtered input and output vectors $\mathbf{U}_f$ and $\mathbf{Y}_f$ are obtained by delaying the corresponding signals. The design of the matrix W gives some freedom to generate a structured set of residuals. One possibility is to select the elements of W such that one measured variable has no impact on a specific residual. Then this residual remains small in the case of an additive fault on this variable, and the other residuals increase [47].

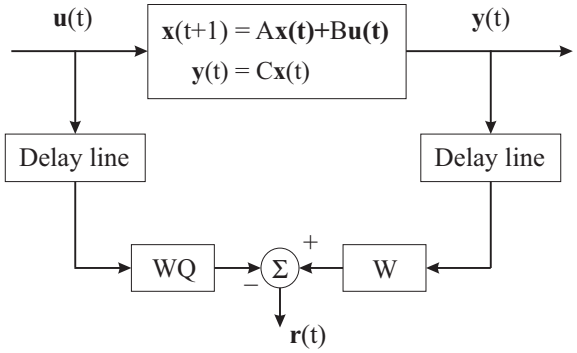

Figure 2.14: Parity equation methods for a MIMO model.

2.7 Change Detection and Symptom Evaluation

Because of the presence of noise, disturbances and other unknown signals acting upon the monitored system, the measured or estimated quantities, such as signals, parameters, state variables or residuals are usually stochastic variables $S_i(t)$, with mean value and variance [6]

$$\bar{S}_i = E\{S_i(t)\}; \qquad \bar{\sigma}_i^2 = E\{[S_i(t) - \bar{S}_i]^2\} \tag{2.52}$$

as normal values for the fault-free process. Analytic symptoms are then obtained as changes

$$\Delta S_i = E\{S_i(t) - \bar{S}_i\}; \qquad \Delta\sigma_i = E\{\sigma_i(t) - \bar{\sigma}_i\} \tag{2.53}$$

with reference to the normal values and $t > t_f$, where t_f is the time instant of fault occurrence.

To separate normal from faulty behavior, usually a fixed threshold

$$\Delta S_{tol} = \epsilon\bar{\sigma}_S, \qquad \epsilon \geq 2 \tag{2.54}$$

has to be selected. By this means, a compromise has to be made between the detection of small faults and false alarms. Methods of change detection, e.g. a likelihood-ration test, Bayes decision, fuzzy or adaptive threshold may improve the binary decision [47].

2.8 Residual Generation Problem

Although the analytical redundancy method for residual generation has been recognized as an effective technique for detecting and isolating faults, the critical problem of unavoidable modeling uncertainty has not been fully solved.

The main problem regarding the reliability of FDI schemes is the modeling uncertainty which is due, for example, to process noise, parameter variations and nonlinearities.

All model-based methods use a model of the monitored system to produce the symptom generator. If the system is not complex and can be described accurately by the mathematical model, FDI is directly performed by using a simple geometrical analysis of residuals.

In real industrial systems however, the modeling uncertainty is unavoidable. The design of an effective and reliable FDI scheme should take into account of the modeling uncertainty with respect to the sensitivity of the faults. Several papers addressed this problem. For example, optimal robust parity relations were proposed [16, 53, 54, 55] and the threshold selector concept was introduced [56]. Robust FDI using the disturbance decoupling technique was also used [24].

The model-based FDI technique requires a high accuracy mathematical description of the monitored system. The better the model represents the dynamic behavior of the system, the better will be the FDI precision. If a FDI method can be developed which is insensitive to modeling uncertainty, a very accurate model is not necessarily needed.

All uncertainties can be are summarized as disturbances acting on the system. Although the disturbance vector is unknown, its distribution matrix can be obtained by an identification procedure. Under this assumption, the "disturbance decoupling" principle can be exploited to design a robust FDI scheme using the UIO [24].

In Chapters 4 and 3 identification tools to improve the design of a robust residual generator will be shown.

2.9 Fuzzy Logic and Neural Networks in FDI

Classical FDI model-based methods of FDD use static and dynamic models of the process. Faults are supposed to appear as state changes caused by malfunctions of the components as well as of the sensors. Such fault indices are often monitored using estimation techniques. The main problem with these techniques is that the precision of the process model affects the accuracy of the detection and isolation system as well as the diagnostic sensibility.

Rule-based expert systems have been also investigated very intensively for fault detection and diagnosis problems [23, 47, 57, 58]. Fault diagnosis using rule-based system needs a database of rules and the accuracy of diagnosis depend on the rules. Moreover, creating a rich and detailed database of rules is usually a time-consuming task and many process experts are needed.

On the other hand, the majority of real industrial processes are nonlinear [24, 25, 59] and cannot be modeled by using a single model for all operating conditions. Since a mathematical model is a description of system behavior, accurate modeling for a complex nonlinear system is very difficult to achieve in practice. Sometime for some nonlinear systems, it can be impossible to describe them by analytical equations. Instead of exploiting complicated nonlinear models obtained by modeling techniques, it is also possible to describe the plant by a collection of local affine fuzzy and non-fuzzy models [60, 61], whose parameters are obtained by identification procedures.

When the process model is only known to a certain extent of precision, pattern recognition methods provide a convenient approach to solve the fault diagnosis problem [9, 22]. In recent years, neural networks (NN) have been used successfully in pattern recognition as well as system identification, and they have been proposed as a possible technique for fault diagnosis, too. NN can handle nonlinear behavior and partially known process because they learn the diagnostic

requirements by means of the information of the training data. NN are noise tolerant and their ability to generalize the knowledge as well as to adapt during use are extremely interesting properties [62, 63, 64, 65, 66].

Some example processes were considered in which FDI was performed by a NN using input and output measurements. In these works the NN is trained to identify the fault from measurement patterns, however the classification of individual measurement pattern is not always unique in dynamic situations, therefore the straightforward use of NN in fault diagnosis of dynamic plant is not practical and other approaches should be investigated.

A NN could be exploited in order to find a dynamic model of the monitored system or connections from faults to residuals. In the latter case, the NN is used as pattern classifier or nonlinear function approximator. In fact, artificial neural networks are capable of approximating a large class of functions, for fault diagnosis of an industrial plant.

In this thesis, in Chapter 4, the identification of fuzzy and non-fuzzy models for the system under diagnosis as well as the application of NN as function approximator will be shown.

2.10 Summary

This chapter has presented a tutorial treatment on the basis principles of model-based FDI.

The FDI problem has been formalized in a uniform framework by presenting mathematical description and definition. Within this framework, the residual generation has been identified as a central issue in model-based FDI.

The residual generator has been summarized in different residual generation structures. The ways of designing residuals for isolation have also been discussed.

The success of fault diagnosis depends on the quality of the residuals. Other FDI methods such as fuzzy logic and qualitative modelling have been briefly discussed.

Applications of the presented FDI techniques will be shown in in Chapters 4 and 5.

Chapter 3

System Identification for Fault Diagnosis

3.1 Introduction

The problem of identifying an unknown system given samples of its behavior is well-known [33, 43, 67] to be ill-posed in the sense of Hadamard [68], as its solution is neither unique nor depends continuously on the given data.

When a priori knowledge on the characteristics of the unknown system is available, the identification procedure can be enhanced. This knowledge may act as a set of constraints shaping the space of models so that identification in this new space is a more tractable problem. As an example, the regularity of the unknown system can be translated into smoothness constraints of some kind, transforming the identification problem into a minimization problem [69, 70].

This point of view can be successfully applied to estimate algebraic and dynamic affine systems from noisy samples, by assuming certain good properties of the noise and of the sampling process [42, 71].

The identification method described in this chapter starts from the results on algebraic case with the purpose of showing the possibility of extending the Frisch scheme [41] to dynamic systems determining the whole family of models compatible with noisy sequences.

A frequency approach for EIV models and its application to the dynamic Frisch scheme identification in still in development [72, 73, 74].

This chapter also addresses the problem of the identification of both linear and nonlinear dynamic systems. In the case of nonlinear nonlinear systems the identification will be performed by exploiting affine, piecewise affine and fuzzy structure. The so-called Frisch scheme procedure is exploited to estimate these models from noisy data.

3.2 The Frisch Scheme in the Algebraic Case

The finite sequence of n variables x_1, x_2, $\cdots$, x_n observed at N different times with $N > n$ is considered. If linear relations exist among these variables, they are described by models of the type

$$a_1 x_1 + a_2 x_2 + \cdots + a_n x_n = 0. \tag{3.1}$$

If X is the $(N \times n)$ matrix storing the previous measures, models (3.1) are described by the columns of a matrix A such that

$$\mathrm{XA} = 0 \tag{3.2}$$

or, equivalently

$$\mathrm{X}^T\mathrm{XA} = 0 \tag{3.3}$$

where $\Sigma = \mathrm{X}^T\mathrm{X}$ is the sample covariance matrix, under a zero-mean assumption for all variables.

When the data are corrupted by noise then the rank$[\Sigma] = n$, so that no relation can be obtained unless the data are modified. In the Frisch scheme, the following assumptions are added:

1. all variables are treated symmetrically and each variable is affected by an unknown amount of additive noise;

2. each noise component is independent of every other noise component and of every variable. Under these conditions, each variable x_i, with $i = 1, \cdots, n$, is defined as

$$x_i = x_i^* + \tilde{x}_i \tag{3.4}$$

where the unknown terms x_i^* are the true value of the i-th variable whilst $\tilde{x}_i$, the additive noises on this variable.

The problem of determining the true data from the available noisy sequences can thus be formulated as follows.

Problem 1. *Given an $(n \times n)$ symmetric positive definite covariance matrix Σ, find all diagonal matrices $\tilde{\Sigma}$ with non-negative elements elements such that $\Sigma^* = \Sigma - \tilde{\Sigma} \geq 0$.*

In this context, the solution of the problem is not univocally definite. The rank of Σ^* may change by varying $\tilde{\Sigma}$, which models the noise and, consequently, the same set of data may be linked by different numbers of linear relations. Even if it does not happen, the problem has infinite solutions; the rank of Σ^*, for instance, is always equal to $(n-1)$ if and only if Σ^{-1} can be reduced to a matrix with strictly positive entries by the transformation $\mathrm{L}\Sigma^{-1}\mathrm{L}$ with $\mathrm{L} = \mathrm{diag}[\pm 1]$. The solution set is the convex simplex the n vertices of which are the least-squares solutions which can be found assuming that one variable is noisy and all others are noise-free [44].

Before solving Problem 1, the following theorem can be considered [44].

Theorem 1. *Given the $(n \times n)$ symmetric positive definite covariance matrix Σ, the maximal variance of the additive noise on the i-th variable, when all others are noise-free, is computed by*

$$\tilde{\sigma}_i = \frac{det[\Sigma]}{det[\Sigma_i]} \tag{3.5}$$

where Σ_i is obtained from Σ by deleting its i-th row and column.

Every allowable noise covariance matrix $\tilde{\Sigma}$ (i.e. such that $\Sigma^* = \Sigma - \tilde{\Sigma} \geq 0$) defines a point $(\sigma_1, \cdots, \sigma_n)$ belonging to the first orthant of the noise space $\Re^n$, which is mapped into one and only one point $(a_1, \cdots, a_n)$ of the solution space $\Re^n$. Moreover, the following result can be proved [44].

Theorem 2. *The solution set defined by all points* $(\sigma_1, \cdots, \sigma_n)$ *defined by the matrix set* $\tilde{\Sigma}$ *is a convex hypersurface belonging to the first orthant of the noise space the section of which, with a plane parallel to a coordinate one, is a hyperbola segment.*

Note that if noise values, corresponding to a rank of Σ^* lower than $n-1$, exist, they belong to the hypersurface defined by Theorem 2. In these conditions, in the parameter space, the solution set might be a collection of convex polyhedral sets lying in the orthants.

The hypersurface defined by Theorem 2 partitions the first orthant of the noise space into two regions. The points over the hypersurface correspond to non-definite matrices Σ^*, those under the hypersurface to positive definite matrices.

3.3 The Frisch Scheme in the Dynamic Case

Let us consider a finite sequence of the variables $u_1(\cdot)$, $\cdots$, $u_r(\cdot)$, $y(\cdot)$ observed with a constant sampling interval. If dynamic linear relations exist among these variables, they can be described by models of the type

$$y^*(t+n) = \sum_{i=0}^{n-1} \alpha_i y^*(t+i) + \sum_{i=0}^{n-1} \sum_{j=1}^{r} \beta_{ij} u_j^*(t+i) \tag{3.6}$$

which represent linear MISO discrete-time systems whose order is n and whose parameters are α_i and β_{ij}.

At first, the following problem is considered.

Problem 2 (realization). *Given a noiseless input–output sequence* $u_1^*(\cdot)$, $\cdots$, $u_r^*(\cdot)$, $y^*(\cdot)$ *generated by a system of type (3.6), determine the order* n *and the parameters* α_i, β_{ij} *of the system.*

The following vectors and matrices are thus defined

$$u_j^{*N}(t+k) = \left[\begin{array}{cccc} u_j^*(t+k) & \dots & u_j^*(t+k+N-1) \end{array} \right]^T \tag{3.7}$$

$$y^{*N}(t+k) = \left[\begin{array}{cccc} y^*(t+k) & \dots & y^*(t+k+N-1) \end{array} \right]^T \tag{3.8}$$

$$X_k(u_j^*) = \left[\begin{array}{cccc} u_j^{*N}(t) & \dots & u_j^{*N}(t+k-2) \end{array} \right] \tag{3.9}$$

$$X_k(y^*) = \left[\begin{array}{cccc} y^{*N}(t) & \dots & y^{*N}(t+k-1) \end{array} \right] \tag{3.10}$$

$$\Sigma_k^*(u_j^* u_j^*) = X_k^T(u_j^*) X_k(u_j^*) \tag{3.11}$$

$$\Sigma_k^*(y^* y^*) = X_k^T(y^*) X_k(y^*) \tag{3.12}$$

$$\Sigma_k^*(y^* u_j^*) = X_k^T(y^*) X_k(u_j^*) = \Sigma_k^{*T}(u_j^* y^*) \tag{3.13}$$

where N is assumed large enough to solve the problem considered.

Let us partition now the matrix Σ_k^* as follows

$$\Sigma_k^* = \left[\begin{array}{cccc} \Sigma_k^*(y^*y^*) & \Sigma_k^*(y^*u_1^*) & \dots & \Sigma_k^*(y^*u_r^*) \\ \Sigma_k^*(u_1^*y^*) & \Sigma_k^*(u_1^*u_1^*) & \dots & \Sigma_k^*(u_r^*y^*) \\ \vdots & \vdots & \ddots & \vdots \\ \Sigma_k^*(u_r^*y^*) & \Sigma_k^*(u_r^*u_1^*) & \dots & \Sigma_k^*(u_r^*u_r^*). \end{array} \right]. \tag{3.14}$$

To solve the realization problem it is possible to consider the sequence of increasing–dimension matrices

$$\Sigma_2^*, \quad \Sigma_3^*, \quad \dots \quad \Sigma_k^*, \quad \dots \tag{3.15}$$

testing their singularity. As soon as a singular matrix Σ_k^* is found then $n = k - 1$ and the parameters $\alpha_0, \dots, \alpha_{n-1}, \beta_{0j}, \dots, \beta_{(n-1)j}$ $(j = 1, \dots, r)$ describe the dependence relationship of the $(n+1)$-th vector of Σ_{n+1}^* on the remaining ones.

In Problem 2 it has been assumed that N is large enough to avoid unwanted linear dependence relationships due to limitations in the dimension of the involved vector spaces; this means $N \geq (r+1)n + 1$. If a lower number of samples is available then only a partial realization problem can be solved.

In the noisy case the following identification problem can be proposed.

Problem 3 (identification). *Given a noisy input-output sequence $u_1(\cdot)$, ..., $u_r(\cdot)$, $y(\cdot)$ univocally determine, if possible, the order n and the parameters α_i, β_{ij} of a model (3.6) of the system which has generated the noiseless sequences $u_1^*(\cdot)$, ..., $u_r^*(\cdot)$, $y^*(\cdot)$.*

Note that in the presence of noise, the procedure described for the solution of Problem 2 would obviously be useless since matrices Σ_k^* would always be non-singular. In the Frisch scheme it is normally assumed that

$$\begin{array}{rcll} u_j(t) & = & u_j^*(t) + \tilde{u}_j(t), & j = 1, \dots, r \\ y(t) & = & y^*(t) + \tilde{y}(t) & \end{array} \tag{3.16}$$

where every noise term $\tilde{u}_j(t)$, $\tilde{y}(t)$ is independent of every other term and only $u_j(t)$ and $y(t)$ are known. Without loss of generality, all the variables may be assumed as having null mean value. Consequently the generic positive definite matrix Σ_k associated with the input-output noise-corrupted sequences may always be expressed as the sum of two terms $\Sigma_k = \Sigma_k^* + \tilde{\Sigma}_k$ where

$$\tilde{\Sigma}_k = \mathrm{diag}[\tilde{\sigma}_y I_k, \tilde{\sigma}_{u_1} I_{k-1}, \dots, \tilde{\sigma}_{u_r} I_{k-1}] \geq 0 \tag{3.17}$$

since no correlation has been assumed among the noise samples at different times. This condition is verified for additive white noise with variance $\tilde{\sigma}_y$ and $\tilde{\sigma}_{u_j}$ on the input-output sequences.

Problem 4. *Given a sequence of increasing–dimension $\Big(\big((r+1)k-r\big) \times \big((r+1)k-r\big)\Big)$ symmetric positive definite covariance matrices*

$$\Sigma_2, \quad \Sigma_3, \quad \dots \quad \Sigma_k, \quad \dots \tag{3.18}$$

find, for each k, all diagonal non-negative definite matrices

$$\tilde{\Sigma}_k = diag[\tilde{\sigma}_y I_k, \tilde{\sigma}_{u_1} I_{k-1}, \dots, \tilde{\sigma}_{u_r} I_{k-1}] \tag{3.19}$$

such that

$$\Sigma_k^* = \Sigma_k - diag[\tilde{\sigma}_y I_k, \tilde{\sigma}_{u_1} I_{k-1}, \dots, \tilde{\sigma}_{u_r} I_{k-1}] \geq 0 \ . \tag{3.20}$$

It is worth observing now that, unlike the algebraic case, for each k the noise space is always $\Re_+^{(r+1)}$, while the parameter space is $\Re^{(r+1)k-r}$.

It can be noted that for each k the solution set of relation (3.20) describes, in the first orthant of the $(\tilde{\sigma}_y, \tilde{\sigma}_{u_1}, \dots, \tilde{\sigma}_{u_r})$ hyperplane, a hypersurface whose concavity faces the origin [44].

In the noise space, the $(r+1)$ solutions $(\tilde{\sigma}_y, 0, \tilde{\sigma}_{u_2}, \dots, \tilde{\sigma}_{u_r})$, $(\tilde{\sigma}_y, \tilde{\sigma}_{u_1}, 0, \dots, \tilde{\sigma}_{u_r})$, $\cdots$, $(\tilde{\sigma}_y, \tilde{\sigma}_{u_1}, \dots, \tilde{\sigma}_{u_{r-1}}, 0)$ correspond to the limit case of noise affecting only the output or the input sequences. This case can be considered as the natural extension to the dynamic case of the computation of least-square solutions.

Previous results hold for every value of k. Since determination of the system order requires the increasing values of k to be tested, it is relevant to analyze the behavior of the associated curves when k varies. This corresponds to a comparison of the admissible solution sets for different model orders. In this context the following result can be proved [44].

Theorem 3. *The solution sets of condition (3.20) for different values of k are non-crossing curves.*

It is also important to observe that, since it is assumes that a system (3.6) has generated the noiseless data, for $k > n$ all the hyper-surfaces of type (3.20) have necessarily at least one common point, i.e. point $(\tilde{\sigma}_{y^*}, \tilde{\sigma}_{u_1^*}, \dots, \tilde{\sigma}_{u_r^*})$ corresponding to the true variances $\tilde{\sigma}_{y^*}$ and $\tilde{\sigma}_{u_j^*}$ of the noise affecting the output and the inputs of the system. The search for a solution for the identification problem can thus start from the determination in the noise space of this point. The following considerations can now be stated.

With reference to the diagonal non-negative definite matrices

$$\tilde{\Sigma}_k = \mathrm{diag}[\tilde{\sigma}_{y^*} I_k, \tilde{\sigma}_{u_1^*} I_{k-1}, \dots, \tilde{\sigma}_{u_r^*} I_{k-1}] \tag{3.21}$$

the following properties hold:

- If $k \leq n$, the matrices Σ_k^* are positive definite.
- If $k > n$, the dimension of the null space of Σ_k^* and, consequently, the multiplicity of its least eigenvalue, is equal to $(k-n)$.
- For $k = (n+1)$, matrix Σ_k^* is characterized by a linear dependence relation among its $(r+1)k - r$ vectors and the coefficients which link the k-th vector of Σ_k^* to the remaining ones are the parameters α_i, β_{ij}, with $i = 0, \dots, n-1$ and $j = 1, \dots, r$, of the system (3.6) which has generated the noiseless sequences.
- For $k > (n+1)$, all linear dependence relations among the vectors of the matrix Σ_k^* are characterized by the same $(r+1)n$ coefficients α_i, β_{ij}.

As an example, Figure (3.1) shows the above properties for a second order ($n = 2$) SISO dynamic system. The point marked by a circle corresponds to the input-output noise variances $\tilde{\sigma}_{y^*}$ and $\tilde{\sigma}_{u^*}$ affecting the measurements.
It is worthy to note how this approach cannot be applied immediately to the identification of real processes, since the hypotheses on the linearity, finite dimensionality and time independence of the system and on the additivity and whiteness of the noise are not usually verified, so that the hyper-surfaces (3.20) have no common point for $k > n$. The definition of a suitable criterion of model selection in such cases was suggested in [75].

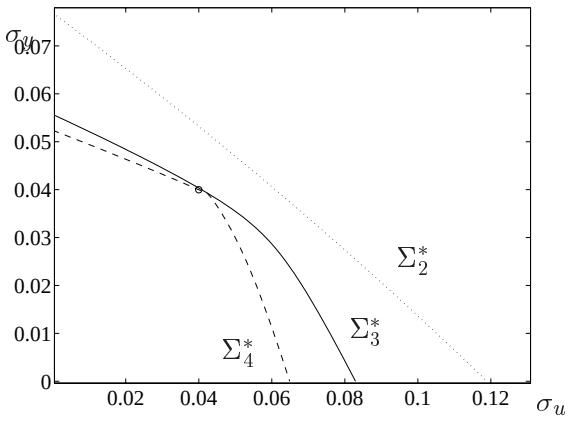

Figure 3.1: Singularity surfaces in the noisy space.

3.4 The Frisch Scheme in the MIMO Case

Multivariable system can be represented by means of canonical models of the type

$$y_i^*(t+\nu_i) = \sum_{j=1}^{m} \sum_{k=0}^{\nu_{ij}-1} \alpha_{ijk} y^*(t+k) + \sum_{j=1}^{r} \sum_{k=0}^{\nu_i-1} \beta_{ijk} u_j^*(t+k) \tag{3.22}$$

where $i = 1, \cdots, m$. r and m are the number of inputs and outputs of the system, respectively [76]. The indices $\nu_{ij} - 1$ satisfy the following relations:

$$\begin{array}{ll} \nu_{ij} = \nu_i & \text{for } i = j \\ \nu_{ij} = \min(\nu_i + 1, \nu_j) & \text{for } i > j \\ \nu_{ij} = \min(\nu_i, \nu_j) & \text{for } i < j. \end{array} \tag{3.23}$$

Model (3.22) decomposes the system into m interconnected subsystems the orders of which are given by the integers ν_i. Such integers completely define the system structure and are coincident with the Kronecker observability invariants of any realization of the system.

Given the sequences $y_i(t)$ $(i = 1, \cdots, m)$ and $u_j(t)$ $(j = 1, \cdots, r)$ generated by the system of the type (3.22), the identification problem consists in univocally determining both the *structure*, i.e. the set of integers ν_1, $\cdots$, ν_m, as well as the characteristic *parameters* α_{ijk} and β_{ijk} of the model (3.22) [76].

The solution of the identification problem is described by Guidorzi in [76] with reference to canonical models, but can easily be generalised to multistructural (overlapping) models.

Advantages associated to the use of these identified models with reference to FDI concern the minimal parametrisation [50], reduced storage, computing time and high efficiency of the related algorithms.

The techniques and properties for MISO systems identification presented in Section 3.3 can be generalised for the MIMO case. Because of these properties, it is possible to conclude that if, starting from a certain structure, the hypersurfaces associated to increasing dimension covariace matrices have only a common point in the noise space, then this point represent the variances

of the noise affecting the input-output sequences. If the noise variances can thus be univocally determined, the identification problem can be reduced to a realization one and a canonical model of the system can be obtained.

From a computational point of view, it can be noted that the search for the noise variances is made in an $(m+r)$-dimensional space and may, therefore, be time expensive. The results given in Section 3.3 and extended to the MIMO case do not exclude the possibility that the previously considered hypersurfaces may be coincident and consequently that non-unique solution exists.

Concluding, it can be stated that no conceptual differences exist between the application of the Frisch scheme to the identification of SISO and MIMO dynamic systems.

3.5 Identification of Nonlinear Dynamic Systems

Industrial processes are nonlinear and cannot be modeled by using a single affine model for all operating conditions. Instead of exploiting complicated nonlinear models obtained by modeling techniques, it is also possible to describe the plant by a collection of affine models. Each submodel approximates the system locally around an operating point and a selection procedure determines which particular submodel has to be used. Such a multimodel structure will be called *multiple model* approach [60]. At each operating point, the behavior of the multiple model is described by a local affine dynamic model.

In this section, the nonlinear dynamic systems will be assumed piecewise affine on the same region of the model so to explore the problem of noise rejection under the same assumption as in the affine theory [42, 43]. Such a multiple model is piecewise affine with non-smooth boundary transition. In order to ensure a smooth transition between models, continuity contraints among local affine models have to be forced. In this context, such a problem will be solved by using an optimization technique.

The contruction of the multiple model from only one set of global input-output measurements is a non-trivial problem since the model structure, a switching function and the local model parameters have to be identified.

In a first stage, the method proposed requires the knowledge of the operating-point regions and of the expected number of local models. Under this assumption, the identification of the structure and of the parameters of each local model can be performed [44].

The contribution of this identification tool is two fold. First, it is shown how to integrate the well-established Frisch scheme method for the identification of affine algebraic systems within a general procedure for nonlinear dynamic system. Second, some interesting properties of such a Scheme can enhance the solution of the optimization problem as well as of the continuity contraint fulfillment.

In the remainder of this chapter, the structure of the multiple model and the identification scheme used to estimate each local affine dynamic model from input–output noisy sequences will be presented. The extension of such theory to the multiple model case and to the analysis of the continuity constraints is also shown. Under the assumption of the Frisch scheme, some conditions ensure that a unique solution exists in the model space. On the other hand, when the Frisch scheme requirements are relaxed, the global identification problem can be transformed into an optimization problem. The presented technique shows how the properties of the Frisch Scheme solutions may simplify the computation of such a problem.

3.6 Multiple Model Structure

The main idea underlying the use of multiple model approach for the modeling of nonlinear dynamic systems is based on the interpretation of a nonlinear regression model. For simplicity, a discrete-time nonlinear SISO model in the following form is considered

$$y(t+n) = F\big(y(t+n-1), \cdots, y(t), u(t+n-1), \cdots, u(t)\big) \tag{3.24}$$

where $y(t+n-1), \cdots, y(t)$ and $u(t+n-1), \cdots, u(t)$ are lagged outputs and inputs of the model, respectively, n is the model order and $F(\cdot)$ a static nonlinear function. In the product space of the model inputs and outputs, the nonlinear mapping $F(\cdot)$ defines a hypersurface in a $\Re^{2n+1}$ subspace. If a sufficient number of samples is acquired, the identification of the nonlinear system can be regarded as an approximation of this hypersurface. In case of multiple model approach, a local approximation of this hypersurface is performed by using affine dynamic models. The operating point is described by all the lagged inputs and output $y(t+n-1), \cdots, y(t)$ and $u(t+n-1), \cdots, u(t)$ which can be collected into a vector $\mathbf{x}(t) = [y(t+n-1), \cdots, y(t), u(t+n-1), \cdots, u(t)]^T$. By using the knowledge of the operating point vector $\mathbf{x}(t)$, the domain $\mathbb{D}$ of the function $F(\cdot)$, with $\mathbb{D} \subset \Re^{2n}$, is divided into a number M of regions R_i in which the local submodels are valid.

The output $y(t+n)$ of the nonlinear dynamic system $F : \Re^{2n} \to \Re$ can be approximated by the multiple model $f(\cdot)$ in the form

$$f\big(\mathbf{x}(t)\big) = \sum_{i=1}^{M} \chi_i\big(\mathbf{x}(t)\big)\,[1, \mathbf{x}^T]\ \mathbf{a}^{(i)} \tag{3.25}$$

where $\mathbf{a}^{(i)} = [a_0^{(i)}, a_1^{(i)}, \ldots, a_{2n}^{(i)}]^T$ are parameter vector and $\mathbb{D}$ is partitioned in M regions $R_1, \ldots, R_M$ such that $\chi_i\big(\mathbf{x}(t)\big) = 1$ if $\mathbf{x}(t) \in R_i$, otherwise $\chi_i\big(\mathbf{x}(t)\big) = 0$. The model is affine in each R_i being $[1, \mathbf{x}^T]\ \mathbf{a}^{(i)}$ the local affine dynamic model.

Since the transitions between the regions should be gradual than abrupt, f is forced to be continuous over the whole $\mathbb{D}$. In such a case, the parameter vectors are constrained to satisfy certain relations stemming from the equality of left and right limits in boundary points common to different regions. Namely, let $\mathbf{x}_0$ be an operating point of both $R_{i'}$ and $R_{i''}$. The model f is continuous only if:

$$\lim_{\substack{\mathbf{x}(t)\to\mathbf{x}_0 \\ \mathbf{x}(t)\in R_{i'}}} f\big(\mathbf{x}(t)\big) = \lim_{\substack{\mathbf{x}(t)\to\mathbf{x}_0 \\ \mathbf{x}(t)\in R_{i''}}} f\big(\mathbf{x}(t)\big) \tag{3.26}$$

i.e. if

$$[1, \mathbf{x}_0^T]\ \mathbf{a}^{(i')} = [1, \mathbf{x}_0^T]\ \mathbf{a}^{(i'')} \tag{3.27}$$

The straightforward application of Equation (3.27) to all the accumulation points common to two neighboring regions leads to an infinite number of constraints. Yet, the following theorem shows that the adoption of regions with straight borders guarantees that only a finite number of them is linearly independent.

Theorem 4. *Let $\mathcal{B}_{i',i''}$ be the set of all the accumulation points common to two neighboring regions $R_{i'}$ and $R_{i''}$. If $\mathcal{B}_{i',i''}$ is convex, and p points $\mathbf{z}_1, \ldots, \mathbf{z}_p \in \mathcal{B}_{i',i''}$ exist for which (3.27) is satisfied, then (3.27) is also satisfied by any point of their convex hull.*

Proof. If $\mathbf{x}$ belongs to the convex hull of $\mathbf{z}_1, \ldots, \mathbf{z}_p$ then p non negative scalars $\alpha_1, \ldots, \alpha_p$ exist such that

$$\sum_{k=1}^{p} \alpha_k = 1 \tag{3.28}$$

and

$$\mathbf{x} = \sum_{k=1}^{p} \alpha_k \mathbf{z}_k. \tag{3.29}$$

Then the continuity constraints $[1\ \mathbf{z}_k^T]\mathbf{a}^{(i')} - [1\ \mathbf{z}_k^T]\mathbf{a}^{(i'')} = 0$ for $k = 1, 2, \ldots, p$, can be combined by means of (3.29) and (3.28) to obtain the thesis. □

Theorem 4 suggests that regions whose boundary are convex polyhedra should be favored. In that case, in fact, continuity can be ensured simply setting the value of the local models only on the vertices of the boundaries. As an l-dimensional local affine model can be forced to assume a certain value in at most $l+1$ affinely independent points, it is surely convenient to triangulate $\mathbb{D}$, i.e. partition it into l-dimensional simplexes. In particular, it will be assumed that the triangulation is such that two simplexes are either disjoint, or have a whole k-dimensional face in common (with $k = 0, 1, \ldots, l-1$).

With this we may compound the finite number of continuity constraints (one for each simplex vertex) in a finite matrix C such that the overall model is continuous if and only if

$$\mathrm{C} \begin{bmatrix} \mathbf{a}^{(1)} \\ \vdots \\ \mathbf{a}^{(M)} \end{bmatrix} = \mathbf{0}. \tag{3.30}$$

3.7 Multiple Model Identification

For each region R_i with $\mathbf{x}(t) \in R_i$, the set $,\ {}_k^{(i)}$ of all admissible noise variance matrices $\tilde{\Sigma}_k^{(i)}$, i.e. those making $\Sigma_k^{(i)} - \tilde{\Sigma}_k^{(i)}$ positive semidefinite, can be defined.

For a SISO model, in an two-dimensional space having σ_u and σ_y as coordinates, according to Section (3.3), $,\ {}_k^{(i)}$ is a convex hypersurface belonging to first orthant.

If the noise characteristics are common to all the regions R_i, as the physical nature of the process generating the noise is independent of the model structure and of the operating point conditions (i.e. the partition of $\mathbb{D}$ into regions) and all assumptions regarding the Frisch Scheme are fulfilled, for all the regions a common noise matrix $\tilde{\Sigma}_k$ exists which must satisfy:

$$\tilde{\Sigma}_k \in \bigcap_{i=1}^{M} ,\ {}_k^{(i)} \tag{3.31}$$

In these circumstances the right-hand side of (3.31) degenerates to a single point in the noise space. Therefore univocal identification of noise and its complete rejection is allowed.

Existence conditions of an unique common noise matrix (3.31) for all the regions can be found in the following theorem.

Theorem 5. *Let $\Sigma_j^{(i)}$ be obtained from $\Sigma^{(i)}$ deleting its $j-$th row and column. If for any j', j'' there are two indices i', i'' such that*

$$\left(\det(\Sigma_{j'}^{(i')}) - \det(\Sigma_{j'}^{(i'')})\right)\left(\det(\Sigma_{j''}^{(i')}) - \det(\Sigma_{j''}^{(i'')})\right) \leq 0 \tag{3.32}$$

and $M > m$ then the right-hand side of (3.31) degenerates into a single point.

Proof. Multiplying (3.32) by $\det(\Sigma^{(i')})\det(\Sigma^{(i'')})$ and dividing it by $\det(\Sigma_{j'}^{(i')})\det(\Sigma_{j'}^{(i'')})\det(\Sigma_{j''}^{(i')})$ $\det(\Sigma_{j''}^{(i'')})$, we obtain

$$\left(\frac{\det(\Sigma^{(i')})}{\det(\Sigma_{j'}^{(i')})} - \frac{\det(\Sigma^{(i')})}{\det(\Sigma_{j''}^{(i')})}\right)\left(\frac{\det(\Sigma^{(i'')})}{\det(\Sigma_{j'}^{(i'')})} - \frac{\det(\Sigma^{(i'')})}{\det(\Sigma_{j''}^{(i'')})}\right) \leq 0 \tag{3.33}$$

From Theorem 1 in [44] it follows that $\frac{\det(\Sigma^{(i)})}{\det(\Sigma_j^{(i)})}$ is the intersection of $\mathcal{, }^{(i)}$ with the $j-$th axis of the noise space. Thus the intersection of $\mathcal{, }^{(i')}$ and $\mathcal{, }^{(i'')}$ with the plane defined by the two axes j' and j'' are of the kind reported in the Figure 3.2 where the continuity and convexity of the $\mathcal{, }^{(i)}$ surface allow for just a single common point.

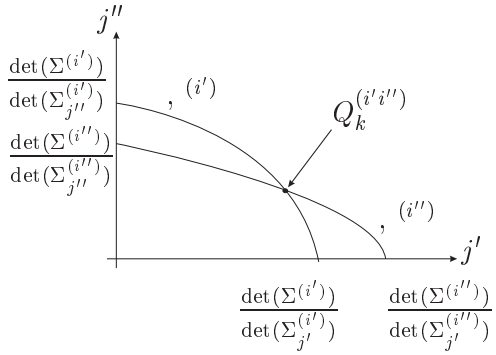

Figure 3.2: An example of $\mathcal{, }^{(i')}$ and $\mathcal{, }^{(i'')}$ surfaces

Yet, if (3.32) holds, then for any other axis j either

$$\left(\det(\Sigma_{j}^{(i')}) - \det(\Sigma_{j}^{(i'')})\right)\left(\det(\Sigma_{j'}^{(i')}) - \det(\Sigma_{j'}^{(i'')})\right) \leq 0$$

or

$$\left(\det(\Sigma_{j}^{(i')}) - \det(\Sigma_{j}^{(i'')})\right)\left(\det(\Sigma_{j''}^{(i')}) - \det(\Sigma_{j''}^{(i'')})\right) \leq 0$$

so that we can ensure that $\mathcal{, }^{(i')}$ and $\mathcal{, }^{(i'')}$ have at least m points in common each on a different coordinate plane. Let us indicate with $Q_1^{(i'i'')}, \ldots, Q_m^{(i'i'')}$ these intersections.

Note now that each $\mathcal{, }^{(i)}$ is included in set of the zeros of $\det(\Sigma^{(i)} - \tilde{\Sigma})$ which is an $(m+1)-$linear function of the noise variances. Thus $\mathcal{, }^{(i')} \cap \mathcal{, }^{(i'')}$ is an $(m-1)-$dimensional hypersurface parametrized by means of m non-linear functions $0 \leq \eta_k^{(i'i'')}(t_1, \ldots, t_{m-1}) \leq 1$,

$t_1, \dots, t_{m-1} \in [0,1]$, such that $\eta_1^{(i'i'')}(1,0,\dots,0) = 1$ while $\eta_k^{(i'i'')}(1,0,\dots,0) = 0$ for $k \neq 1$, $\eta_2^{(i'i'')}(0,1,\dots,0) = 1$ while $\eta_k^{(i'i'')}(0,1,\dots,0) = 0$ for $k \neq 2$ etc.

This parameterization allows to express any point $P \in , ^{(i')} \cap , ^{(i'')}$ as

$$P = \sum_{k=1}^{m} Q_k^{(i'i'')} \eta_k^{(i'i'')}(t_1, \dots, t_{m-1})$$

where the convexity of each $, ^{(i)}$ makes each $\eta^{(i'i'')}$ monotonic and $\sum_{k=1}^{m} \eta_k^{(i'i'')} \geq 1$.

Since (3.32) holds for any couple of axes we may find a set of $m+1$ pairs (i', i'') such that the corresponding set of points $Q^{(i'i'')}$ have at least two elements on different coordinate planes.

The intersection of all the corresponding $, ^{(i)}$ cannot contain more than one point. As the same intersection cannot vanish the right-hand side of (3.31) degenerate to that single point. □

Under these assumptions, as an example, the singularity hypersurfaces regarding two regions R_i and R_j for two different second order local models are depicted in Figure (3.3). The hypersurfaces share the common point $(\tilde{\sigma}_{y^*}, \tilde{\sigma}_{u^*})$ representing the variances of the noises which affect the data.

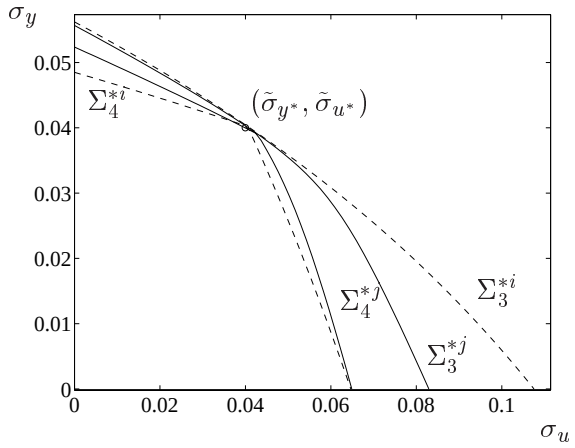

Figure 3.3: An example of singularity surfaces in two regions R_i and R_j.

The structure k and the parameters $\mathbf{a}^{(i)}$ (with $i = 1, \cdots, M$) of each local dynamic model can be identified by the following equation

$$(\Sigma^{(i)}{}_k - \tilde{\Sigma}_k)\mathbf{a}^{(i)} = \mathbf{0}. \tag{3.34}$$

It is worthy to note how this approach cannot be applied immediately in the identification of real processes, even if the Frisch Scheme hypotheses still hold, since exact matching of the noise characteristics from region to region cannot be assumed. The hypersurface intersection in the right side of (3.31) degenerates in an empty set so that a common noise matrix $\tilde{\Sigma}_k$ cannot be found.

Yet, a set of points $\tilde{\Sigma}^{(1)}_{k_1} \in , {}^{(1)}_{k_1}, \ldots, \tilde{\Sigma}^{(M)}_{k_M} \in , {}^{(M)}_{k_M}$ exists each of them very near to the others. To find them we need to solve the optimization problem

$$\begin{aligned} J = \min_{\tilde{\Sigma}_k} \quad & \sum_{i=1}^{M} \Big(\|\lambda_{min}\big(\Sigma^{*(i)}_k\big)\| + \|\lambda_{min}\big(\Sigma^{*(i)}_{(k+1)}\big)\| \Big), \\ \text{s.t.} \quad & C\ \mathrm{A} = \mathbf{0}, \\ \text{with} \quad & (\Sigma^{(i)}_k - \tilde{\Sigma}^{(i)}_k)\mathbf{a}^{(i)} = \mathbf{0}. \end{aligned} \tag{3.35}$$

where $\mathrm{A} = [{\mathbf{a}^{(1)}}^T, \ldots, {\mathbf{a}^{(M)}}^T]^T$ while $\lambda_{min}(\cdot)$ represents the minimal eigenvalue of the matrices $\Sigma^{*(i)}_k$ and $\Sigma^{*(i)}_{(k+1)}$. An example of such a situation is depicted in Figure (3.4). The common noise point (marked with a circle) among singularity surfaces is lost.

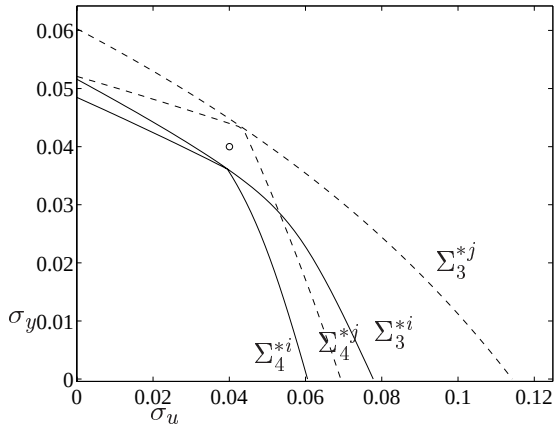

Figure 3.4: Singularity surfaces in two regions R_i and R_j with non-stationary noise.

The described procedure requires the computation of the minimum of the sums of the absolute value of the minimum eigenvalues of two increasing order hypersurfaces, $\Sigma^{*(i)}_k$ and $\Sigma^{*(i)}_{(k+1)}$, corresponding to local dynamic models, $\mathbf{a}^{(i)}$, identified by the Frisch Scheme which yield to a continuous multiple model, $C\ \mathrm{A} = \mathbf{0}$. The definition of the minimum eigenvalue criterion was suggested in [75] to estimate model order in linear dynamic identification.

3.8 Simplifying the Optimization Problem

The minimization problem in (3.35) has a simple cost function, J, but quite complex constraints. The aim of this Section is to discuss the role and structure of such constraints.

Well-known results [42, 43] ensure that, once that the noise is identified, the corresponding $\mathbf{a}^{(i)}$ satisfying $(\Sigma^{(i)}_k - \tilde{\Sigma}_k)\mathbf{a}^{(i)} = \mathbf{0}$ is unique and can be expressed as an affine combination

$$\mathbf{a}^{(i)} = \sum_j w^{(i)}_j\ {}^{*(i)}_{\mathbf{a}_j} \tag{3.36}$$

of the solutions $\overset{*(i)}{\mathbf{a}}_j$, obtained assuming that only the input ($\tilde{\sigma}_{u^*} \neq 0$) or the output ($\tilde{\sigma}_{y^*} \neq 0$) noise variance is non-null. These solutions are nothing but the "dynamic" ordinary least square solutions of a dynamic regression problem [44].

If $\mathbf{w}$ is the weight vector of the solutions $\overset{*(i)}{\mathbf{a}}_j$, from (3.36) and (3.30), the following is obtained

$$\overset{*}{\mathrm{CA}}\mathbf{w} = \mathbf{0}. \tag{3.37}$$

The null subspace $\ker(\overset{*}{\mathrm{CA}})$ can be computed a-priori and only its elements with non-negative components give raise to a continuous model. In this simple case, as the weight vector is constrained by $\sum_j w_j^{(i)} = 1$ for $i = 1, 2, \ldots, M$, the subset of continuous model is a manifold with not more than $\mathrm{corank}(\overset{*}{\mathrm{CA}}) - M$ dimensions.

An explicit parameterization of such manifold can be obtained by considering the following general results for nonlinear algebraic system identification.

Theorem 6. *For each region R_i, all the submodels satisfying (3.34) contain the point*

$$\begin{aligned} \bar{\mathbf{x}}^{(i)} &= \frac{1}{N_i}\sum_{j=1}^{N_i}\mathbf{x}_j^{(i)} \\ \bar{y}^{(i)} &= \frac{1}{N_i}\sum_{j=1}^{N_i} y_j \end{aligned} \tag{3.38}$$

Proof. Let us consider the Eq. (3.34). In that Equation, the matrix $\tilde{\Sigma}^{(i)}$ has a the first row with all zero entries, therefore, multiplying the first row of the matrix $\Sigma^{(i)}$ by the column vector $[\mathbf{a}^{(i)} - 1]^T$, we obtain:

$$N_i + \mathbf{a}^{(i)}\sum_{j=1}^{N_i}\mathbf{x}_j^{(i)} - \sum_{j=1}^{N_i} y_j = 0$$

dividing the above equality by N_i the thesis is proved. □

Indicate with $\mathbf{z}_1^{(i)}, \ldots, \mathbf{z}_{m+1}^{(i)}$ be the vertices of the simplex R_i and indicate with $\mathbb{I}_k^{(i)}$ the set of values assumed in $\mathbf{z}_k^{(i)}$ by all the submodels satisfying (3.34). The following Theorem holds

Theorem 7. *The set $\mathbb{I}_k^{(i)}$ is an interval going from $\min_{j=1}^{m+1}[1\ \mathbf{z}_k^{(i)}]\ \overset{*(i)}{\mathbf{a}}_j$ to $\max_{j=1}^{m+1}[1\ \mathbf{z}_k^{(i)}]\ \overset{*(i)}{\mathbf{a}}_j$.*

Proof. If the submodel satisfies (3.34), then its parameter vector $\mathbf{a}^{(i)}$ satisfies (3.36)

$$[1\ \mathbf{z}_k^{(i)}]\ \overset{*(i)}{\mathbf{a}} = \sum_{j=1}^{m+1} w_j^{(i)}[1\ \mathbf{z}_k^{(i)}]\ \overset{*(i)}{\mathbf{a}}_j$$

Hence, $\mathbb{I}_k^{(i)}$ is a one dimensional convex set, i.e. an interval spanning from the minimum to the maximum attainable values. □

The two above theorems can be effectively exploited in the algebraic case, when $m = 1$ if we assume that $\mathbb{D}$ is the interval between $\mathbf{z}_{\min}$ and $\mathbf{z}_{\max}$. In this case R_i are intervals and can be sorted so that $\mathbf{z}_{\min} = \mathbf{z}_1^{(1)} < \mathbf{z}_2^{(1)} = \mathbf{z}_1^{(2)} < \mathbf{z}_2^{(2)} = \mathbf{z}_1^{(3)} < \ldots < \mathbf{z}_2^{(M)} = \mathbf{z}_{\max}$. Theorem 7 also simplifies as $\mathbb{I}_k^{(i)}$ goes from $\min\{[1\ \mathbf{z}_k^{(i)}]\ \overset{*(i)}{\mathbf{a}}_1, [1\ \mathbf{z}_k^{(i)}]\ \overset{*(i)}{\mathbf{a}}_2\}$ to $\max\{[1\ \mathbf{z}_k^{(i)}]\ \overset{*(i)}{\mathbf{a}}_1, [1\ \mathbf{z}_k^{(i)}]\ \overset{*(i)}{\mathbf{a}}_2\}$.

Further on, indicate with Θ_i a transformation such that given an interval $I = [\alpha, \beta]$ produces the interval $\Theta_i(I) = [2\bar{y}^{(i)} - \beta, 2\bar{y}^{(i)} - \alpha]$. Theorem 6 guarantees that $\Theta_i(\mathbb{I}_k^{(i)}) = \mathbb{I}_{3-k}^{(i)}$ and that, for any parameter vector satisfying (3.34) if $[1\ \mathbf{z}_k^{(i)}]\mathbf{a}^{(i)} \in I$ then $[1\ \mathbf{z}_{3-k}^{(i)}]\mathbf{a}^{(i)} \in \Theta_i(I)$. With this the following Theorem holds

Theorem 8. *A model is continuous if and only if it assumes at $\mathbf{z}_2^{(M)}$ a value in the interval*

$$\Theta_M\left(\mathbb{I}_1^{(M)} \cap \Theta_{M-1}\left(\mathbb{I}_1^{(M-1)} \cap \ldots \Theta_2\left(\mathbb{I}_1^{(2)} \cap \Theta_1\left(\mathbb{I}_1^{(1)}\right)\right)\right)\right)$$

Proof. Proceed by induction on M. For $M = 1$ the thesis is trivial as all the models satisfying (3.34) assume at $\mathbf{z}_2^{(1)}$ a value within $\mathbb{I}_2^{(1)} = \Theta_1(\mathbb{I}_1^{(1)})$.

Assume now that a model is continuous in the first $M-1$ regions if and only if it assumes at $\mathbf{z}_2^{(M-1)}$ a value within $\Theta_{M-1}\left(\mathbb{I}_1^{(M-1)} \cap \ldots \Theta_2\left(\mathbb{I}_1^{(2)} \cap \Theta_1\left(\mathbb{I}_1^{(1)}\right)\right)\right)$.

Yet, all the submodels satisfying (3.34) in the M-th region assume at $\mathbf{z}_1^{(M)} = \mathbf{z}_2^{(M-1)}$ values within $\mathbb{I}_1^{(M)}$. As continuity means coincidence of left and right limits, a model is continuous on the first M regions if and only if it assumes at $\mathbf{z}_1^{(M)}$ a value within the intersection of $\mathbb{I}_1^{(M)}$ and the above interval. If we finally apply Θ_M we obtain the set of values characterizing the continuous models at $\mathbf{z}_2^{(M)}$ as indicated in the Theorem statement. □

The previous observations can be effectively exploited to simplify the optimization problem (3.35). The computation is performed by forcing continuity constraints among the boundaries of the local models containing the mean value of the data in each region R_i. In fact, as continuity means coincidence of left and right limits in each region, a multiple model is continuous on the j-th region if and only if its vertices assume the same values of the local models in the neighboring regions.

Because different models in each region can be identified according to (3.36) and (3.34), several continuous piecewise affine dynamic models can be built up.

The optimum multiple model is estimated computing the minimum the sum of the minimum eigenvalues corresponding to the local dynamic models identified by the Frisch Scheme which form the different continuous multiple models.

In Chapter 5 an example concerning the identification of a nonlinear process using piecewise affine models will be presented.

3.9 Fuzzy Modeling from Noisy Data

This section proposes a novel approach for the identification on nonlinear dynamic processes using fuzzy models approach. The technique presented concerns the identification and design of a nonlinear fuzzy inference system based on Takagi-Sugeno (TS) fuzzy models [61].

As the non-fuzzy case, a nonlinear dynamic process can be, in fact, described as a composition of several TS models selected according to the process operating conditions.

The following sections also address a method for the identification and the optimal selection of the local TS models from a sequence of noisy measurements acquired from the process.

3.10 Fuzzy Multiple Inference Identification

In recent years the application of fuzzy logic to control theory has gained increasing attention in both fundamental research and application. The key idea of this method consists in exploiting fuzzy set theory to express cause-effect relations in expert systems.

The proposed fuzzy technique is mainly useful when an model of the process under investigation has to be estimated. Therefore, the method presented will be used in the model-based FDI context.

The majority of real industrial processes are, in fact, nonlinear [25, 59] and cannot be modeled by using a single model for all operating conditions. Since a mathematical model is a description of system behavior, accurate modeling for a complex nonlinear system is very difficult to achieve in practice. Sometime for some nonlinear systems, it can be impossible to describe them by analytical equations. Instead of exploiting complicated nonlinear models obtained by modeling techniques, it is also possible to describe the plant by a collection of local linear models [60] obtained by identification procedures.

In particular, fuzzy logic is exploited to define a TS fuzzy model [61]. The TS fuzzy model for nonlinear dynamic systems is described by a number of local linear models. Each submodel approximates the system locally around an operating point and a selection procedure determines which particular submodel has to be used. As stated previously, such a multimodel structure is be called multiple model approach [60].

Under such a fuzzy logic scheme, a number of local linear models are designed and the estimate of outputs is given by a fuzzy fusion of local outputs.

In this algorithm, the different operating points are self-selected with a fuzzy clustering method [77, 78, 79]. On the basis of knowledge of the operating-point regions, the identification of the structure and the parameters of each local TS model can be performed [42, 43, 44].

3.11 Fuzzy Model Structure

This section deals with the decomposition of input-output data $u(t)$ and $y(t)$ $(t = 1, \ldots, N)$, acquired from a nonlinear SISO system, into fuzzy subsets which can be approximated by local affine input-output models. Each submodel represents the system behavior around the operating point.

Fuzzy clustering can be used as a tool to obtain partitioning of data into subsets, which can be approximated by local linear models.

It is assumed that the dynamics of the system under observation can be described by the following EE model [42, 43],

$$y(t) = f\big(\mathbf{x}(t)\big) + \varepsilon(t) \tag{3.39}$$

where $y(t)$ is the system output, $\mathbf{x}(t)$ is a collection of a finite number of inputs and outputs, $\mathbf{x}^T(t) = [y(t-1), \ldots, y(t-n), u(t-1), \ldots, u(t-n)]$, $f(\cdot)$ describes the input-output link, while $\varepsilon(t)$ reflects the fact that $y(t)$ is not an exact function of $\mathbf{x}(t)$. n is an integer related to the system order.

The objective of fuzzy clustering is to partition the set of observed inputs and outputs $\{\mathbf{x}(t)\}_t$ of an unknown dynamic system into a number M of fuzzy subsets. Each subset, R_i, representing an operating condition of the dynamic system, can be approximated by a linear dynamic model.

Partition of the data set into fuzzy subset can be achieved, for instance, by using the well-established Gustafson-Kessel (GK) clustering algorithm in [80].

Each cluster R_i ($i = 1, \cdots, M$) obtained by fuzzy partitioning is regarded as a local approximation of the nonlinear system. The global EE model (3.39) can be conveniently represented using local affine TS rules [61] $y_i(t)$:

$$\mathbf{x}(t) \ \in \ R_i \Rightarrow y_i(t) = \theta_i^T \mathbf{x}(t) \tag{3.40}$$

where θ_i is the i-th parameter vector of the i-th submodel, with $i = 1, \cdots, M$.

The TS fuzzy model is a simple way to describe a nonlinear dynamic system using local linear models. With this TS model a dynamic system can be linearized around a number of operating points. The global system behavior is described by a fuzzy fusion of all linear model outputs:

$$\hat{y}(t) = \frac{\sum_{i=1}^{M} \mu_i\big(\mathbf{x}(t)\big)\, y_i(t)}{\sum_{i=1}^{M} \mu_i\big(\mathbf{x}(t)\big)} \tag{3.41}$$

in which $\hat{y}(t)$ is the estimate of the output $y(t)$ at the instant t. The results of clustering are M, the membership functions $\mu_i(\cdot)$ and the subsets of input-output data $\{\mathbf{x}_i(t)\}_{i=1}^{M}$ with $\mathbf{x}_i(t) \in R_i$ [78]. These subsets can be processed according the Frisch Scheme identification procedure [41, 44], in order to estimate the θ_i and n parameters for each submodels.

3.12 Conclusions

In this section off-line procedures were presented for the identification of both linear and nonlinear static and dynamic system from data affected by noise. Linear, piecewise affine and fuzzy models were exploited.

For the case of piecewise affine and fuzzy models, the multiple model approach consists in using several local affine submodels each describing a different operating condition of the process.

The identification algorithm exploited to estimate parameters and orders of the local affine submodels is based on the well-established Frisch Scheme method for linear systems.

For the nonlinear case, in order to obtain a continuous piecewise affine prototype describing the input-output behavior of the process, continuity constraints between local linear dynamic models have to be forced.

For non-fuzzy models, such a continuity constrained problem was solved by using an optimization technique. The properties of the solutions obtained by the Frisch Scheme enhance the fulfillment of the contraints.

The method proposed requires a priori knowledge of the operating point vector structure as well as the expected number of local models.

Chapter 4

Residual Generation

4.1 Introduction

The most important task in model-based FDI techniques is the generation of residuals which are independent of disturbances. The method is based on disturbance decoupling principle. In this approach, uncertain factors in system modeling or identification are considered to act by means of an unknown input, the disturbance, on a linear system model.

The disturbance vector is unknown but its distribution matrix is usually assumed known. However, in the following, it will be shown how to estimate the disturbance distribution matrix, under the assumption that the system can be identified with an equation error model.

Based on the disturbance distribution matrix, obtained by modeling or identification procedure, the unknown input can be decoupled form the residual.

The principle of the UIO is to make the state (or output) estimation error decoupled from the unknown inputs or disturbances. Since the residual is a weighted output estimation error, it may be decoupled from each disturbance.

This approach was originally propose by Watanabe and Himmelblau [37], who considered the sensor FDI problem for systems with modeling uncertainties. Later, the approach was generalized by Frank [23, 28] in order to perform the FDI of both sensors and actuators. Very important contributions to this subject can be found in [24, 35, 47].

The first step in the disturbance decoupled residual generation consists in designing an UIO. This chapter shows how to obtain the structure of a full order UIO for FDI purpose. The design of an UIO will be presented from a mathematical point of view as well as the necessary and sufficient existence conditions.

Unlike some other works, in which the reduced order structure is exploited, this chapter is based exclusively on the use of the full order UIO. In fact, for a full order UIO, there is more design freedom available to achieve other required performance, after the disturbance decoupling conditions have been satisfied. As an example, the remaining design of freedom can be exploited to obtain directional residuals [24].

UIO or other disturbance decoupling based residual generation approaches require that the unknown input distribution matrix must be known a priori. The actual unknown input itself does not need to be known.

When uncertainties are caused by modeling errors, linearization errors, parameter variations, etc, such a disturbance decoupling approach cannot directly applied because the distribution

matrix is normally unknown. To solve this problem, which is of importance in real industrial system applications, some investigators have suggested an approach exploiting *estimated* [24] distribution matrices. In Section 4.7, the author of this thesis will suggest a method using *identified* distribution matrices.

The last approximate strategy has extended the application of disturbance decoupling-based residual generation to actual process FDI.

Some simulation results applied to a real industrial power plant and using identified disturbance distribution matrix technique will be shown in Chapter 5.

Finally, techniques exploiting fuzzy models and NNs are presented in order to perform residual generation and fault identification, respectively.

4.2 Unknown Input Observer

This section deals with the design of observers for discrete-time, time-invariant, linear dynamic systems with an additive unknown disturbance term. From a mathematical point of view, these systems are described by the following model

$$\begin{cases} \mathbf{x}(t+1) &= \mathrm{A}\mathbf{x}(t) + \mathrm{B}\mathbf{u}(t) + \mathrm{E}\mathbf{d}(t) \\ \mathbf{y}(t) &= \mathrm{C}\mathbf{x}(t) \end{cases} \tag{4.1}$$

where, $\mathbf{x}(t) \in \Re^n$ is the state vector, $\mathbf{y}(t) \in \Re^m$ is the output vector, $\mathbf{u}(t) \in \Re^r$ the known input vector and $\mathbf{d}(t) \in \Re^q$ the unknown input vector. A, B, C, E are known matrices with appropriate dimensions.

It is worthy to note how the unknown term $\mathrm{E}\mathbf{d}(t)$ can be used to describe an additive disturbance, different kinds of modeling uncertainties (noise, unmodelled nonlinear terms, time-varying dynamics, etc.) as well as fault terms.

The unknown term may also appear in the output equation, i.e.

$$\mathbf{y}(t) = \mathrm{C}\mathbf{x}(t) + \mathrm{E}_y\mathbf{d}(t) \tag{4.2}$$

but this case is not considered because the disturbance term $\mathrm{E}_y\mathbf{d}(t)$ can be nulled by using a transformation of the output signal $\mathbf{y}(t)$ [24].

For some systems (4.1), there is the term relating the control input $\mathbf{u}(t)$ in the output equation, i.e.

$$\mathbf{y}(t) = \mathrm{C}\mathbf{x}(t) + \mathrm{D}\mathbf{u}(t). \tag{4.3}$$

However, the term $\mathrm{D}\mathbf{u}(t)$ is omitted in this thesis since this does not affect the generality of the discussion on the observer design.

Definition 1. *An observer is defined as* **Unknown Input Observer** *for the system described by Eqs. (4.1), if its state estimation error vector* $\mathbf{e}_x(t)$ *approaches zero asymptotically, regardless of the presence of the unknown input term in the system.*

The problem of designing an observer for unknown inputs has been studied for nearly two decades and after the paper of Wang [81], many approaches for the design of both full-order

and reduced-order UIO have been proposed (geometric and algebraic methods, singular value decomposition and matrix inversion techniques, linear transformation algorithms) [24].

In this chapter, a full-order UIO structure is used and a mathematical method for designing UIO is presented. The necessary and sufficient conditions for this observer to exist are also recalled. These conditions are easy to verify and the design procedure is easy to implement.

4.3 UIO Mathematical Description

The full-order UIO has the following mathematical form

$$\begin{cases} \mathbf{z}(t+1) &= \mathrm{F}\mathbf{z}(t) + \mathrm{TB}\mathbf{u}(t) + \mathrm{K}\mathbf{y}(t) \\ \hat{\mathbf{x}}(t) &= \mathbf{z}(t) + \mathrm{H}\mathbf{y}(t) \end{cases} \tag{4.4}$$

where $\mathbf{z}(t) \in \Re^n$ is the state of the UIO, $\hat{\mathbf{x}}(t)$ the estimated state vector $\mathbf{x}(t)$, whilts F, T, H and K are matrices to be designed to achieve the unknown input decoupling.

The observer described by Eqs. (4.4) is depicted in Figure (4.1).

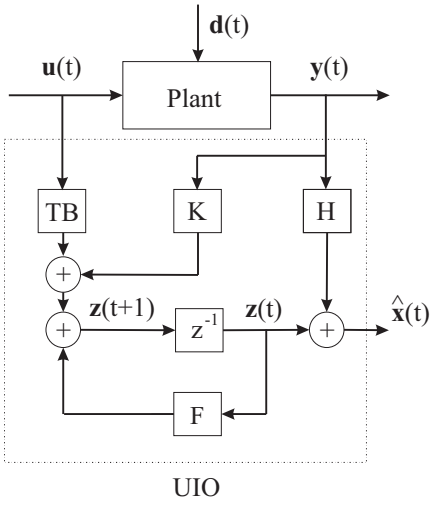

Figure 4.1: The UIO structure.

The state estimation error obtained by the UIO (4.4) applied to the system (4.1) is described by the equation

$$\begin{aligned} \mathbf{e}_x(t+1) &= [\mathrm{A} - \mathrm{HCA} - \mathrm{K}_1\mathrm{C}]\mathbf{e}_x(t) + \big[\mathrm{F} - (\mathrm{A} - \mathrm{HCA} - \mathrm{K}_1\mathrm{C})\big]\mathbf{z}(t) \\ &+ \big[\mathrm{K}_2 - (\mathrm{A} - \mathrm{HCA} - \mathrm{K}_1\mathrm{C})\big]\mathbf{y}(t) \\ &+ \big[\mathrm{T} - (\mathrm{I} - \mathrm{HC})\big]\mathrm{B}\mathbf{u}(t) + (\mathrm{HC} - \mathrm{I})\mathrm{E}\mathbf{d}(t) \end{aligned} \tag{4.5}$$

where $\mathrm{K} = \mathrm{K}_1 + \mathrm{K}_2$.

If the following relations hold

$$\begin{array}{lcl} (\mathrm{HC}-\mathrm{I})\mathrm{E} & = & 0 \\ \mathrm{I}-\mathrm{HC} & = & \mathrm{T} \\ \mathrm{A}-\mathrm{HCA}-\mathrm{K}_1\mathrm{C} & = & \mathrm{F} \\ \mathrm{FH} & = & \mathrm{K}_2 \end{array} \tag{4.6}$$

the state estimation error will then be

$$\mathbf{e}_x(t+1) = \mathrm{F}\mathbf{e}_x(t). \tag{4.7}$$

This means that, if all the eigenvalues of F are stable, $\mathbf{e}_x(t)$ will approach zero asymptotically, i.e. $\hat{\mathbf{x}} \to \mathbf{x}$. Hence, according to the Definition 1, the observer described by Eqs. (4.4) is an UIO for the system (4.1).

The design of this UIO consists in solving Eqs. (4.6) and making all eigenvalues of the system matrix F be stable.

The following theorem states existence conditions for the UIO.

Theorem 1. *Necessary and sufficient conditions for the existence of an UIO (4.4) for the system defined by (4.1) are [24]:*

(i) $rank(\mathrm{CE}) = rank(\mathrm{E})$,

(ii) $(\mathrm{A}_1, \mathrm{C})$ *is a detectable pair,*

where $\mathrm{A}_1 = \mathrm{A} - \mathrm{E}(\mathrm{CE})^+\mathrm{CA}$.

A special solution for the matrix H in conditions (4.6) is [24]

$$\mathrm{H}^* = \mathrm{E}(\mathrm{CE})^+ \tag{4.8}$$

where $(\cdot)^+$ is the pseudoinverse of the matrix CE.

It is worthy to note that the number of independent row of the matrix C must not be less than the number of the independent columns of the matrix E to satisfy condition *(i)* in Theorem 1. It means that the maximum number of disturbances which can be decoupled cannot be larger than the number of the independent measurements. Moreover, without unknown inputs in the system, by setting T = I, H = 0 and E = 0, the observer (4.4) will be a simple Luenberger observer. In such a situation, condition *(i)* in Theorem 1 is clearly hold true and condition *(ii)* is equal to the detectability of couple (A, C).

4.4 UIO Design Procedure

It can be seen how K_1 is a free matrix of parameters in the design of an UIO. After K_1 is computed, in order to stabilize the dynamic system matrix F, other parameter matrices in the UIO can be computed by the relation $\mathrm{K} = \mathrm{K}_1 + \mathrm{K}_2$ and conditions (4.6). Some design freedom left in the choice of K_1 may be exploited to make the diagnostic residual has directional characteristics. In this thesis, because the input-output link of the MIMO system under investigation

is obtained by means of the identification of a collection of MISO models, this further degree of freedom will not be used in the residual design.

Under these assumptions, if the pair (A_1, C) is observable, in order to stabilize the system matrix $F = A_1 - K_1C$, the pole placement routine available in the Control System Toolbox for MATLAB® [82] can be used.

If (A_1, C) is not observable, an observable canonical decomposition should be applied to the pair [24]. If (A_1, C) is detectable, the matrix F can be stabilized.

4.5 FDI Schemes Based on UIO

The main task of FDI is to generate residual signals which have to be sensitive to faults themselves. According to Chapter 2, a system with faults concerning system inputs and outputs can be represented as

$$\begin{cases} \mathbf{x}(t+1) &= A\mathbf{x}(t) + B\mathbf{u}(t) + B\mathbf{f}_u(t) \\ \mathbf{y}(t) &= C\mathbf{x}(t) + \mathbf{f}_y(t) \end{cases} \tag{4.9}$$

where A, B and C are constant matrices of appropriate dimensions obtained by means of the identification procedures recalled in Chapter 3.

The vectors $\mathbf{f}_u(t) = [f_{u_1}(t) \dots f_{u_r}(t)]^T$ and $\mathbf{f}_y(t) = [f_{y_1}(t) \dots f_{y_m}(t)]^T$ assume values different from zero only in the presence of faults.

Usually these signals are described by step and ramp functions representing abrupt and incipient faults (bias or drift), respectively.

With reference to Chapter 2, the actual measured signals $\mathbf{u}(t)$ and $\mathbf{y}(t)$ are modeled as

$$\begin{cases} \mathbf{u}(t) &= \mathbf{u}^*(t) + \tilde{\mathbf{u}}(t) \\ \mathbf{y}(t) &= \mathbf{y}^*(t) + \tilde{\mathbf{y}}(t) \end{cases} \tag{4.10}$$

in which, the sequences $\tilde{\mathbf{u}}(t)$ and $\tilde{\mathbf{y}}(t)$ are usually described as white, zero–mean, uncorrelated Gaussian noises.

To univocally isolate a fault concerning one of the *system outputs*, $\mathbf{f}_y(t)$, under the hypothesis that inputs are fault–free, $(\mathbf{f}_u(t) = \mathbf{0})$, a bank of classical dynamic observers or KF is used (Figure (4.2)).
This observer configuration represents the Dedicated Observer Scheme (DOS) [23].

The number of these estimators is equal to the number m of system outputs, and each device is driven by a single output and all the inputs of the system.

In this case a fault on the i–th output affects only the residual function of the output observer or filter driven by the i–th output.

To univocally isolate a fault concerning one of the *system inputs*, $\mathbf{f}_u(t)$, under the assumption that outputs are fault-free, $(\mathbf{f}_y(t) = \mathbf{0})$, a bank of UIO or UIKF is used (Figure (4.3)).
Such a solution is known as Generalized Observer Scheme (GOS) [23].

The number of these devices is equal to the number r of control inputs.

The i-th device is driven by all but the i–th input and all outputs of the system and generates a residual function which is sensitive to all but the i–th input fault.

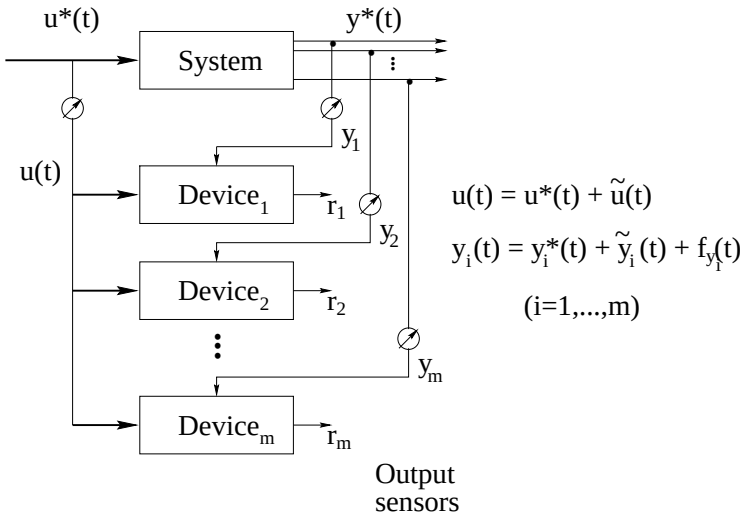

Figure 4.2: Bank of estimators for output residual generation.

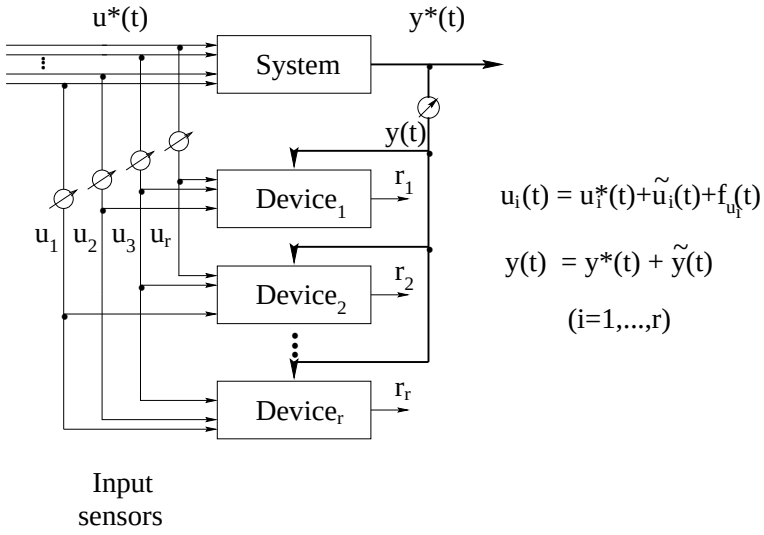

Figure 4.3: Scheme for system inputs FDI.

In this way the detection of single input measurement faults is possible, since a fault on the i–th input affects all the residual functions except that of the device which is insensitive to the i-th input.

In order to summarize the isolation capabilities of the presented schemes, Table (4.1) shows the "fault signatures" in case of a single fault in each input–output signal.

	u_1	u_2	...	u_r	y_1	y_2	...	y_m
r_{UIO_1}	0	1	...	1	1	1	...	1
r_{UIO_2}	1	0	...	1	1	1	...	1
$\vdots$	$\vdots$	$\vdots$	$\vdots$	$\vdots$	$\vdots$	$\vdots$	$\vdots$	$\vdots$
r_{UIO_r}	1	1	...	0	1	1	...	1
r_{O_1}	1	1	...	1	1	0	...	0
r_{O_2}	1	1	...	1	0	1	...	0
$\vdots$	$\vdots$	$\vdots$	$\vdots$	$\vdots$	$\vdots$	$\vdots$	$\vdots$	$\vdots$
r_{O_m}	1	1	...	1	0	0	...	1

Table 4.1: Fault signatures.

The residuals which are affected by the input and output faults are marked with the presence of '1' in the correspondent table entry, while an entry '0' means that the input or output fault does not affect the correspondent residual.

Note how multiple faults in the system outputs can be isolated since a fault on the i–th output signal affects only the residual function r_{O_i} of the output observer driven by the i–th output, but all the UIO or UIKF residual functions r_{UIO_i}. On the other hand, multiple faults on the inputs can not be isolated by means of this technique since all the residual functions are sensitive to faults regarding different inputs.

With reference to Figure (4.2), in order to diagnose a fault on the i–th *system output* when the measurement noises are negligible ($\tilde{\mathbf{u}}(t) \cong 0$, $\tilde{\mathbf{y}}(t) \cong 0$) and $\mathbf{f}_u(t) = \mathbf{0}$ the model of the i–th observer ($i = 1, 2, \ldots, m$) has the form

$$\mathbf{x}^i(t+1) = \mathrm{A}^i\mathbf{x}^i(t) + \mathrm{B}^i\mathbf{u}(t) + \mathrm{K}^i\big(y_i(t) - \mathrm{C}^i\mathbf{x}^i(t)\big) \tag{4.11}$$

where $\mathbf{x}^i(t)$ is the observer state vector and the triple (A^i, B^i, C^i) is a minimal state–space representation (completely observable) of the link among the inputs of the process and its i–th output $y_i(t)$. Such a triple can be obtained by means of the realization procedure, summarized in Chapter 3, starting from a MISO identified model.

The entries of K^i must be designed in order to assign to the $(A^i - K^iC^i)$ matrix stable eigenvalues chosen suitably within the unit circle.

In this situation and in the absence of faults, i.e. $\mathbf{f}_y(t) = \mathbf{0}$, it can be verified that for the i-th output residual $\lim_{t\to\infty} r_i(t) = \lim_{t\to\infty} \big(y_i(t) - C^i\mathbf{x}^i(t)\big) = 0$ and the rate of convergence depends on the position of the eigenvalues of the $(A^i - K^iC^i)$ matrix inside the unit circle.

In the presence of a fault (step or ramp signal) on the i–th process output only the i–th output residual reaches a value different from zero and this situation leads to a complete failure diagnosis.

With reference to the devices for the FDI of the inputs, depicted in Figure (4.3), the structure of the i-th UIO ($i = 1, 2, \ldots, r$) for residual generation [24], under the assumptions $\tilde{\mathbf{u}}(t) \cong \mathbf{0}$, $\tilde{\mathbf{y}}(t) \cong \mathbf{0}$ and $\mathbf{f}_y(t) = \mathbf{0}$, is the following

$$\begin{cases} \mathbf{z}^i(t+1) &= \big(\mathrm{T}^i\mathrm{A} - \mathrm{K}^i\mathrm{C}\big)\mathbf{z}^i(t) + \mathrm{J}^i\mathbf{u}(t) + \mathrm{S}^i\mathbf{y}(t) \\ \mathbf{r}^i(t) &= \mathrm{L}_1^i\mathbf{z}^i(t) + \mathrm{L}_2^i\mathbf{y}(t) \end{cases} \tag{4.12}$$

where $\mathbf{z}^i(t) \in \Re^n$ denotes the observer state vector, $\mathbf{r}^i(t) \in \Re^m$ is the residual vector and F^i, J^i, S^i, L_1^i and L_2^i are matrices to be designed with appropriate dimensions. Let T^i be a linear transformation of the state $\mathbf{x}(t)$ of the system and define the state estimation error as $\mathbf{e}_x^i(t) = \mathbf{z}^i(t) - \mathrm{T}^i\mathbf{x}(t)$. On the suppositions $\tilde{\mathbf{u}}(t) = \mathbf{0}$, $\tilde{\mathbf{y}}(t) = \mathbf{0}$, and $\mathbf{f}_y(t) = \mathbf{0}$, it can be shown that the dynamics of the state estimation error becomes

$$\mathbf{e}_x^i(t+1) = \mathrm{F}^i\mathbf{e}_x^i(t) + \big(\mathrm{F}^i\mathrm{T}^i - \mathrm{T}^i\mathrm{A} + \mathrm{S}^i\mathrm{C}\big)\mathbf{x}(t) + (\mathrm{J}^i - \mathrm{T}^i\mathrm{B})\mathbf{u}(t) - \mathrm{T}^i\mathrm{B}\mathbf{f}_u(t), \tag{4.13}$$

whilst the residual vector is given by

$$\mathbf{r}^i(t) = \mathrm{L}_1^i\mathbf{e}_x^i(t) + (\mathrm{L}_1^i\mathrm{T}^i + \mathrm{L}_2^i\mathrm{C})\mathbf{x}(t). \tag{4.14}$$

It can be seen that if

$$\begin{cases} \mathrm{F}^i\mathrm{T}^i - \mathrm{T}^i\mathrm{A} + \mathrm{S}^i\mathrm{C} &= 0, \\ \mathrm{J}^i &= \mathrm{T}^i\mathrm{B}, \\ \mathrm{L}_1^i\mathrm{T}^i + \mathrm{L}_2^i\mathrm{C} &= 0, \end{cases} \tag{4.15}$$

Equations (4.13) and (4.14) become

$$\begin{cases} \mathbf{e}_x^i(t+1) &= \mathrm{F}^i\mathbf{e}_x^i(t) + \mathrm{T}^i\mathrm{B}\mathbf{f}_u(t), \\ \mathbf{r}^i(t) &= \mathrm{L}_1^i\mathbf{e}_i(t). \end{cases} \tag{4.16}$$

The matrices T^i, K^i, J^i, S^i, L_1^i and L_2^i can be constructed satisfying the following equations.

Under the hypothesis of observability of the system and in the absence of input faults, it can be seen that the i-th residual vector reaches zero as t approaches infinity and the rate of convergence depends on the position of the eigenvalues of F^i matrix inside the unit circle.

The hypothesis of system observability always holds because the transformation of the ARX input-output model into state-space representation leads to completely observable systems [33].

If the linear transformation T^i is chosen as [83]

$$\mathrm{T}^i = \mathrm{I}_n - \mathrm{B}_i(\mathrm{C}\mathrm{B}_i)^+\mathrm{C} \tag{4.17}$$

where B_i is the i-th column of B matrix and K^i is selected such that $\mathrm{F}^i = \mathrm{T}^i\mathrm{A} - \mathrm{K}^i\mathrm{C}$ is asymptotically stable, then, the solutions to (4.15) are obtained as

$$\begin{cases} \mathrm{F}^i &= \mathrm{T}^i\mathrm{A} - \mathrm{K}^i\mathrm{C}, \\ \mathrm{S}^i &= \mathrm{K}^i + \mathrm{F}^i\mathrm{B}_i(\mathrm{C}\mathrm{B}_i)^+, \\ \mathrm{J}^i &= \mathrm{T}^i\mathrm{B}, \\ \mathrm{L}_1^i &= -\mathrm{C}, \\ \mathrm{L}_2^i &= \big[\mathrm{I}_m - (\mathrm{C}\mathrm{B}_i)(\mathrm{C}\mathrm{B}_i)^+\big]. \end{cases} \tag{4.18}$$

The selection of the B_i matrix in Equations (4.17) and (4.18) sets to zero the i-th column of the J^i matrix. That is, the estimation error and then the residual of the i-th UIO become independent of the i-th system input.

Under the hypothesis of observability of the system (4.9) and in the absence of input fault ($\mathbf{f}_u(t) = \mathbf{0}$), it can be seen that the i–th residual vector reaches zero as t approaches infinity and the rate of convergence depends on the position of the eigenvalues of $\mathrm{T}^i\mathrm{A} - \mathrm{K}^i\mathrm{C}$ matrix inside the unit circle.

In the presence of a fault on the i–th input, the i–th residual reaches asymptotically zero while the residuals of the $r-1$ remaining observers are sensitive to the fault signal and this situation leads to a complete fault diagnosis for the process inputs.

The design of these UIO requires the knowledge of a minimal form model $(\mathrm{A}, \mathrm{B}, \mathrm{C})$ for the system (4.9). Such a triple can be computed by using a realization procedure from a MIMO identified model. On the other hand, if the process in mathematically described by m MISO models, the triple $(\mathrm{A}, \mathrm{B}, \mathrm{C})$ can be directly obtained by grouping the $(\mathrm{A}^i, \mathrm{B}^i, \mathrm{C}^\mathrm{i})$ representations $(i = 1, 2, \ldots, m)$.

4.6 Kalman Filtering and FDI from Noisy Measurements

With reference to Eqs. (4.10), when the signal to noise ratios $\|\mathbf{u}^*(t)\|_2^2/\|\tilde{\mathbf{u}}(t)\|_2^2$ and $\|\mathbf{y}^*(t)\|_2^2/\|\tilde{\mathbf{y}}(t)\|_2^2$ are low, a bank of KF must be employed to improve the performance of the FDI system. Even in this situation, the mathematical formulation of the classical KF and of the UIKF is similar to the one described by Equations (4.11) and (4.12) [24].

The essential difference regards the feedback matrix K^i which becomes time–dependent and is computed by solving a Riccati equation. The solution of this equation requires the knowledge of the covariance matrices of the input and the output noises which can be identified by means of the dynamic Frisch scheme [84].

With reference to the time-invariant, discrete-time, linear dynamic system described by Eq. (2.1) the i-th KF for the i-th output has the structure [38]

$$\mathbf{x}_F^i(t+1|t) = A\mathbf{x}_F^i(t|t) + Bu(t) \tag{4.19}$$

$$y_F^i(t+1|t) = C_i\mathbf{x}_F^i(t+1|t) \tag{4.20}$$

$$P(t+1|t) = AP(t|t)A^T + Q \tag{4.21}$$

$$K_i(t+1) = P(t+1|t)C_i^T\left[C_iP(t+1|t)C_i^T + R\right]^{-1} \tag{4.22}$$

$$\mathbf{x}_F^i(t+1|t+1) = \mathbf{x}_F^i(t+1|t) + K_i(t+1)\left[y_i(t+1) - \hat{y}_F^i(t+1|t)\right] \tag{4.23}$$

$$\begin{aligned} P(t+1|t+1) = {} & \left[I - K_i(t+1)C_i\right]P(t+1|t)\left[I - K_i(t+1)C_i\right]^T + \\ & + K_i(t+1)RK_i^T(t+1). \end{aligned} \tag{4.24}$$

The variables $\mathbf{x}_F^i(t+1|t)$ and $y_F^i(t+1|t)$ are the one step prediction of the state and of the output of the process, respectively. $\mathbf{x}_F^i(t|t)$ is the state estimation given by the filter, C_i the i-th row of the output distribution matrix C, $P(t+1|t)$ is the covariance matrix of the one step prediction error $\mathbf{x}(t+1) - \mathbf{x}_F^i(t+1|t)$ whilst $P(t|t)$ is the covariance matrix of the filtered state error $\mathbf{x}(t) - \mathbf{x}_F^i(t|t)$. Q is the covariance matrix of the input vector noise $\tilde{u}(t)$ and R is the

variance of the i-th component of the output noise $\tilde{\mathbf{y}}(t)$. $K_i(t+1)$ is the time-variant gain of the filter and $y_i(t)$ is the i-th component of the measured output $\mathbf{y}(t)$.

It can be proved that the innovation $e_i(t+1) = y_i(t+1) - y_F^i(t+1|t) = y_i(t+1) - C_i \mathbf{x}_F^i(t+1|t)$ is a zero-mean white process when all the assumptions regarding the system (2.1) and the statistical characteristics of the noises (2.4) are completely fulfilled. A Riccati equation is obtained by substituting Eq. (4.21) into Eq. (4.24). The solution of this equation converges to a steady state solution when the pair (A, C_i) is completely observable and the pair (A, D) is completely reachable, where D is a matrix such that $Q = DD^T$.

In the presence of a fault on the i-th output ($f_{y_i}(t) \neq 0$), the stochastic properties (mean-value, variance and whiteness, etc) of the innovation process $e_i(t)$ change abruptly so that the fault detection can be based on these variations [85].

Finally, note how multiple faults in outputs can be isolated since a fault on the i-th output affects only the innovation of the KF driven by the i-th output and all the innovation of the filters with unknown input.

On the other hand, with reference to UIKF [39, 40], a single fault on the i-th input affects all the filter innovations except that of the filter with unknown input which is insensitive to the i-th input. UIKF design procedure similar to (4.18) can be found in [39, 40].

4.7 Residual Robustness to Disturbances

All model-based FDI methods use a model of the monitored system to produce the symptom generator. If the system is not complex and can be described accurately by the mathematical model, FDI is directly performed by using a simple geometrical analysis of residuals.

In real industrial systems however, the modeling uncertainty is unavoidable. The design of a reliable FDI scheme should take into account of the modeling uncertainty with respect to the sensitivity of the faults.

The model-based FDI technique requires a high accuracy mathematical description of the monitored system. The better the model represents the dynamic behavior of the system, the better will be the FDI precision. If a FDI method can be developed which is insensitive to modeling uncertainty, a very accurate model is not necessarily needed.

All uncertainties can be summarized as disturbances acting on the system. Although the disturbance vector is unknown, its distribution matrix can be obtained by an identification procedure. Under this assumption, the disturbance decoupling principle can be exploited to design a fault detection scheme using UIOs.

Under the hypothesis that the system can be described as an equation error model, this section has studied the method of obtaining the disturbance distribution matrix from the fault-free system data, by taking into account the equation error term.

The UIO performing the disturbance decoupling can be designed from the equation error model.

In the following, in fact, it is assumed that the monitored system, depicted in Figure (4.4), can be described by a linear, discrete-time equation error model of the type

$$y_i^*(t) = \sum_{k=1}^{n} \alpha_{ik} y_i^*(t-k) + \sum_{j=1}^{r} \sum_{k=1}^{n} \beta_{ikj} u_j^*(t-k) + \varepsilon_i(t). \tag{4.25}$$

where $y_i^*(t)$ $(i = 1, \ldots, m)$ is the i-component of the system output vector $\mathbf{y}^*(t)$, whilts u_j^* the j-component of the control input vector $\mathbf{u}^* \in \Re^r$. n, α_{ik} and β_{ikj} are the parameters to be determined by an identification approach. The term $\varepsilon_i(t)$ takes into account the modeling error, which is due to process noises, parameter variations, etc.

As depicted in Figure (4.4), in real applications the input and output sensor signals $\mathbf{u}(t)$ and $\mathbf{y}(t)$ are affected by faults.

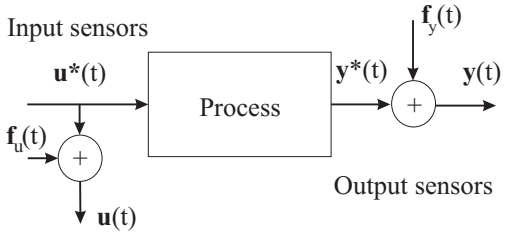

Figure 4.4: The monitored system.

By using the transfer function description, system (4.25) can be rewritten in the form

$$y_i^*(t) = \mathrm{F}_i(z)\mathbf{u}^*(t) + \mathrm{G}_i(z)\varepsilon_i(t) \tag{4.26}$$

and its structure is depicted in Figure (4.5), in which z is the unitary advance operator.

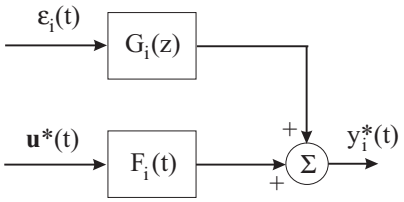

Figure 4.5: The structure of the equation error model.

The symptom generation is implemented by means of dynamic observers with unknown inputs, in order to produce a set of signals from which it will be possible to diagnose faults associated to outputs. This choice should minimize the effects of disturbances, which act as a source of false alarms.

The design of the UIO requires the knowledge of a state-space model of the system under investigation. In particular, in this section, in order to design the UIO, the identification of a number of MISO models ($m = 1$), of the type of (4.26) equal to the number of the output variables has been chosen.

Under no-fault conditions, it can be proved that a state-space formulation of the input-output equation error model (4.25) for the i-th output becomes

$$\left\{ \begin{array}{lcl} \mathbf{x}_i(t+1) & = & \mathrm{A}_i\mathbf{x}_i(t) + \mathrm{B}_i\mathbf{u}(t) + \mathrm{E}_i\varepsilon_i(t) \\ y_i(t) & = & \mathrm{C}_i\mathbf{x}_i(t) + \mathrm{F}_i\varepsilon_i(t), \quad t = 1, 2, \ldots \end{array} \right. \tag{4.27}$$

where the matrices $\mathrm{A}_i(n \times n)$, $\mathrm{B}_i(n \times r)$, $\mathrm{C}_i(1 \times n)$, $\mathrm{E}_i(n \times 1)$ and F_i are functions of the α_{ik} and β_{ikj} parameters [33].

If the vector $\varepsilon_i(t)$ is considered as a disturbance and E_i, F_i its distribution matrices, terms $\mathrm{E}_i\varepsilon_i(t)$ and $\mathrm{F}_i\varepsilon_i(t)$ represent uncertainties acting upon the system.

The i-th residual (symptom) generator using an UIO is thus described as

$$\begin{cases} \mathbf{z}_i(t+1) &= \mathrm{N}_i\mathbf{z}_i(t) + \mathrm{L}_i y_i(t) + \mathrm{G}_i\mathbf{u}(t) \\ \mathbf{r}_i(t) &= y_i(t) - \mathrm{C}_i\big(\mathbf{z}_i(t) - \mathrm{D}_i y_i(t)\big) \end{cases} \tag{4.28}$$

where $\mathrm{z}_i(t) \in \Re^n$ denotes the i-th observer state vector, $\mathrm{C}_i\big(\mathrm{z}_i(t) - \mathrm{D}_i y_i(t)\big)$ represents the estimate of $y_i(t)$ whilst $\mathbf{r}_i(t)$ is the residual vector. A design procedure is used for finding suitable matrices N_i, L_i, G_i and D_i with appropriate dimension.

With the choices

$$\begin{cases} \mathrm{D}_i &= -\mathrm{E}_i(\mathrm{C}_i\mathrm{E}_i)^{-1}, \\ \mathrm{P}_i &= \mathrm{I} + \mathrm{D}_i\mathrm{C}_i, \\ \mathrm{G}_i &= \mathrm{P}_i\mathrm{B}_i, \\ \mathrm{L}_i &= \mathrm{P}_i\mathrm{A}_i\mathrm{E}_i(\mathrm{C}_i\mathrm{E}_i)^{-1}, \end{cases} \tag{4.29}$$

if N_i can be chosen suitably, so that

$$\mathrm{L}_i\mathrm{C}_i - \mathrm{P}_i\mathrm{A}_i = -\mathrm{N}_i\mathrm{P}_i \tag{4.30}$$

$\mathbf{r}_i(t)$ will asymptotically approach zero in the absence of faults, $\mathbf{f}_u(t) = \mathbf{0}$ and $\mathbf{f}_y(t) = \mathbf{0}$.

4.8 Residual Generation via Parameter Estimation

With reference to an input-output SISO EIV model of order n in the form

$$\sum_{i=0}^{n} \alpha_i y(t-i) = \sum_{i=1}^{n} \beta_i u(t-i) \tag{4.31}$$

in which $u(t)$ represents the input, $y(t)$ the output, a KF can be used to estimate α_i and β_i model parameters.

The KF, in fact, used as parameter estimator [86], can be exploited in order to detect changes in parameters α_i and β_i due to faults which affect input and output measurements $u(t)$ and $y(t)$.

The system to design the filter is the following

$$\begin{cases} \theta(t+1) &= \theta(t) + \omega(t) \\ y(t) &= \theta(t)P(t) + \varepsilon(t) \end{cases} \tag{4.32}$$

where the vector $\theta = [\alpha_n, \ldots, \alpha_1, \beta_n, \ldots, \beta_1]$ collects the model parameters and the measurement vector $P(t) = [y(t-n), \ldots, y(t-1), u(t-n), \ldots, u(t-1)]$. $\omega(t)$ is a white process, in order to take into account the parameter variations for non stationary processes whilst $\varepsilon(t)$ the output error term.

Residuals can be generated, for instance, by comparing the estimate of the parameters θ given by Ordinary Least Squares (OLS) or Recursive Least Squares (RLS) and the one computed by the KF (4.32). On the other hand, fault free and faulty parameters $\theta(t)$ computed by (4.32) in fault free and faulty conditions can be compared.

Standard deviation of the $\varepsilon(t)$ process can be evaluated via OLS, while the one of the $\omega(t)$ white process has to be tuned in order to obtain an accurate parameter estimate.

An application of such a method will be shown in Section 5.8.

4.9 Residual Generation via Fuzzy Models

This section exploits the approach for FDI in nonlinear dynamic processes using multiple model approach. In particular, as described in Section 3.11, the method uses Takagi-Sugeno (TS) fuzzy models.

The nonlinear dynamic process is, in fact, described as a composition of several Takagi-Sugeno models selected according to the process operating conditions.

The FDI scheme adopted to generate residuals from the measured noisy sequences $\mathbf{u}(t)$ and $\mathbf{y}(t)$ is designed by means of the nonlinear TS fuzzy identified models.

In the following, it is assumed that the monitored system, depicted in Figure (4.6), can be described by a model of the type (3.39) in Section 3.11. $\mathbf{y}(t) \in \Re^m$ is the system output vector and $\mathbf{u}(t) \in \Re^r$ the control input vector.

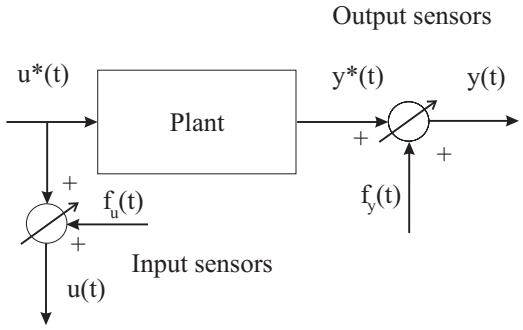

Figure 4.6: The structure of the monitored system.

In real applications measured variables $\mathbf{u}^*(t)$ and $\mathbf{y}^*(t)$ are affected by noise. $\mathbf{f}_u(t)$ and $\mathbf{f}_y(t)$ are faults affecting system inputs and outputs.

As presented in Chapter 2, there are different approaches to generate the residuals from which it will be possible to diagnose faults associated to system inputs and outputs. In this thesis, fuzzy models are used to estimate the outputs of the system from the input-output measurements.

As depicted in Figure (4.7), residuals can be generated by the comparison of measured $\mathbf{y}(t)$ and estimated $\hat{\mathbf{y}}(t)$ outputs

$$\mathbf{r}(t) = \mathbf{y}(t) - \hat{\mathbf{y}}(t). \tag{4.33}$$

The symptom evaluation is obtained by a logic device which processes the redundant signals computed by the residual generation in order to detect when a fault occurs. In such a case, faults can be detected by using a simple thresholding logic.

4.10 Fault Identification Using Neural Networks

This section presents the problem of the estimation of the size of faults occurring in the inputs and outputs of a dynamic system.

The fault detection and identification system involves a bank of dynamic observers and utilizes NNs in order to classify observer residuals into fault classes.

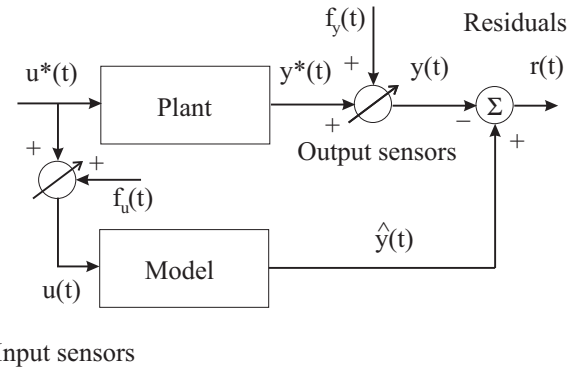

Figure 4.7: The residual generation scheme.

A NN is exploited in order to find the connection from a particular fault regarding system inputs and outputs to a particular residual. In such a way the observers generate a residual outputs which not depend on the dynamic characteristics of the plant, but only on faults. Therefore, the NN classify static patterns of residuals, which are uniquely related to particular fault conditions independently from the plant dynamics.

Moreover, in the following, the structure of the NN used for fault classification is detailed. NN may be classified as *supervised*, in which a teacher is used to train the network, and as *unsupervised*, in which input patterns are clustered into groups collecting similar inputs.

An important member of the first class of NN is the *MultiLayer Perceptron* (MLP), which can approximate any mapping $f : \Re^n \mapsto \Re^m$ with arbitrary degree of accuracy. A multilayer perceptron comprises several layers of simple computation units called neurons. The mathematical description of a neuron is:

$$y_i = f_a(\mathbf{w_i}^T \mathbf{p} + \mathbf{b_i})$$

where $\mathbf{p}$ is the input pattern and $\mathbf{b}_i$, $\mathbf{w}_i$ are the parameter vectors of the neuron and y_i is neuron output. The function f_a is an activation function, generally nonlinear.

Another kind of NNs, namely *Radial Basis Function* (RBF) networks, belonging to the class of the Generalized Regression Network, has been considered.

The hidden layer is composed of radial basis neurons performing a nonlinear mapping of the input space. Unnormalized Gaussian functions given by the equation,

$$G = e^{-\|\mathbf{x}-\mathbf{c}\|^2/\delta^2} \tag{4.34}$$

in which $\|\cdot\|$ denotes the Euclidean norm, $\mathbf{x}$ is the m-dimensional input vector, $\mathbf{c}$ the centers and δ the width of the gaussian functions, are the most common functions in the hidden node, but several other functions have been proposed [66].

In the output layer linear neurons have to be used in order to perform the function approximation. The parameters of NNs are obtained with the training procedure.

Centers of the Gaussian functions are the most troublesome values to tune. In particular, the network architecture can be implemented by using a "non-exact" solution. An "exact" design solution requires one hidden neuron for each training pattern.

4.11 Summary

The purpose of this chapter has been the study of UIO-based residual generation methods and a full-order UIO structure has been recalled.

The existence conditions and design procedures for such UIO have also been presented.

The design procedure proposed in the chapter is very easy to verify and implement, since the pole placement routine in Control System Toolbox for MATLAB can be used.

The main advantage of the full-order UIO is that there is more design freedom available (even if it is not exploited in this thesis) after the unknown input decoupling conditions have been satisfied. The remaining freedom may be used to generate directional residuals for fault isolation.

UIO-based FDI methods have been studied for many year but the number of applications is very limited. The main problem is, in fact, that the unknown input distribution matrix, required for designing UIOs, is unknown for most real systems.

Under simple assumptions, the chapter has shown how UIO-based disturbance decoupling technique can be used in practical systems, in which the disturbance distribution matrix is not known.

When measurements are affected by noises, KF and UIKF can be exploited.

Finally, a residual generation technique exploiting fuzzy models was presented while the identification of faults concerning system inputs and outputs can be performed by means of static NNs.

Chapter 5

Fault Diagnosis Applications

5.1 Introduction

In the following section, several simulated and real application examples are presented in order to test the FDI techniques studied in Chapter 4 in connection with identification procedures presented in Chapter 3.

Complete design procedures for fault detection, isolation and identification of actuators, components, input and output sensors of industrial processes described in Chapters 2 and 4 are applied.

The fault diagnosis is performed by using banks of dynamic observers and UIO or, when the measurement noises are not negligible, banks of KF and UIKF [87].

Single faults on the actuators, components, input and output sensors and multiple faults on the output sensors are considered and simulated on the monitored systems.

As explained in Chapter 3, FDI methods applied do not require any physical knowledge of the processes under observation since the input–output links are obtained by means of identification schemes using EE and EIV models.

In case of noisy measurements, the identification technique (Frisch scheme) recalled in Chapter 3 for EIV models gives also the variances of the input–output noises, which are required in the design of the KF.

The procedure has been applied to different models of a real and simulated power plants.

In order to analyze the diagnostic effectiveness of the FDI system in the presence of abrupt changes or drifts in measurements, faults modeled by step or ramp functions have been generated.

The results obtained by this approach indicate that the minimal detectable faults on the various sensors are of interest for the industrial diagnostic applications.

The following processes are described.

- MIMO Simulink® model of a real single-shaft industrial gas turbine with variable Inlet Guided Vane (IGV) angle working in parallel with electrical mains.

- MIMO real 120MW power plant of Pont sur Sambre. It is a double-shaft industrial gas turbine working in parallel with electrical mains.

- MIMO Simulink prototype of a real single-shaft industrial gas turbine.

5.2 FDI of an Industrial Gas Turbine using Dynamic Observers

The technique for input-output sensor FDI presented in this thesis is applied to the model of a real single-shaft industrial gas turbine with variable IGV angle working in parallel with electrical mains in a cogeneration plant [88].

Concerning the machine layout shown in Figure (5.1), the input control sensors are used for the measurement of:

$u_1(t)$, Inlet Guide Vane (IGV) angular position (α);
$u_2(t)$, fuel mass flow rate (M_f).

The output sensors are those used for the measurement of the following variables:

$y_1(t)$, pressure at the compressor inlet (p_{ic});
$y_2(t)$, pressure at the compressor outlet (p_{oc});
$y_3(t)$, pressure at the turbine outlet (p_{ot});
$y_4(t)$, temperature at the compressor outlet (T_{oc});
$y_5(t)$, temperature at the turbine outlet (T_{ot});
$y_6(t)$, electrical power at the generator terminal (P_e).

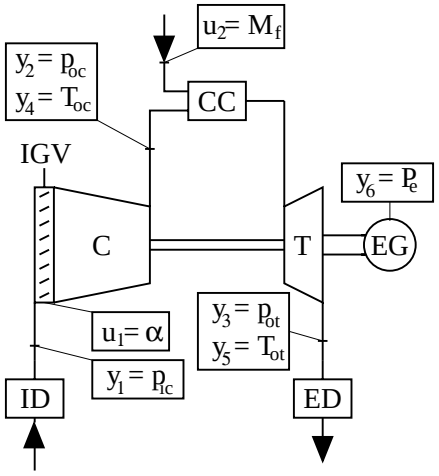

Figure 5.1: Layout of the single-shaft industrial gas turbine with highlighted the monitored sensors.

The gas turbine main features under ISO design conditions are shown in Tab. (5.1).
The measurement sensor of gas turbine rotational speed are not considered since the operation of the machine in parallel with electrical mains is at constant rotational speed.

The measurements of ambient temperature and relative humidity were also not considered, since they are not directly used by the gas turbine control system. The ambient temperature in particular, which is an important parameter for gas turbine performance, is taken into account by the machine control system by means of the measurements of compressor outlet pressure.

Air mass flow rate [kg/s]	24.4
Cycle pressure ratio (P_{oc}/P_{ic})	9.1
Electrical power (P_e) [kW]	5220
Exhaust temperature (T_{ot})[K]	796
Fuel mass flow rate (M_f) [kg/s]	0.388
IGV angle range ($\Delta\alpha$) [deg]	17

Table 5.1: Gas turbine main cycle parameters (ISO design conditions).

This pressure indeed depends on the compressor mass flow rate which, in turn, depends on ambient temperature [88].

The design of the different observer configurations necessary to isolate a fault regarding one of the input-output sensors requires the knowledge of a state-space model of the system under investigation.

The first step was the identification of a number of input-output models MISO equal to the number of the output variables.

The i-th model ($i = 1, \ldots, 6$) is driven by $u_1(t)$ and $u_2(t)$ and gives the prediction $\hat{y}_i(t)$ of the i-th output $y_i(t)$.

Other model input variables should be the boundary conditions (i.e., ambient pressure and temperature, fuel lower heating value and composition); they were not considered as model inputs since they were assumed to be constant.

The time series of data used to identify the models were generated with a nonlinear dynamic model which simulates the gas turbine operation. The nonlinear model was previously developed and validated by means of measurements taken during transients on a gas turbine in operation [88] and presents an accuracy of less than 1% for all the measured variables and for a range of ambient temperature $0 \div 40^oC$ and load conditions $70 \div 100\%$.

The time series of data generated with the nonlinear dynamic model simulates measurements taken on the machine with a sampling rate of 0.1 s and without noise due to measurement uncertainty which, instead, is always present in the real measurement systems.

In order to simulate the measurements taken on the actual instrumentation, the following noise signals were fixed:

- IGV angular position measurement:

  standard deviation of $\tilde{u}_1(t) = 1\%$ of the mean value of the signal $u_1(t)$ (α);

- fuel mass flow rate measurement:

  standard deviation of $\tilde{u}_2(t) = 2\%$ of the mean value of the signal $u_2(t)$ (M_f);

- pressure measurements:

  standard deviations of $\tilde{y}_1(t)$, $\tilde{y}_2(t)$, $\tilde{y}_3(t) = 0.4\%$ of the mean values of the signals $y_1(t)$ (p_{ic}), $y_2(t)$ (p_{oc}) and $y_3(t)$ (p_{ot}), respectively;

- compressor outlet temperature measurement:

  standard deviation of $\tilde{y}_4(t) = 0.6\%$ of the mean value of the signal $y_4(t)$ (T_{oc});

- turbine outlet temperature measurement:

  standard deviation of $\tilde{y}_5(t) = 0.7\%$ of the mean value of the signal $y_5(t)$ (T_{ot});

- electrical power measurement:

  standard deviation of $\tilde{y}_6(t) = 0.5\%$ of the mean value of the signal $y_6(t)$ (P_e);

These noise levels are typical of the standard instrumentation of the real industrial gas turbine used to validate the nonlinear dynamic model [87].

The procedure used to transform the input-output MISO model into state–space representation is available in literature [33].

Since these six state-space descriptions are driven by the same two inputs, they can be easily aggregated into a single MIMO model which is the starting point for the design of the different observer configurations.

This model was tested in different operating condition and it has always provided an output reconstruction error variable in the range of $10^{-3} \div 10^{-9}$.

The parameters of each input-output model have shown remarkable properties of robustness with respect to the amplitudes of the noises corrupting the data. As an example, Table (5.2) shows the parameter variations of the input-output model relative to the p_{ic} measurement versus the measurement noise. In this situation, the different measurement noises were assumed all of equal size.

Moreover, different time series of data generated by the gas turbine nonlinear model were exploited in order to identify the input-output models. These models have always provided an output reconstruction error lower than 10^{-3}.

Noise	0 %	2 %	10 %	20 %
α_2	-0.9963	-0.9941	-0.9513	-0.9325
α_1	1.9963	1.9949	1.9712	1.9486
β_{11}	0.9205	0.9368	0.9680	0.9458
β_{12}	-0.9176	-0.9455	-0.9682	-0.9864
β_{21}	0.0044	0.0178	0.0176	0.0220
β_{22}	-0.0044	-0.0092	-0.0108	-0.0197

Table 5.2: Parameter variation of the p_{ic} ARX model versus measurement noise.

In order to assess the technique for diagnosing sensor faults, gas turbine operating conditions with different sensor faults were simulated by using the nonlinear dynamic model of the machine.

Faults in single input-output sensors were generated by producing positive and negative variations (step functions of different amplitudes) in the input-output signals. A positive and negative fault occurring respectively at the instant of the minimum and maximum values of the observer residuals were chosen since these conditions represent the worst case in failure detection.

Moreover, it was decided to consider a fault during a transient since, in this case, the residual error due to model approximation is maximum (see Figures (5.2) and (5.5)) and therefore it represents the most critical case.

The fault occurring on the single sensor causes alteration of the sensor signal and of the residuals given by observers using this signal as input. These residuals indicate fault occurrence according to whether their values are lower or higher than the thresholds fixed in fault-free conditions.

In order to determine the thresholds above which the faults are detectable, the simulation of different amplitude faults in the sensor signals was performed. The threshold value depends on the residual error amount due to the ARX model approximation and on the real measurement noises $\tilde{u}(t)$ and $\tilde{y}(t)$. In Table (5.3) the values fixed for the observer residual thresholds are shown.

measurement	positive threshold	negative threshold
T_{oc}	+0.85	-0.85
T_{ot}	+0.20	-0.22
p_{ot}	+0.022	-0.024
p_{oc}	+0.55	-0.65
p_{ic}	+0.022	-0.0225
P_e	+2.0	-2.2
M_f	+1.1	-1.1
α	+0.27	-0.41

Table 5.3: Fault detectability thresholds.

The positive and negative thresholds were settled on the basis of fault-free residuals generated by different time series of simulated data. A margin of 10% between the positive and negative thresholds and the maximum and minimum values were respectively imposed.

In Figures (5.2), (5.3) and (5.4) an example of the residuals given by UIO (Section 4.2) for the diagnosis of M_f input sensor is shown.

In particular, Figure (5.2) shows the fault-free residual generated by the input observer driven by the signal of M_f input sensor and insensitive to the signal of IGV input sensor. In this condition, it is possible to determine the thresholds above which the fault on the M_f sensor can be detected.

The eigenvalues of the state distribution matrix of the UIO are placed near to 0.2 in order to maximize the fault detection sensibility and promptness and to minimize the occurrence of false alarms.

Figure (5.3) shows how a fault of +4% on the mean value of M_f signal at the instant of minimal residual value causes an abrupt change of the residual.

In Figure (5.4) the change of the residual at the instant of its maximum is instead due to a fault of -4% on the mean value of M_f signal. These fault amplitudes are the minimal detectable in order to identify the fault as soon as it occurs.

Figures (5.5), (5.6) and (5.7) illustrate an example of the diagnostic technique for output sensor fault regarding the p_{ot} signal.

Figure (5.5) shows the fault-free residual obtained from the difference between the values computed by the observer (Section 4.5) of the output $y_3(t)$ (p_{ot} signal) and the one given by the sensor.

Obviously, the non zero value of the residual is due to the identified model approximation

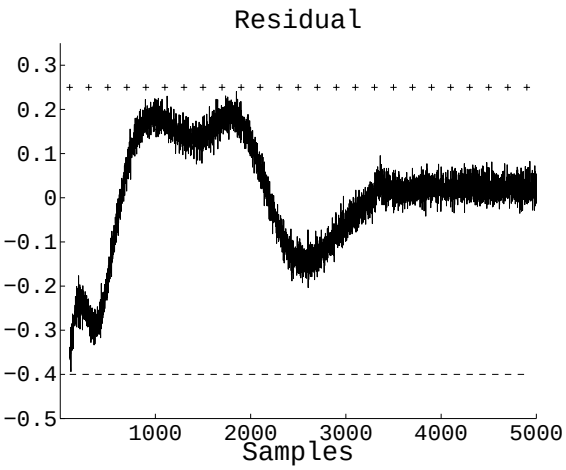

Figure 5.2: Fault-free residual function of the UIO driven by the M_f signal with minimum positive ('+') and negative ('-') thresholds.

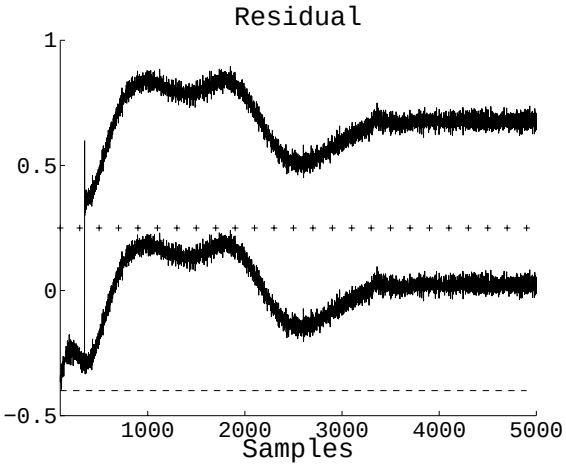

Figure 5.3: Residual function of the UIO driven by the M_f signal in the presence of positive failure.

and actual measurement noise.
The eigenvalues of the state distribution matrix of output observers are placed between 0 and 0.2 in order to maximize the fault detection sensibility and promptness and to minimize the occurrence of false alarms.

In Figure (5.6) the abrupt change of p_{ot} residual caused by a fault of +5% on the mean value of p_{ot} signal occurring at the instant of the minimum residual value is shown.
Figure (5.7) shows the behavior of the residual with the same fault as the previous case (changed sign) occurring when the residual itself assumes maximal value.

The instantaneous peaks which appear in Figures (5.6) and (5.7) are generated by the abrupt change related to the fault occurrence and may be used as incipient detector of anomalous

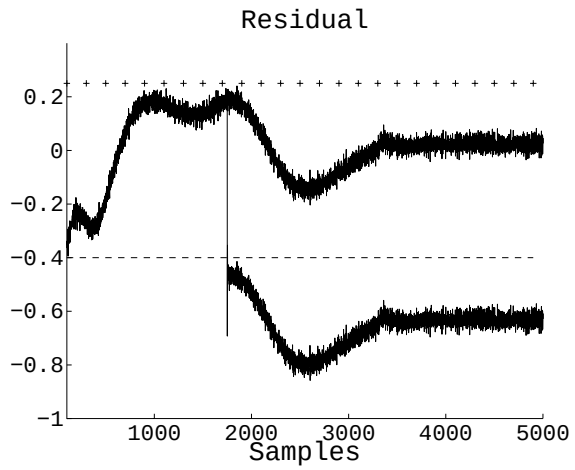

Figure 5.4: Residual function of the UIO driven by the M_f signal in the presence of negative failure.

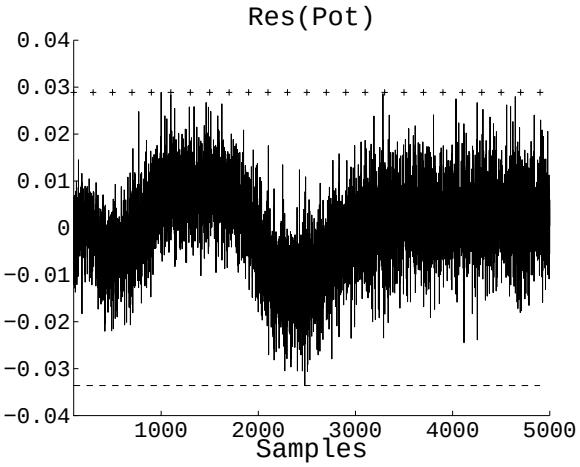

Figure 5.5: Fault-free residual function of output observer driven by p_{ot} signal with minimum positive ('+') and negative ('-') thresholds.

behavior of the sensors.

In order to analyze the diagnostic effectiveness of the FDI system in the presence of drifts in measurements, faults modeled by ramp functions were generated.

In Figures (5.8) and (5.9) the residual functions of the UIO observer driven by α signal and of the output observer regarding the T_{oc} signal are shown as an example. The two ramp faults start at the sample 2500 and reach constant final values at the sample 4000. These values are equal to 4% of the mean values of α and to 5% of the mean values T_{oc}.

To summarize the performance of the FDI technique, the minimal detectable faults on the various sensors referred to the mean signal values are collected in Table (5.4), in case of step faults, and in Table (5.5), in case of ramp faults.

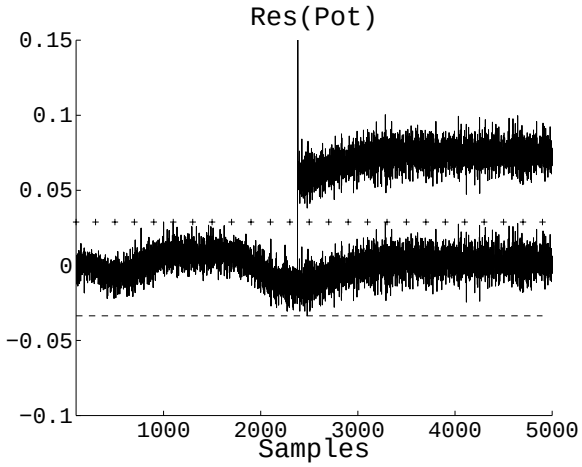

Figure 5.6: Residual function of output observer driven by p_{ot} signal with positive failure.

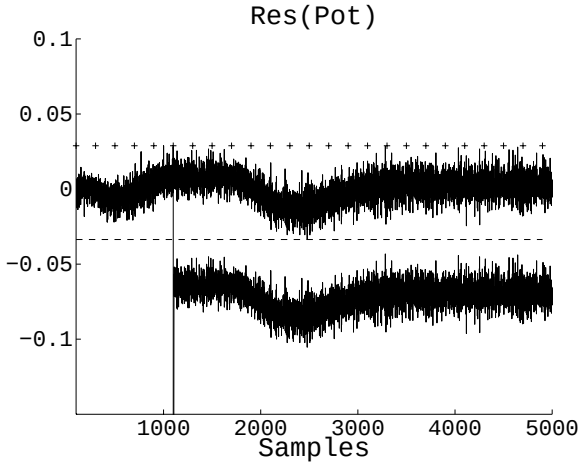

Figure 5.7: Residual function of output observer driven by p_{ot} signal with negative failure.

α	M_f	p_{ic}	p_{oc}	p_{ot}	T_{oc}	T_{ot}	P_e
4%	4%	5%	7%	5%	5%	2.5%	1.7%

Table 5.4: Minimal detectable step faults.

The minimum values shown in Table (5.4) are relative to the case in which the fault must be detected as soon as it occurs. If a delay in detection is tolerable the amplitude of the minimal detectable fault is lower.

Table (5.5) shows how ramp faults can not be immediately detected, since the delay in the corresponding alarm normally depends on fault mode.

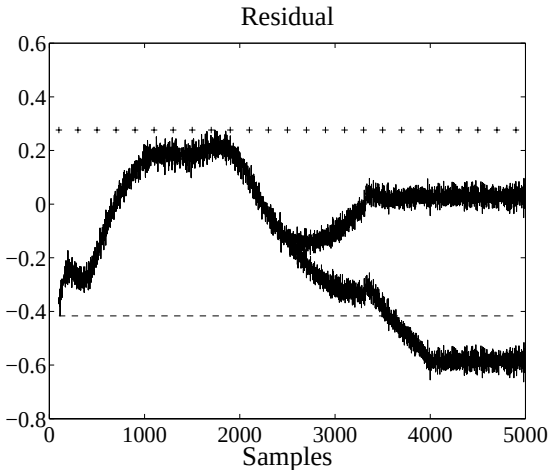

Figure 5.8: Residual function of the UIO driven by the α signal in the presence of a drift in the α measurement.

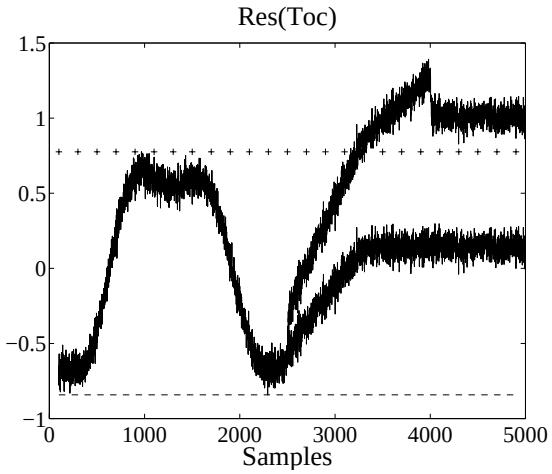

Figure 5.9: Residual function of the output observer regarding the T_{oc} signal in the presence of a drift in the T_{oc} measurement.

5.3 FDI of the Gas Turbine using Kalman Filters

In this section, a bank of KF is presented in order to diagnose malfunctions of the gas turbine sensors. This technique seems to be robust with respect to the modeling uncertainties, the system parameter variations and the measurement noise, which can obscure the performance of a fault detection system by acting as a source of false alarms [89].

The procedure exploited in this section requires the design of different KF configurations and the basic scheme is the standard one: a set of measured variables of the system is compared with the corresponding signals estimated by filters to generate residual functions.

The diagnosis can be performed by detecting the changes of these residuals caused by a fault.

measurement	fault	detection delay [s]
T_{oc}	5 %	50
T_{ot}	3 %	100
p_{ot}	5.5 %	75
p_{oc}	7.5 %	0
p_{ic}	6 %	50
P_e	6 %	100
M_f	4 %	150
α	4 %	100

Table 5.5: Minimal detectable ramp faults.

The fault diagnosis of input sensors uses a number of KF equal to the number of input variables. Each filter is designed to be insensitive to a different input of the system. Output sensor faults affecting a single residual are detected by means of a classic KF, driven by a single output and all the inputs of the system.

The results and improvements obtained by using this technique are compared with the ones presented in Section 5.2.

Also the design of the different KF configurations necessary to isolate a fault in one of the input-output sensors requires the knowledge of a state-space model of the system under investigation.

Measurement noises $\tilde{\mathbf{u}}(t)$ and $\tilde{\mathbf{y}}(t)$ with standard deviations reported in Table (5.6) were then added to the input-output time series generated with the nonlinear model.

α	M_f	p_{ic}	p_{oc}	p_{ot}	T_{oc}	T_{ot}	P_e
1.08 deg	0.0076 kg/s	0.41 KPa	3.66 kPa	0.41 kPa	3.59 K	5.59 K	23.90 kW

Table 5.6: Measurement noise standard deviation.

As recalled in Section 4.5, the detection strategy which is commonly chosen in connection with KF methods for failures detection, consists in monitoring the residuals or KF innovations.

Because of the linear property of the model and because of the additive effect of the faults on the system, it may easily be shown that the effect of the change on the innovation is also additive.

Any abrupt change in measurements due to a fault is reflected in a change in the mean value and in the standard deviation of innovations.

In particular, since the KF produces zero-mean and independent white residuals with the system in normal operation, a method for FDI consists in testing how much the sequence of innovations has deviated from the white noise hypothesis. As explained in Section 2.7, the tests which are performed on the innovations $r(t)$ are the usual ones for zero-mean and variance, as cumulative sum algorithms

$$\overline{r}(t) = E[r(t)] = \frac{1}{t}\sum_{j=1}^{t} r(j) \tag{5.1}$$

and

$$\sigma_r^2(t) = E[r^2(t)] = \frac{1}{t}\sum_{j=1}^{t} r^2(j) \tag{5.2}$$

and independence, as χ^2-type

$$\begin{aligned} R_r^t(\tau) &= \frac{1}{t}\sum_{j=1}^{t} r(j)r(j+\tau), \\ \zeta_r^M(t) &= \frac{t}{R_r^t(0)^2}\sum_{\tau=1}^{M}\left(R_r^t(\tau)\right)^2 \end{aligned} \tag{5.3}$$

computed in a growing window. The parameter $\zeta_r^M(t)$ is a chi-squared random variable with M degrees of freedom.

If a system abnormality occurs, the statistics of $r(t)$ change, so the comparison of $\overline{r}(t)$ and $\zeta_r^M(t)$ with a threshold ϵ fixed under no faults conditions, becomes the detection rule (2.14). In particular, such threshold can be settled as in a Section 5.2 or, with the aid of chi-squared tables, $\epsilon = \chi_\beta^2(M)$ can be computed as a function of the false-alarms probability β and of the window size M.

As in Section 5.2, in order to determine the thresholds above which the faults are detectable, the simulation of different amplitude faults in the sensor signals was performed. Now threshold values depend on the residual error amount due to the model approximation and on the real measurement noises $\tilde{\mathbf{u}}(t)$ and $\tilde{\mathbf{y}}(t)$.

In Figures (5.10), (5.11) and (5.12) the examples of the statistical tests (5.1), (5.2) and (5.3), respectively, of the residual generated by the KF with unknown input for the diagnosis of α input sensor are shown.

In particular, Figure (5.10) shows the mean value computed by Eq. (5.1) and generated by the KF driven by the signal of α input sensor and insensitive to the signal of the M_f input sensor. A fault of 3% on the maximal value of α signal causes an abrupt change in the mean value of the residual computed in a growing window.
Such fault also affects the standard deviation of the same residual, as depicted in Figure (5.11). The standard deviation was computed by using Eq. (5.2) in a growing window. The thresholds (marked with '+' and '-') were fixed in fault-free conditions as well as by imposing an acceptable false-alarms rate.

Figure (5.12) shows how the same fault causes a change in the whiteness of the residual given by Eq. (5.3). The whiteness value of 20.1 was calculated by assuming that $M = 8$ and $\beta = 0.05$.

Under this condition, it is possible to determine the limit values above which the fault on the α sensor (and also the M_f sensor) can be detected.

It is important to note that, in order to achieve the maximal input fault detection capability, the residual corresponding to the most sensitive filter to a failure on the α input was selected. Figures (5.13), (5.14) and (5.15) illustrate an example of the previous statistical tests for the output sensor fault of 2% on the maximal value of p_{ic} signal occurring at the sample $t = 1500$.

Figure (5.13) shows the mean value (5.1) of the residual obtained from the difference between the values computed by the KF regarding the output $y_1(t)$ (p_{ic} signal) and the ones measured

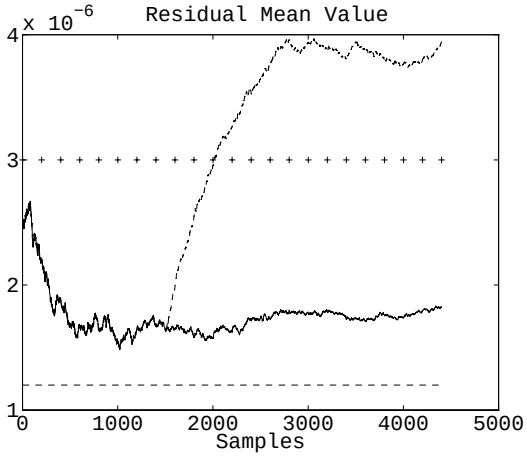

Figure 5.10: Mean value of the residual computed by using KF with unknown input in a growing window.

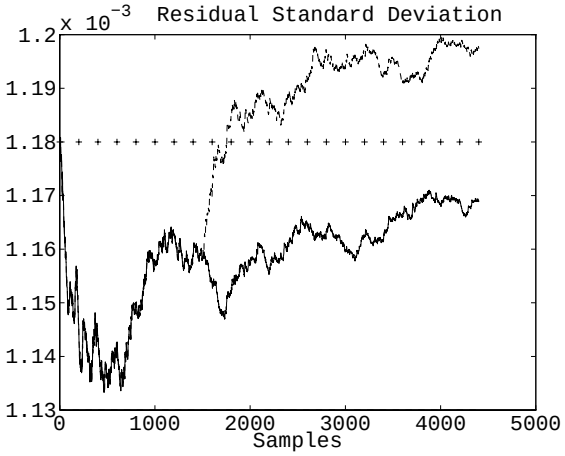

Figure 5.11: Standard deviation of the residual computed by using a KF with unknown input in a growing window.

by the sensor. Obviously, the non-zero value of the residual in fault-free conditions is due to the model approximation and to the actual measurement noise.
Figure (5.14) shows the behavior of the standard deviation (5.2) of the residual with the same fault as the previous case.
Figure (5.15) shows the abrupt change in the whiteness (5.3) of p_{ic} residual.
Tables (5.7) and (5.8) summarize the performance of the enhanced fault detection and isolation technique and collect the minimal detectable fault on the various sensors, in case the mean value and the whiteness of the residuals are respectively monitored.

The minimal detectable fault values in Tables (5.7) and (5.8) are expressed as percentage of the maximal signal values and are relative to the case in which the occurrence of a fault must be detected as soon as possible.

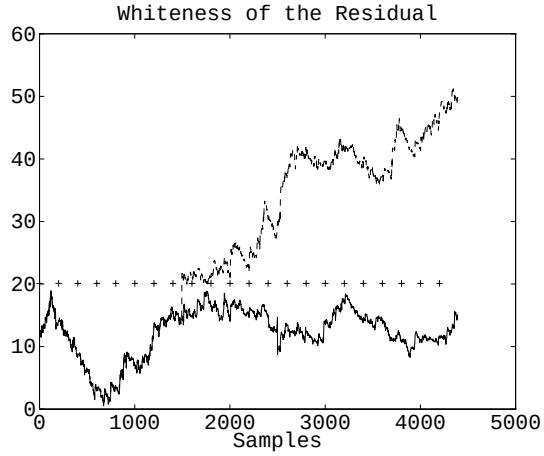

Figure 5.12: Whiteness of the residual computed by using a KF with unknown input in a growing window.

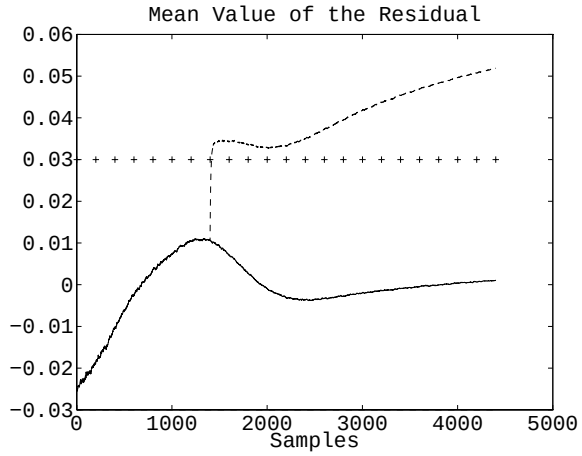

Figure 5.13: Mean value of p_{ic} residual computed by using a growing window.

α	M_f	p_{ic}	p_{oc}	p_{ot}	T_{oc}	T_{ot}	P_e
3%	3%	2.5%	4%	1.5%	2%	2.5%	3%

Table 5.7: Minimum detectable faults by monitoring residual mean value .

α	M_f	p_{ic}	p_{oc}	p_{ot}	T_{oc}	T_{ot}	P_e
2%	2.5%	0.75%	1%	0.75%	2%	0.8%	1.5%

Table 5.8: Minimum detectable faults by monitoring residual whiteness.

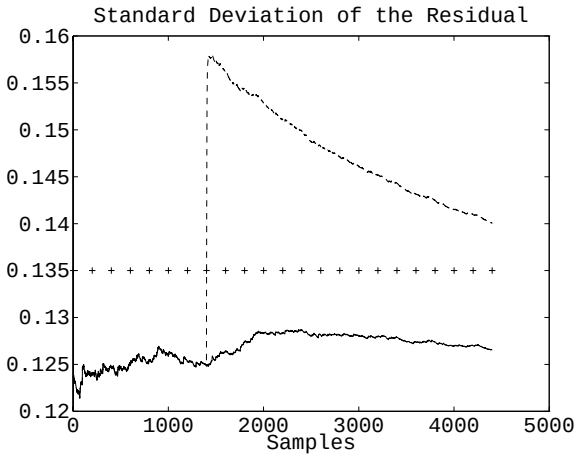

Figure 5.14: Standard deviation of p_{ic} residual computed by using a growing window.

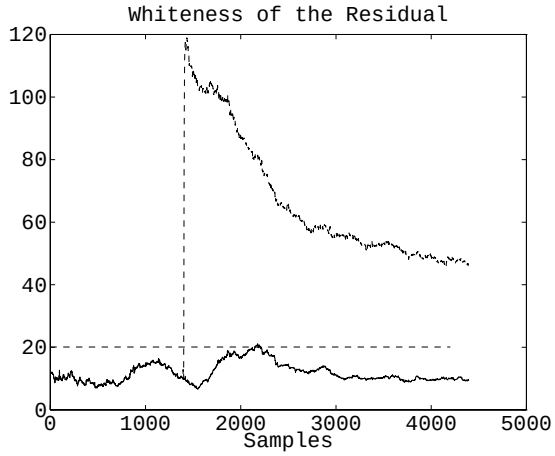

Figure 5.15: Whiteness of p_{ic} residual computed by using a growing window.

In order to compare improvements with this fault detection and isolation technique, the minimal detectable faults obtained by using observers and geometrical analysis of residuals collected in Table (5.4) in Section 5.2 have to be considered.

It ensues that the values of the faults obtained by using statistical tests on KF innovations, collected in Tables (5.7) and (5.8), are lower than the ones reported in Table (5.4).

5.4 Sensor Fault Identification Using Neural Networks

In this section, the problem of detect and isolate the occurrence of faults regarding control sensors of the single shaft industrial gas turbine is studied [90, 91].

Faults modeled by step functions create changes in several residuals obtained by using dynamic observers of the process under examination.

A NN is exploited in order to find the connection from a particular fault regarding input and output sensors to a particular residual. In such a way the observers generate a residual outputs which not depend on the dynamic characteristics of the plant, but only on sensors faults. Therefore, the NN classify static patterns of residuals, which are uniquely related to particular fault conditions independently from the plant dynamics.

A NN is exploited in order to find the connection from a particular fault regarding input and output sensors to a particular residual. In such a way the observers generate a residual outputs which not depend on the dynamic characteristics of the plant, but only on sensors faults. Therefore, the NN classify static patterns of residuals, which are uniquely related to particular fault conditions independently from the plant dynamics.

A number of residuals equal to the number of the outputs of the process is obtained by difference between the values computed by observers and the ones measured by the sensors.

The detection and isolation of output sensor faults is indeed very easy, since each output measurement is directly connected to a single residual generator. This lucky situation does not hold for the inputs, and the relation between input faults and residuals should be determined.

Solution of such problem was obtained by monitoring changes in residuals by means of a geometrical analysis of residuals or it can be implemented by using special testing methods, e.g. a whiteness and a chi-squared test of the residual of the KF. A solution instead exploiting the learning capability of NN is presented.

In order to find the relationships existing between input sensor faults and residuals, the NN is applied in order to classify the residual computed by observers according to the operation of the process. In such a case the decision methods by using classification do not need to take into account the dynamic property of the process, as the observers residuals not depend on it.

The classification method is typically an off-line procedure in which the fault mode is first defined and the data (residuals) is collected.

The classification of process residuals can be carried out in accordance to the information about different faults. Then, it is known that certain residual patterns correspond to the normal operation and other patterns correspond to the faulty operation. With this kind of data the training of the NN is performed.

The NN implemented by the Neural Network Toolbox for MATLAB are *Multilayer Perceptron* and *Radial Basis Function* NN described in Section 4.10. They are both able to approximate any continuous function with an arbitrary degree of accuracy, provided with a sufficient number of neurons.

The technique for input-output sensor fault detection, isolation and identification presented in this section was applied to the gas turbine simulated model of Figure (5.1) introduced in Section 5.2.

Firstly, a RBF network has been considered.

The simulations basically concern two aspects, namely the generation of pattern for the NN training and the fault diagnosis validation. The first step regarded the generation of pattern of residuals and fault signals.

The training set includes simulated faults on the sensors of variables M_f and IGV. A six inputs-one output RBF network has been trained by using steady-state residual sequences composed of 1100 samples and shown in Figures (5.16) and (5.17).

Figure (5.16) shows the six steady-state residuals used as inputs for the training of the network whilst Figure (5.17) corresponds to the output target.

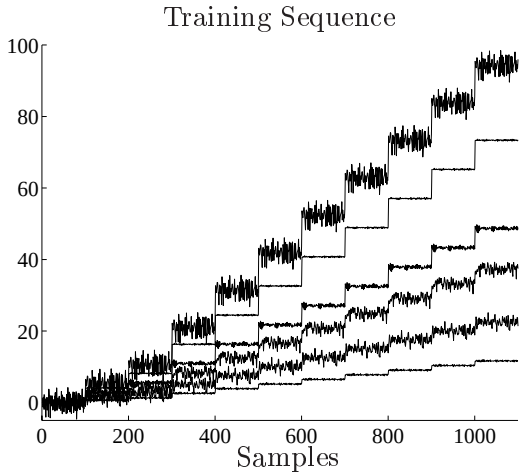

Figure 5.16: NN input pattern

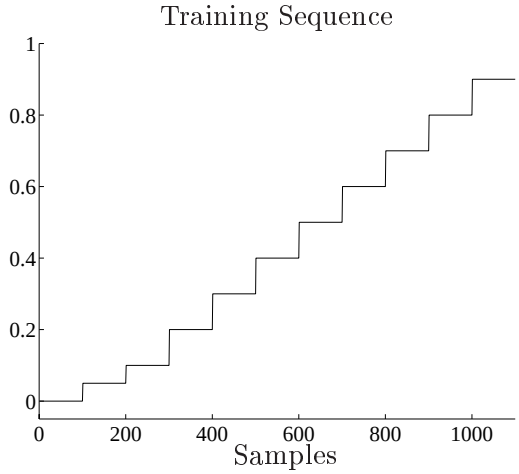

Figure 5.17: Output pattern of the NN.

The sequences considered comprise 11 fault conditions, namely no fault and faults varying from a 5%, 10% to 90% of the maximum value of input measurements. Each fault condition is composed of 100 samples.

The network training is performed with a trial and error procedure to arrange the number of hidden neurons in respect to the network output error. Even if an output error goal (SSE) of less than 0.1 was reached (sometimes with more than 100 hidden neurons), generalization properties were unsatisfactory.

A different supervised NN architecture was then considered, namely a feed-forward MLP network [90]. Such a NN consists of an input layer, one or more hidden layers and an output layer. A six inputs-one output MLP network was designed with one hidden layer. Since the network is used as function approximator, in the input and hidden layers sigmoidal neurons were implemented, whilst the output layer was made of a single linear neuron. A back-propagation

algorithm with adaptive learning rate was exploited to update network parameters.

The training patterns were the ones used for the RBF network. The selection of training parameters in the back-propagation algorithm as well as the tuning of the number of hidden neurons of the network were difficult. In particular the convergence of the network depends on the number of the neuron in the hidden layer. The momentum term has varied in a range of $0.7 \div 0.9$.

In the Tables (5.9) and (5.10), the results of training sessions regarding the inputs M_f and IGV are shown, respectively, for different values of neurons and epochs.

Input layer	Hidden layer	SSE after 70000 epochs
15	15	0.27
15	20	0.264
20	50	**0.127**

Table 5.9: Training results concerning the M_f sensor.

Input layer	Hidden layer	SSE after 70000 epochs
15	15	0.17
15	20	0.24
20	30	**0.108**

Table 5.10: Training results concerning the IGV sensor.

Even if the SSE value is usually fixed in a range of $0.01 \div 0.001$, due to the noisy environment, the network architectures providing the lowest SSE were chosen. These values allow estimating the input sensor fault amplitude with an accuracy of at least 1%. Minimal fault values concerning both input sensors are collected in the Table (5.11). They are indicated by (NN). These minimum detectable faults can be compared with the ones obtained by using statistical tests on KF innovations as well as geometrical analysis of residuals generated by means of output dynamic observers.

Method	M_f	IGV
(NN)	3%	2.5%

Table 5.11: Minimal detectable step faults.

The fault sizes are expressed as per cent of the mean signal values.

It can be noted how the values of the faults obtained by using statistical tests on KF innovations are lower than the ones obtained with geometrical analysis of dynamic observer residuals and they appear comparable to the ones estimated by NN. However, the minimal detectable faults on the various input sensors seem to be adequate to the industrial diagnostic applications. The improvements achieved are not free of charge: they have been obtained with a procedure of greater complexity and, consequently, with a growing computational cost.

5.5 Power Plant of Pont sur Sambre Identification and FDI

The technique for robust output sensor FDI introduces in Section 4.7 was applied to real data from the 120MW power plant of Pont sur Sambre [92]. It consists of a double-shaft industrial gas turbine working in parallel with electrical mains.

The block-diagram of the plant is shown in Figure (5.18) where the numbers refer to: 1 - super heater (radiation), 2 - super heater (convection), 3 - super heater, 4 - reheater, 5 - dampers, 6 - condenser, 7 - drum, 8 - water pump and 9 - burner.

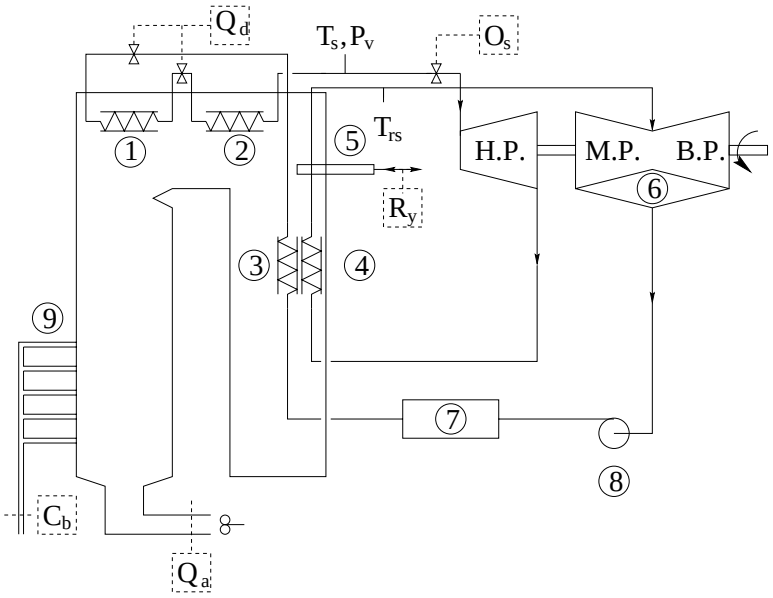

Figure 5.18: The structure of the power plant.

The available data from the control inputs were 2200 samples from normal operating records of C_b (gas flow), O_s (turbine valves opening), Q_d (super heater spray flow), R_y (gas dampers) and Q_a (air flow). The data from the output sensors were the corresponding values of P_v (steam pressure), T_s (main steam temperature) and T_{rs} (reheat steam temperature). The sampling time was of 10 seconds and since this value is very little with respect to the time constants of the plant, it has been increased to about 60 seconds. The number of samples has thus been reduced to 367. Their plots are reported in Figures (5.19) and (5.20).
The computational procedure which has been performed on the data is the identification of the triple (A_i,B_i,C_i) and of disturbance distribution matrix E_i (4.27) from the equation error model ($i = 1, \ldots, m$) corresponding to the MISO subsystem (4.27) which links each output with the five ($r = 5$) inputs (see Chapter 3). Moreover, the triple (A,B,C) from the EIV model and the estimation of the input-output noise variances were obtained. The matrices A, B and C were obtained by grouping the A_i, B_i and C_i ($i = 1, \ldots, m$) corresponding to the MISO subsystem which links each output with the five ($r = 5$) inputs. Three subsystems ($m = 3$) with order two have thus been considered.

The design of the UIO (4.28) requires, in fact, the knowledge of a minimal form model

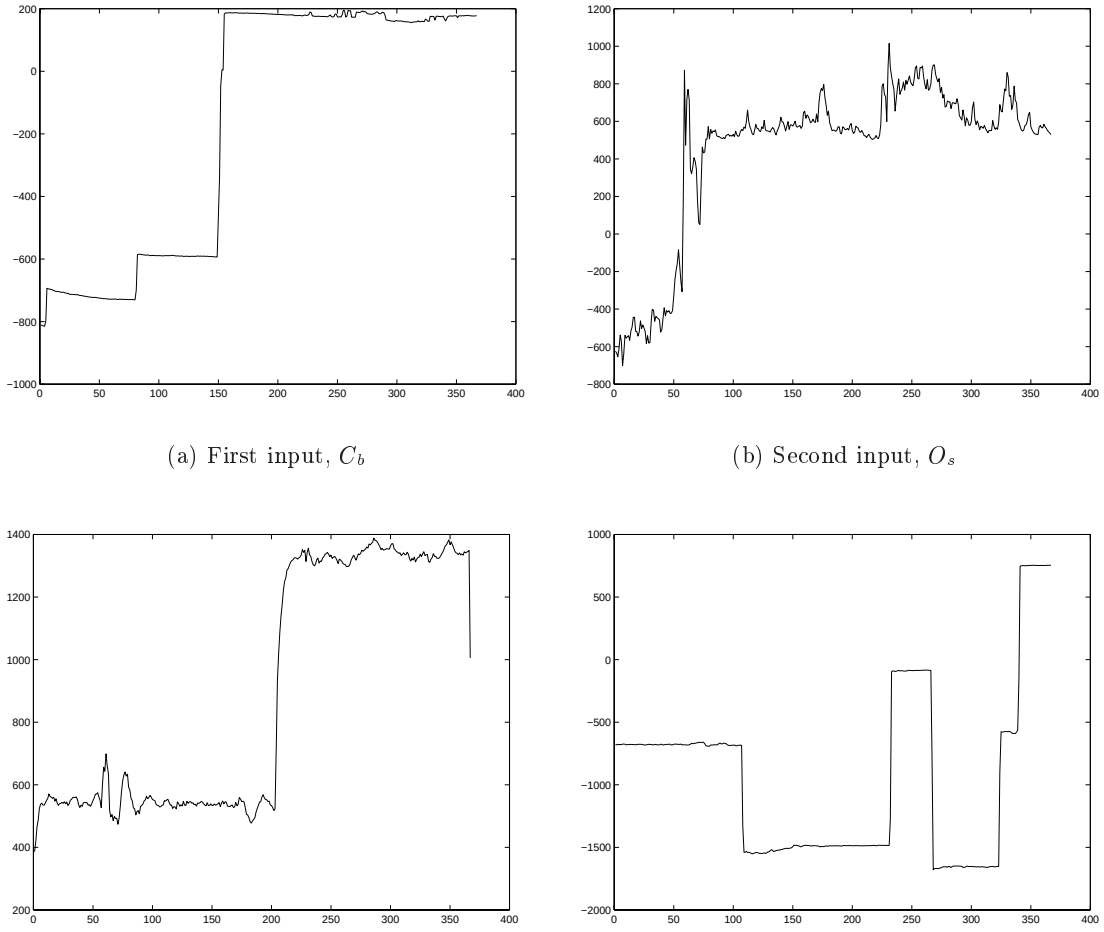

(a) First input, C_b

(b) Second input, O_s

(c) Third input, Q_d

(d) Fourth input, R_y

Figure 5.19: First four input of the power plant.

(A, B, C) for the system under investigation.

The determination of the order of every subsystem has been performed by considering the FPE, AIC and MDL identification criteria [33].

Faults in a single output sensor were generated by producing positive and negative variations (step and ramp functions of different amplitudes) in the output signals. A positive and negative fault occurring respectively at the instant of the minimum and maximum values of the observer were chosen since these conditions represent the worst case in failure detection.

Moreover, it was decided to consider a fault during a transient since, in this case, the residual error due to model approximation is maximum and therefore it represents the most critical case.

The fault occurring on the single sensor causes alteration of the sensor signal and of the residuals given by observers and filters using this signal as input. These residuals indicate fault occurrence according to whether their values are lower or higher than the thresholds fixed in

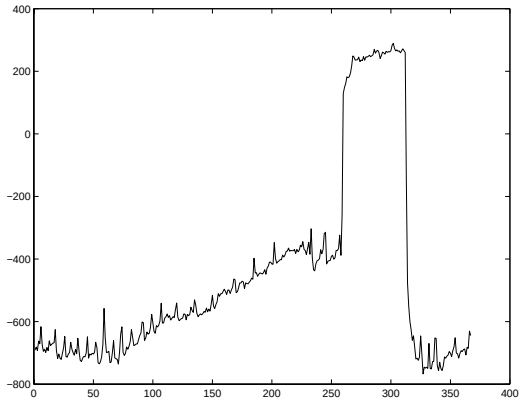

(a) Fifth input, Q_a

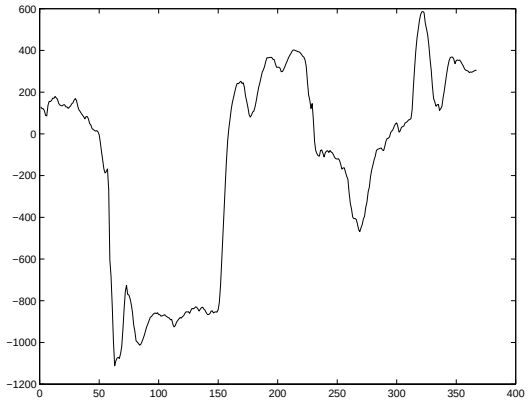

(b) First output, P_v

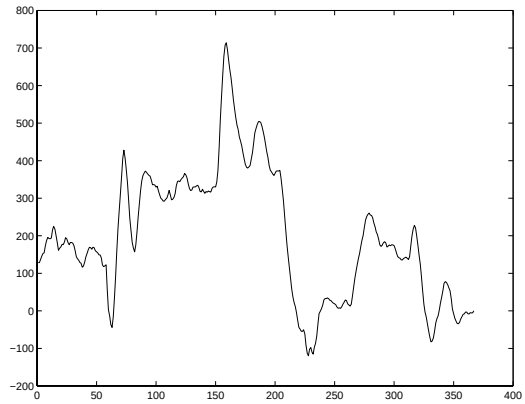

(c) Second output, T_s

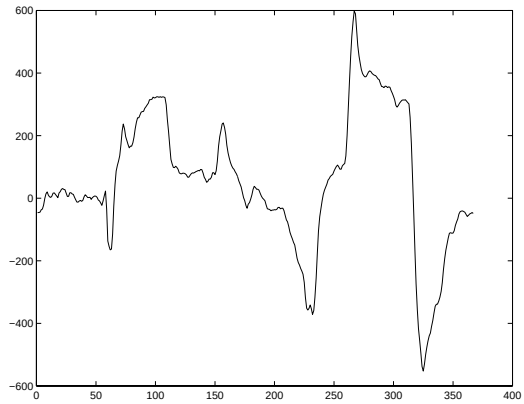

(d) Third output, T_{rs}

Figure 5.20: Last input and three output of the power plant.

fault-free conditions.

In order to determine the thresholds above which the faults are detectable, the simulation of different amplitude faults in the sensor signals was performed. The threshold value depends on the residual error amount due to the model approximation. These thresholds were settled on the basis of fault-free residuals. A margin of 10% between the thresholds and the residual values was imposed.

In Figures (5.21) and (5.22) an example of the residuals given by UIO (4.28) for the diagnosis of O_s input sensor is shown.

In particular, Figure (5.21) shows the fault-free residual generated by the input observer driven by the signal of O_s input sensor $u_2(t)$ and insensitive to the signal of C_b input sensor $u_1(t)$. In this condition, it is possible to determine the thresholds above which the fault on the O_s sensor can be detected.

The eigenvalues of the UIO state distribution matrix (Equations (4.18) with $i = 1$) of the

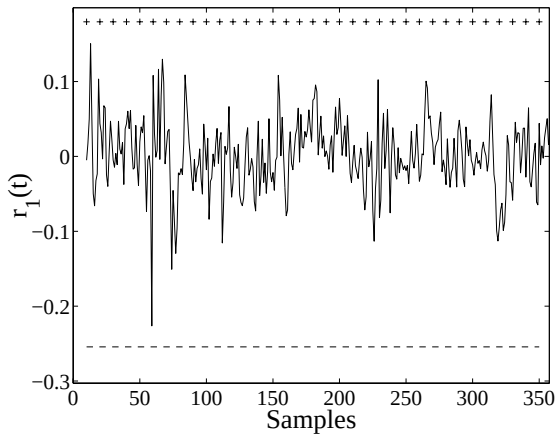

Figure 5.21: Fault-free residual function $r_1(t)$ of the UIO driven by the O_s signal with minimum positive ('+') and negative ('-') thresholds.

input observer are placed near to 0.2 in order to maximize the fault detection sensibility and promptness and to minimize the occurrence of false alarms.

Figure (5.22) shows how a fault of 25% on the mean value of O_s signal at the sample $T = 150$ causes an abrupt change of the residual.

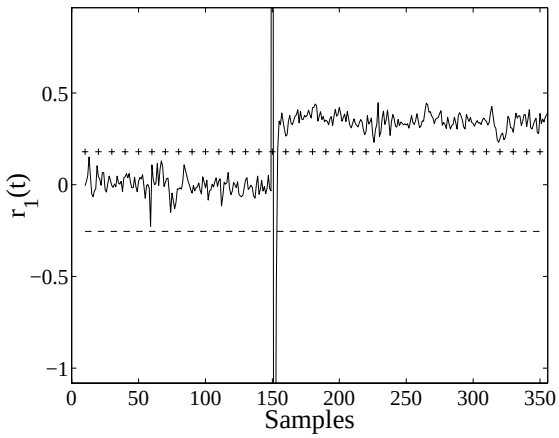

Figure 5.22: Residual function $r_1(t)$ of the UIO driven by the O_s signal in the presence of a failure.

Figures (5.23) and (5.24) illustrate an example of the diagnostic technique for output sensor fault regarding the T_{rs} signal.

Figure (5.23) shows the fault-free residual (Eq. (4.11)) obtained from the difference between the values computed by the observer of the output $y_3(t)$ (T_{rs} signal) and the one given by the sensor $y_3(t)$. Obviously, the non zero value of the residual is due to the ARX model approximation and actual measurement noise.

The eigenvalues of the state distribution matrix (matrix $(A^i - K^i C^i)$ in Eq. (4.11) with $i = 3$)

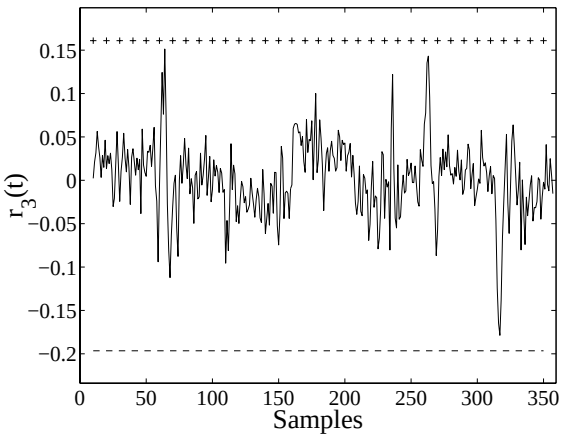

Figure 5.23: Fault-free residual function $r_3(t)$ of output observer driven by T_{rs} signal with minimum positive ('+') and negative ('-') thresholds.

of output state observer are placed between 0 and 0.2 in order to maximize the fault detection sensibility and promptness and to minimize the occurrence of false alarms.

In Figure (5.24) the abrupt change of T_{rs} residual caused by a fault of 10% on the mean value of T_{rs} signal occurring at the instant of $T = 150$ is shown.

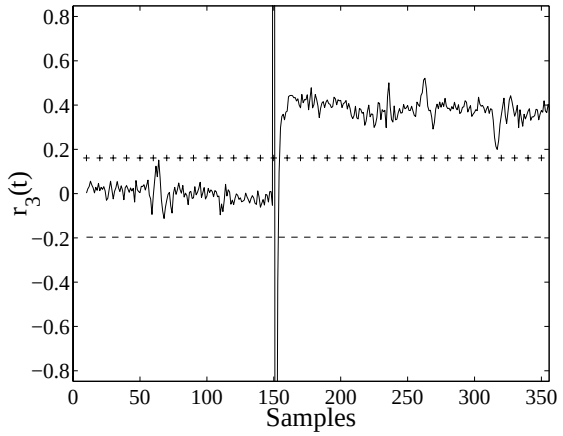

Figure 5.24: Residual function $r_3(t)$ of output observer driven by T_{rs} signal with a failure.

The instantaneous peaks which appear in Figures (5.22) and (5.24) are generated by the abrupt change related to the fault occurrence and may be used as incipient detector of anomalous behavior of the sensors.

To summarize the performance of the FDI technique using classical observers and UIO, the minimal detectable failures on the various sensors referred to the mean signal values are collected in Table (5.12), in case of step and ramp faults.
Finally, Table (5.13) reports the mean square values of the output estimation errors corresponding to the state–space systems obtained by the equation errors models in deterministic case.

Sensor	C_b	O_s	Q_d	R_y	Q_a	P_v	T_s	T_{rs}
Step	30%	25%	20%	40%	45%	15%	5%	10%
Ramp	40%	30%	35%	55%	50%	40%	20%	30%

Table 5.12: Minimal detectable step and ramp faults with classical observers and UIO.

An improvement on the performance of the FDI device was obtained by using classical KF and UIKF. The noises affecting the input–output measurements were identified by using the Frisch scheme method.

Output	P_v	T_s	T_{rs}
Equation error	0.0146	0.0273	0.0051

Table 5.13: The three output estimation errors with equation error models.

Also in this case, the comparison of the residuals with the thresholds fixed under no fault conditions remains the detection rule.

Table (5.14) shows the minimal detectable faults in stochastic case.

Sensor	C_b	O_s	Q_d	R_y	Q_a	P_v	T_s	T_{rs}
Step	25%	15%	12%	35%	35%	10%	3%	5%
Ramp	35%	20%	20%	45%	40%	30%	5%	8%

Table 5.14: Minimal detectable step and ramp faults with classical KF and UIKF.

Table (5.15) reports the mean square values of the output estimation errors when EIV models identified by the dynamic Frisch scheme are used.

Output	P_v	T_s	T_{rs}
EIV	0.0026	0.0018	0.0012

Table 5.15: The three output estimation errors with EIV models.

Compared with the ones concerning the deterministic case, the output estimation errors with EIV models are smaller because the noise rejection is achieved by means of the dynamic Frisch scheme. Consequently, the residuals obtained by KF are more sensitive to a fault occurring on the sensors. Moreover, smaller thresholds can be placed on the residual signals to declare the occurrence of faults.

5.6 Disturbance Decoupled Observers for Sensor FDD

Under the hypothesis that the system under investigation can be described as an equation error model, this section has presented the method of obtaining the disturbance distribution matrix

from the fault-free system data, by taking into account the equation error term. The UIO performing the disturbance decoupling can be designed from the equation error model [93].

The identification scheme exploited to extract the disturbance distribution matrix from input-output data was illustrated in Section 4.7. In previous section the characteristics of the industrial process, such as the 120MW power plant of Pont sur Sambre, used to illustrate the method proposed in this thesis, were shown. The results obtained by using UIO which perform the diagnosis of faults regarding output sensors are shown below. These results can be compared with the ones obtained without disturbance decoupling recalled in Section 5.5.

Table (5.16) reports the mean square values of the output estimation errors given by the FDI observers without disturbance decoupling. These values are very large and they cannot be used to detect faults reliability.

Slight better results than the previous ones have been obtained by using a technique presented in [89] where the process was described as an errors-in-variables model and the Frisch scheme dynamic system identification was performed (Section 3.3).

KF were exploited to detect step and ramp faults.

P_v	T_s	T_{rs}
581.25	51.46	55.88

Table 5.16: The three output estimation errors without disturbance decoupling.

The mean square errors of the output estimation errors obtained by using the KF are collected in Table (5.17).

Output	P_v	T_s	T_{rs}
KF	181.92	28.42	33.69

Table 5.17: The three output estimation errors with KF.

A meaningful improvement on the performance of the FDI device was obtained by using the UIO exploiting the disturbance decoupling technique presented in Section 4.7.

Table (5.18) shows the minimal detectable faults concerning system outputs in case of disturbance decoupling.

Sensor	P_v	T_s	T_{rs}
Step	5%	1%	1.7%
Ramp	20%	4.5%	4.7%

Table 5.18: Minimal detectable step and ramp faults with UIO.

Table (5.19) reports the mean square values of the output estimation errors when UIO is used.

Compared with the ones concerning classical observers, residuals are very small because disturbance decoupling is achieved, and consequently, their increase can be significantly detected when a fault occurs on the sensors. Moreover, smaller thresholds can be placed on the residual signals to declare the occurrence of faults.

This demonstrates the improved efficiency of the FDI technique when decoupling of disturbances is performed.

Output	P_v	T_s	T_{rs}
UIO	20.45	12.24	15.55

Table 5.19: The three output estimation errors with disturbance decoupling.

5.7 Fuzzy Models and Fault Diagnosis of an Industrial Process

This section proposes an approach for FDI in the power plant of Pont sur Sambre using the multiple model approach presented in Section 3.11.

Such a technique concerns the identification and design of a fuzzy system based on Takagi-Sugeno fuzzy models.

The nonlinear dynamic process is, in fact, described as a composition of several TS models selected according to the process operating conditions.

The FDI scheme adopted to generate residuals exploits the nonlinear TS fuzzy model [94].

With reference to the fuzzy identification method presented in Section 3.11 and implemented using the Fuzzy Modeling and Identification Toolbox for Matlab [79] the GK clustering algorithm was used with $M = 4$ clusters for each output (operating conditions) and $n = 3$ the number of shifts of inputs and outputs.

After clustering, the system parameters θ_i, with $i = 1, \cdots, M$ for each output, were estimated using the dynamic Frisch scheme identification method. The model was then validated on a separate data set.

In fault-free conditions, Table (5.16) reported the mean square values of the output estimation errors $\mathbf{r}(t)$ given by classical observers using a single model for all operating conditions. These values are very large and they cannot be used to detect faults reliability.

A meaningful improvement has been obtained by using the identification technique presented in Section 3.11 where the process is described as a collection of fuzzy TS models identified using Frisch scheme method.

The i-th output $y_i(t)$ of the plant ($i = 1, \cdots, m$ and $m = 3$) can be characterized as a TS fuzzy multiple-input single-output (MISO) model (3.41) with $r = 5$ inputs.

The mean square errors of the output estimation errors $\mathbf{r}(t)$, under no-fault conditions, are collected in Table (5.20).

Output	P_v	T_s	T_{rs}
Multiple model approach	10.46	8.90	6.91

Table 5.20: The three output estimation errors with fuzzy multiple model.

The corresponding results are shown in Figures (5.7), (5.7) and (5.7).
These figures compares the outputs of the plant calculated using the fuzzy multiple model with the actual process outputs on a validation data set.

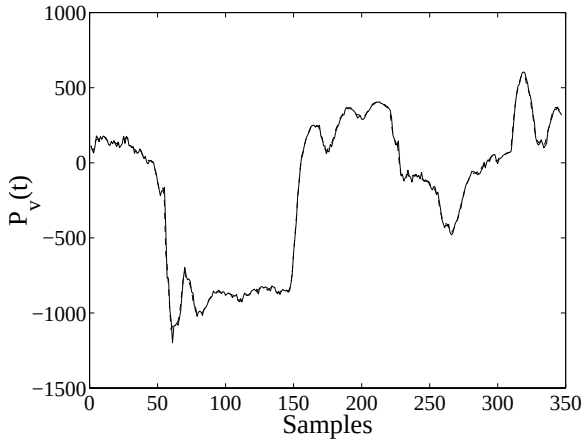

Figure 5.25: Predicted and measured $P_v(t)$ output.

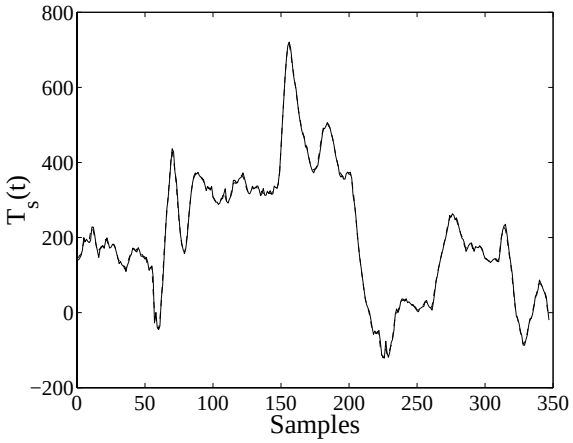

Figure 5.26: Predicted and measured $T_s(t)$ output.

Therefore, as depicted in Figure (5.28), residuals can be generated by the comparison of the measured and estimated outputs.

$$\mathbf{r}(t) = \hat{\mathbf{y}}(t) - \mathbf{y}(t). \tag{5.4}$$

The dashed line corresponds to the i-th predicted output ($i = 1, \cdots, 3$), $\hat{y}_i(t)$, and the solid line to the measured one, $y_i(t)$. The fuzzy multiple model approximates the real process very accurately.

The results indicate that the composite model can serve as reliable predictor for the real process. Using this model, a model-based approach for fault diagnosis can be exploited and applied to the actual power plant.

Single faults were generated by adding step and ramp signals in the input and output measurements. It was decided to consider fault occurrences during a transient since, in this case, the residual error due to model approximation is maximum and therefore it represents the most

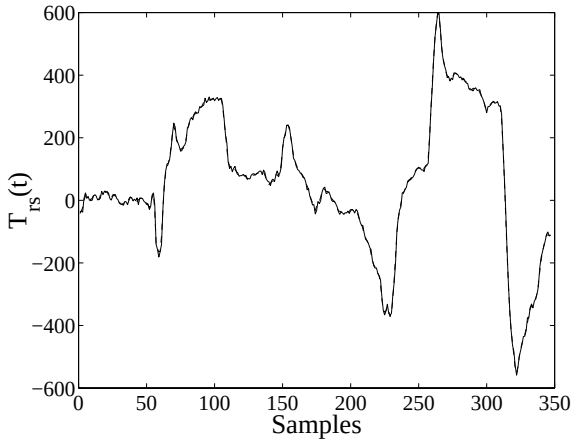

Figure 5.27: Predicted and measured $T_{rs}(t)$ output.

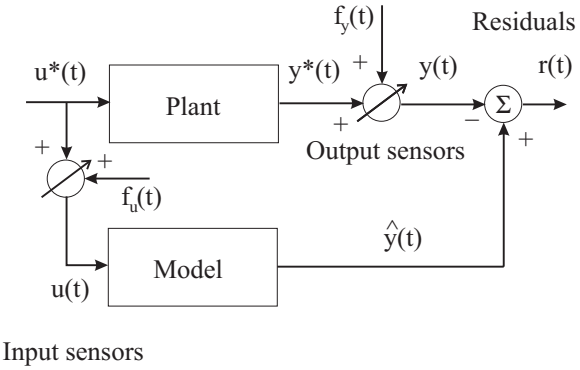

Figure 5.28: The residual generation scheme.

critical case in failure detection.

The fault occurring on the system output causes alteration of the signal $\mathbf{y}(t)$ and of the residuals $\mathbf{r}(t)$ given by the predictive model (3.41) using $\mathbf{u}(t)$ as input. Residuals indicate fault occurrence according to (2.14) whether their values are lower or higher than the thresholds fixed in fault-free conditions.

To summarize the performance of the FDI technique, the minimal detectable faults on the various outputs, expressed as per cent of the mean values of the relative signals, are collected in Table (5.14), in case of step and ramp faults.

The minimum values shown in Table (5.14) are relative to the case in which the fault must be detected as soon as it occurs.

The results were obtained by using a single model for all operating conditions. If a delay in detection is tolerable the amplitude of the minimal detectable fault is lower.

It can be noted how faults modeled by ramp functions may not be immediately detected, since the delay in the corresponding alarm normally depends on fault mode.

An improvement of the FDI performance has been obtained by using the fuzzy multiple

model. Model parameters were identified under the assumptions of the dynamic Frisch scheme.

Table (5.21) summarize the performance of the enhanced FDI technique and collect the minimal detectable fault on the various output signals. The fault sizes are expressed as per cent of the signal mean values.

Sensor	P_v	T_s	T_{rs}
Step	3%	1%	2%
Ramp	10%	8%	6%

Table 5.21: Minimal detectable step and ramp faults with multiple model.

The values shown in Table (5.21) are relative to the case in which the occurrence of a fault must be detected as soon as possible.

The residuals obtained by using multiple model approach are more sensitive to a fault occurring on the system outputs, since the corresponding output estimation errors are smaller. Noise rejection is, in fact, achieved by means of the dynamic Frisch Scheme identification method. Moreover, smaller thresholds can be placed on the residual signals to declare the occurrence of faults.

It results that the values of the faults obtained by using fuzzy multiple model approach, collected in Table (5.21), are lower than the ones reported in Table (5.14).

Moreover, the minimal detectable faults on the various sensors seem to be adequate to the industrial diagnostic applications, by considering also that the minimal detectable faults can be reduced if a delay in detection promptness is tolerable. However, these improvements are not free of charge: they have been obtained with a procedure of greater complexity and, consequently, with a growing computational cost.

5.8 Actuator, Process and Sensor FDD of a Turbine Prototype

In this section the application of output observers designed in both deterministic and stochastic environments for FDI of a prototype of a real single-shaft industrial gas turbine is presented [95].

The method uses classical output observers designed using ARX models in case of high signal to noise ratios, or KF obtained by means of EIV models. As shown in Chapter 3, the last situation the identification technique is based on the rules of the Frisch scheme, based on the traditional application to the analysis of economic systems. This approach gives a reliable model of the plant under investigation, as well as providing variances of the input-output noises.

The Simulink prototype, depicted in Figure (5.29), can be described by the closed-loop scheme in Figure (5.30), in which the faults $\mathbf{f}_u$, $\mathbf{f}_s$, $\mathbf{f}_c$ and $\mathbf{f}_y$ are likely to occur in the real plant. They represent actuator, system, controller component and output sensor multiplicative faults, respectively. In particular, they can be modeled as ramp functions.

The problem considered regards the detection and isolation of the faults on the basis of the knowledge of the measured $y_i(t)$ and estimated $\hat{y}_i(t)$ sequences concerning the i-th turbine output.

The structure of the fault detection device is depicted in Figure (5.31).

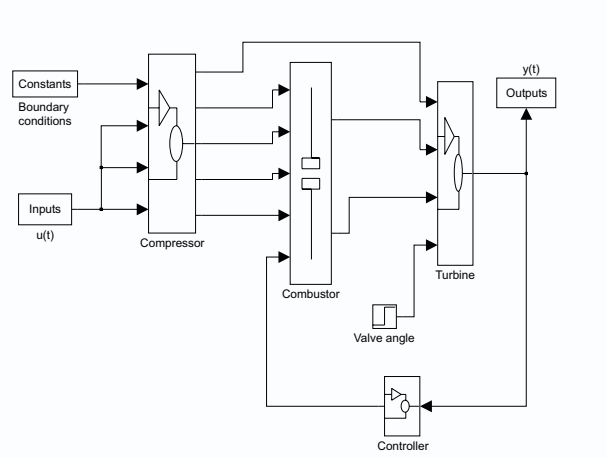

Figure 5.29: Turbine Simulink prototype.

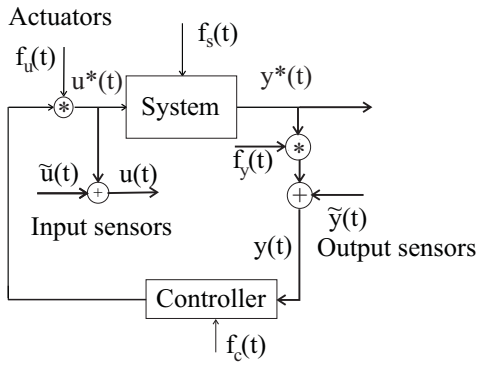

Figure 5.30: Turbine closed-loop scheme.

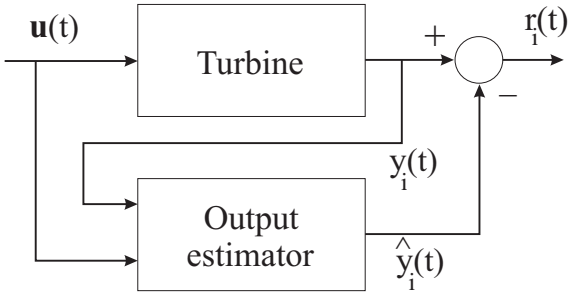

Figure 5.31: Logic diagram of the residual generator.

The residual generator is implemented by means of dynamic observers or KF, in order to produce a set of signals from which it will be possible to isolate faults associated to actuators, components and sensors.

The isolation is obtained by processing the most sensitive output measurement $y_i(t)$ to a particular fault. With this technique, it will be possible to univocally detect faults.

With reference to Figure (5.31) the residual signal $r_i(t)$ $(i = 1, \ldots, m)$ are differences between estimated signal $\hat{y}_i(t)$ (given by observer or KF) and the actual one $y_i(t)$ supplied by the i-th output sensor.

Moreover, it is assumed that only a single fault may occur in the actuators, components or output sensors of the plant.

The time series of data used to identify the models were generated with the nonlinear Simulink prototype and they simulate measurements taken on the machine with a sampling rate of 0.08s with noise due to measurement uncertainty of the real measurement systems.

The nonlinear Simulink model of the gas turbine was validated in steady state conditions against engine measurements where available, and against the prediction of a more rigorous steady state gas turbine model where measurements were not available. The Simulink model variables were found to be within 5% of the measured and rigorous modeled values. For the majority of variables the accuracy was within 1%.

In the dynamic case no model validation has been carried out as yet.

Input dynamics are shown in Figures (5.32) and (5.33). Input measurements present an accuracy of 5%.

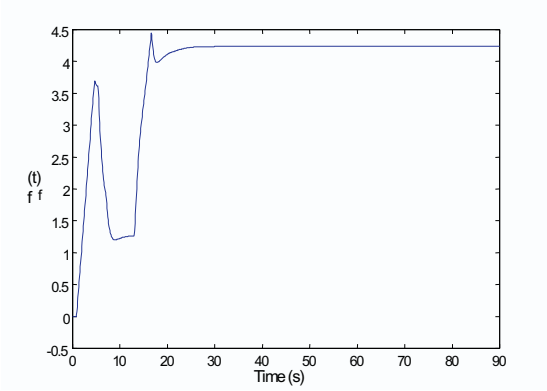

Figure 5.32: First input for the turbine.

Among all the output measurements available from the Simulink model ($m = 28$), only four output signals ($m = 4$) were chosen. They correspond to the output signals which are the most sensitive to an actuator, component or output sensor fault.

Four dynamic third order ($n = 3$) MISO models, each corresponding to the most sensitive output to a different fault, were identified. The i-th model (with $i = 1, \ldots, m$, $r = 2$ and $m = 4$) is driven by $u(t)$ and and gives the prediction of the i-th output $\hat{y}_i(t)$.

Each model was tested in different operating conditions and it has always provided an output reconstruction error lower than 1%.

Four gradually developing faults were considered as follows:

1. Compressor contamination, $f_s(t)$;

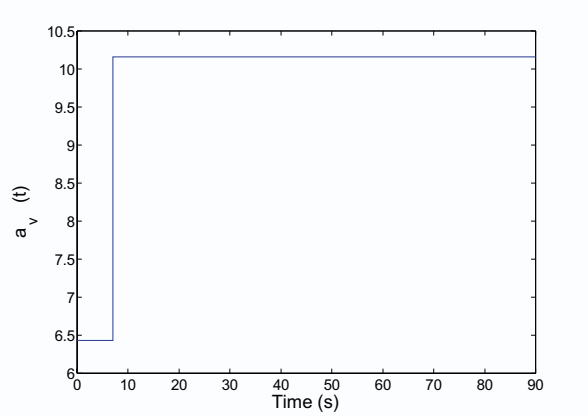

Figure 5.33: Second input for the turbine.

2. Thermocouple sensor fault, $f_y(t)$;
3. Turbine seal damage, $f_s(t)$;
4. Actuator damage, $f_u(t)$.

These slowly developing multiplicative faults were modeled by ramp functions.

Failure *case 1* represents fouling of the surfaces of the compressor blades, which reduces air flow modifying the blade aerodynamics and consequently changes the surface roughness.

The signal corresponding to compressor air flow is depicted in Figure (5.34), while the fault signal is shown in Figure (5.35).

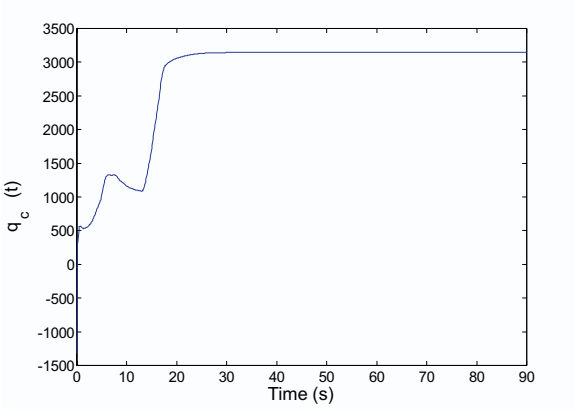

Figure 5.34: Compressor air flow rate.

The fault detection of a fault $f_s(t)$ regarding the compressor was performed by using the output observer configuration exploited for the FDI of output sensor faults. The inputs $\mathbf{u}(t)$ and the output $y_i(t)$ feed the observer to estimate the signal $\hat{y}_i(t)$ itself. The poles of the output observer for the signal were chosen near to 0.4.

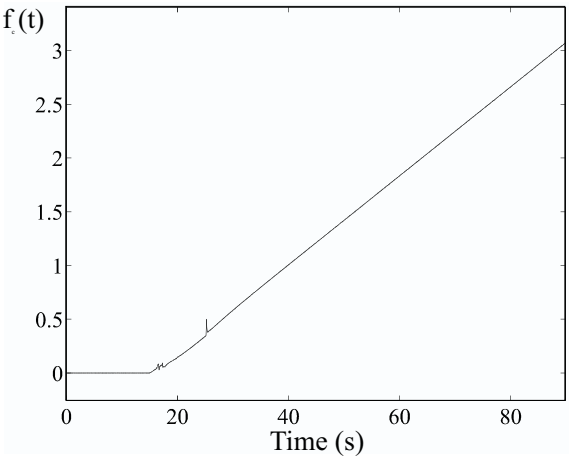

Figure 5.35: Dynamics of the compressor fault.

Figure (5.36) shows the fault-free (solid line) and the faulty residual (dotted line) generated by the first output observer.

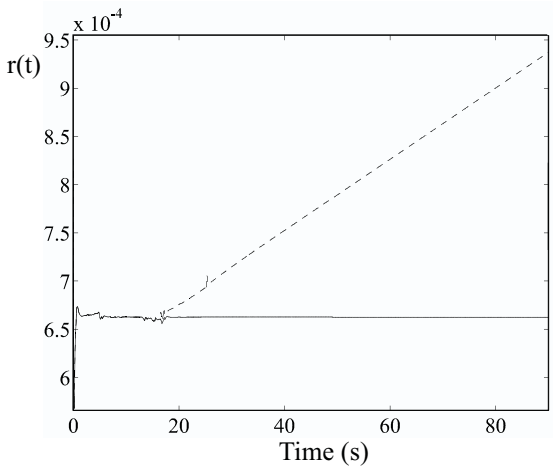

Figure 5.36: Fault-free and faulty residual.

Failure *case 2* represents the malfunctioning of a thermocouple in the gas path leading to a slowly increasing or decreasing reading over time (5.37).
In order to diagnose a single fault $f_y(t)$ on the i-th output temperature sensor, an output observer driven by $\mathbf{u}(t)$ and by the output temperature signal $y_i(t)$ is designed. The output signal is depicted in Figure (5.38).
Figure (5.39) shows the fault-free (continuous line) and faulty (dotted line) residual obtained from the difference between the values computed by the observer related to the output and the one given by the sensor. Obviously, the non zero value of the residual is due to the model approximation.

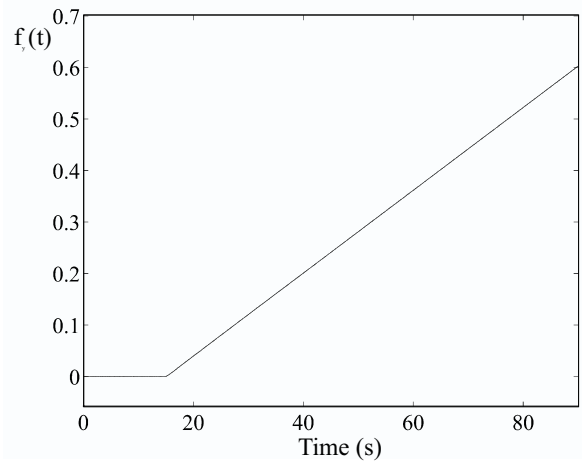

Figure 5.37: Fault on the temperature sensor.

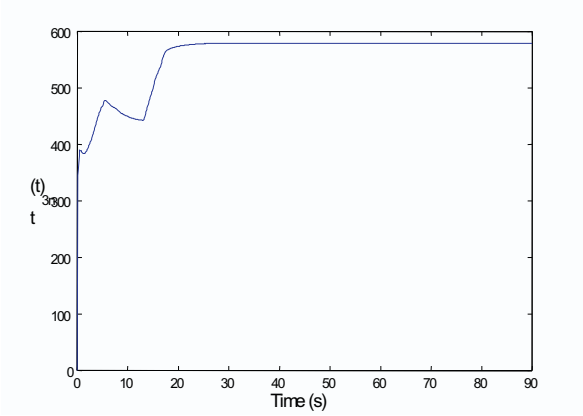

Figure 5.38: Output signal from the temperature sensor.

The step appearing in Figure (5.39), is generated by the instantaneous difference between measured and estimated output and at the instant related to the fault occurrence.
Failure *case 3* represents failure $f_s(t)$ of a component of the turbine. This results in a reduction in turbine efficiency. The fault is modeled as a gradual reduction in turbine efficiency over time.

In order to detect such a fault, an output observer fed by the inputs $\mathbf{u}(t)$ and the $y_i(t)$ output measurement concerning a pressure signal and sensitive to the fault, is designed. In Figure (5.40) the signal $f_s(t)$ representing the turbine component fault is depicted.
Figure (5.41) depicts the output signal $y_i(t)$ which drives the observer to estimate $\hat{y}_i(t)$. Its eigenvalues were chosen near 0.2.
The fault free and the faulty residual generated by the system depicted in Figure (5.31) are shown in the Figure (5.42).
Failure *case 4*, $f_u(t)$, depicted in Figure (5.43), represents a malfunction of the turbine actuator. For the diagnosis of the actuator, $f_u(t)$, the output measurement represented in Figure (5.44),

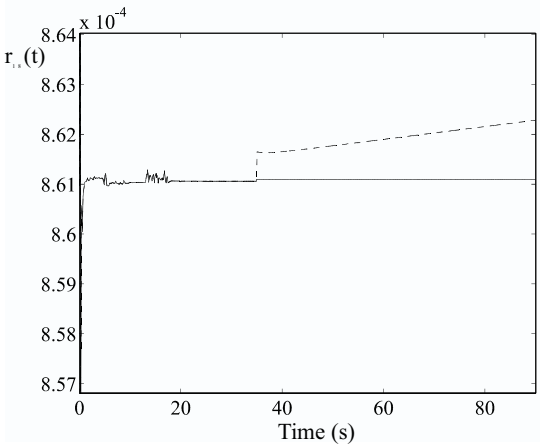

Figure 5.39: Residuals from the temperature sensor.

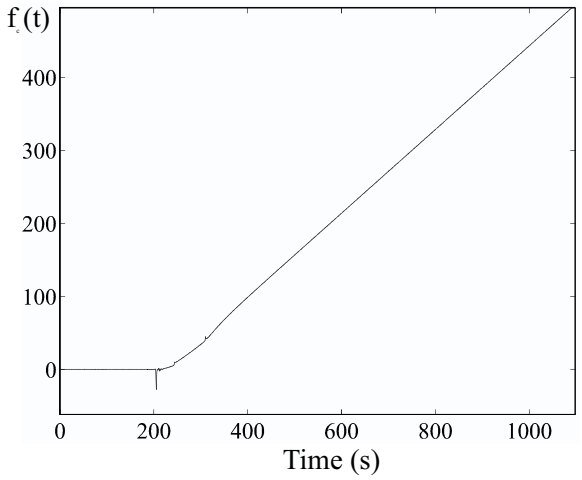

Figure 5.40: Turbine fault signal.

was considered. In particular, the inputs of the turbine, $\mathbf{u}(t)$ and the outputs $y_i(t)$, affected by $f_u(t)$, drive the output observer to estimate the signal $\hat{y}_i(t)$.
In such a case, because of the dynamics of the signal $f_u(t)$, the effects of the fault on the output measurement, as well as the fault shape, can not be described by using a ramp function.

Figure (5.45) shows how the fault occurring on the single sensor causes alteration of the residuals given by the output observer using the signal $\mathbf{u}(t)$ and $y_i(t)$ as inputs. These residuals indicate a fault occurrence when their values are lower or higher than the thresholds fixed in fault-free conditions.

Figure (5.45) the shows the fault-free (solid line) and faulty (dotted line) residual obtained from the difference between the value computed by the observer $\hat{y}_i(t)$ related to the output $y_i(t)$ and the one given by the sensor $y_i(t)$ itself.
In order to improve the fault detection capabilities of the proposed method regarding the *case*

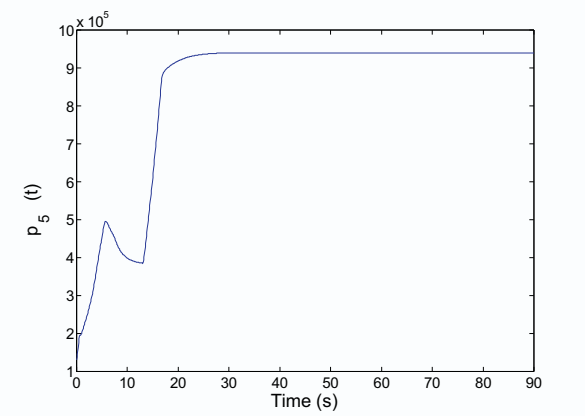

Figure 5.41: Turbine output signal.

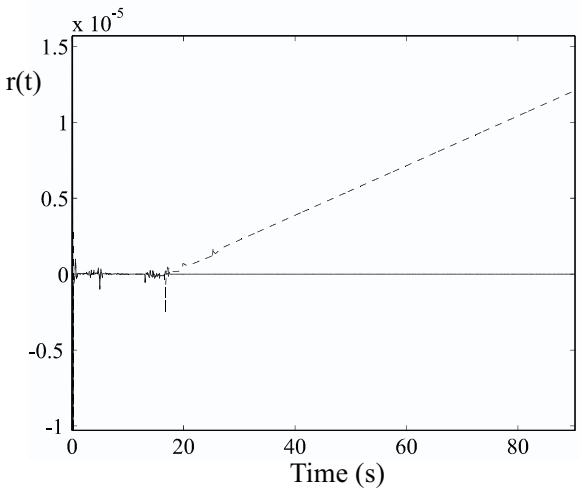

Figure 5.42: Turbine output signal.

4, the technique presented in Section 4.8 is exploited. It concerns the use of a KF as parameter estimator, in order to detect changes in parameters due to faults affecting input and output measurements.

With reference to system (4.32), Figure (5.46) depicts the recursive estimation of the most sensitive parameter in $\theta(t)$ to a fault concerning the input of the turbine. Solid line (KF) represents the estimate given by the KF, while, the dotted one (OLS) is the one computed by the OLS method. Note how the real process, with and as inputs $\mathbf{u}(t)$ and $y_i(t)$ as output, is non stationary and the estimates are different.

Figure (5.47) shows the change of the most sensitive parameter due a fault, by using the KF for a third order ARX model (4.31), with covariance matrices for the $\varepsilon(t)$ and $\omega(t)$ processes estimated from the OLS.

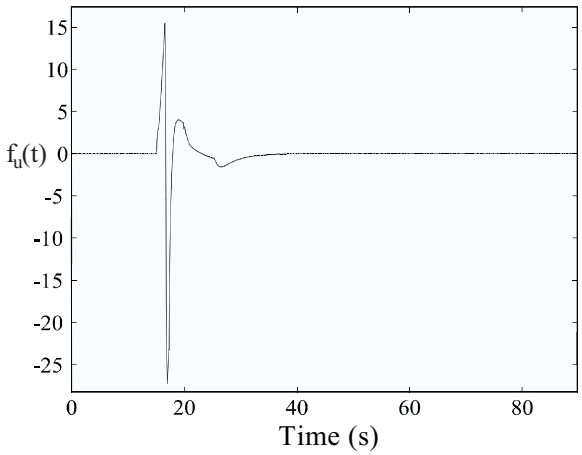

Figure 5.43: Turbine actuator fault.

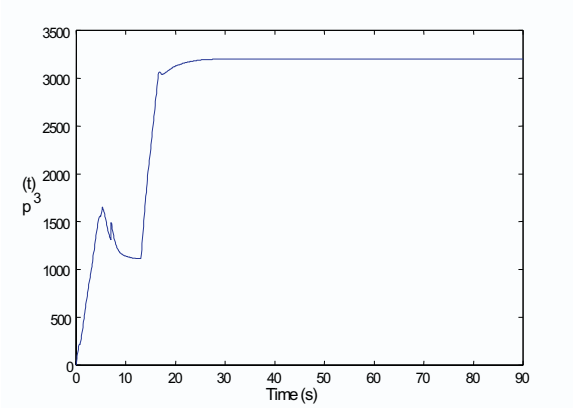

Figure 5.44: Turbine output measurement.

In the following, the FDI technique based on KF designed in case of noisy measurement is presented. Such a design is enhanced by processing the noisy data according to the identification method presented in Chapter 3.

In Figures (5.48), (5.49), (5.50) and (5.51) the examples of the turbine FDI performed by using the residual generated by the KF with two inputs $\mathbf{u}(t)$ and one output $y_i(t)$ are shown.

In particular, Figure (5.48) shows the fault-free and faulty residuals generated by the KF for the i-th output measurement when a fault $f_s(t)$ *case 1* occurs. The i-th filter is driven by the input sensor signals $\mathbf{u}(t)$ and the signal $y_i(t)$ itself. A fault of 5% on the value of the signal at the instant $t = 15$s causes a change in the value of the residual computed in fault-free condition.

It is important to note that, in order to achieve the maximal fault detection capability, the residual corresponding to the most sensitive filter to a failure on the measurement was selected. Figure (5.49) concerns the fault $f_y(t)$ affecting the temperature output sensor and occurring at the instant $t = 15$s *case 2*. Its amplitude is 5% of the output signal $y_i(t)$. It shows the fault free and faulty residuals regarding the signal obtained from the difference between the

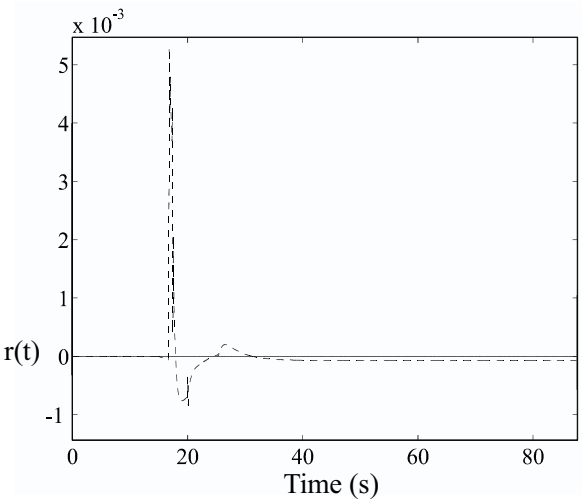

Figure 5.45: Fault free and faulty residuals concerning the turbine actuator.

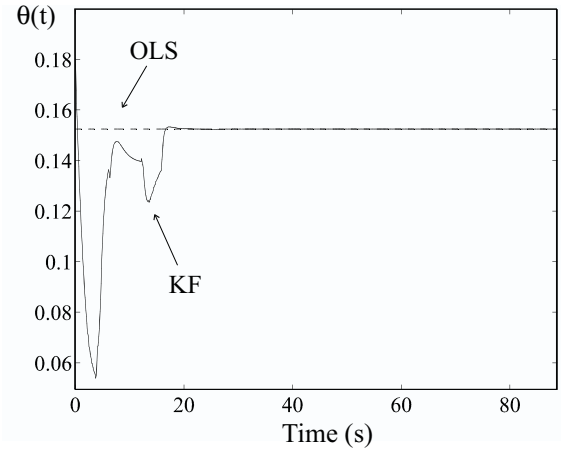

Figure 5.46: Parameter variations.

estimate of $\hat{y}_i(t)$ computed by the KF in Equations (4.19) and the ones measured by the sensor, $y_i(t)$. Obviously, the non-zero value of the residual in fault-free conditions is due to model approximation and to the actual measurement noise.

Figure (5.50) shows the behavior of the residuals when a fault $f_s(t)$ *case 3* occurs at the instant $t = 15$s. Fault amplitude is 5% of the monitored signal for the FDI of a component of the turbine. It depicts the fault-free residual and its change due to the fault occurrence, as the previous cases.

Finally, Figure (5.51) shows the change in the fault-free residual concerning the actuator fault $f_u(t)$ *case 4*. The fault is 5% of the monitored signal $y_i(t)$ and it occurs at the instant $t = 15$s. The faulty residuals is also shown.

Table (5.22) summarizes the performance of the FDI technique both in the deterministic and

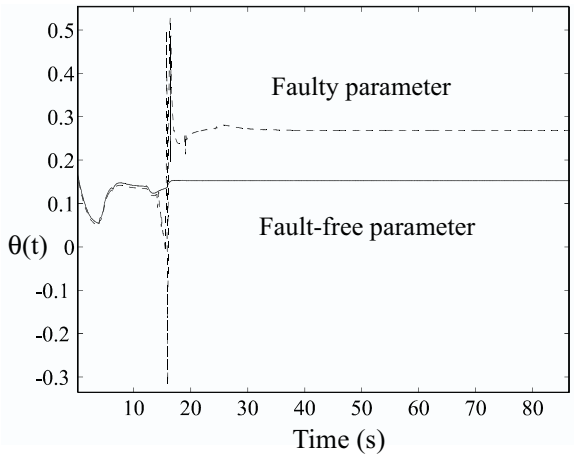

Figure 5.47: Parameter variations in case of actuator fault occurrence.

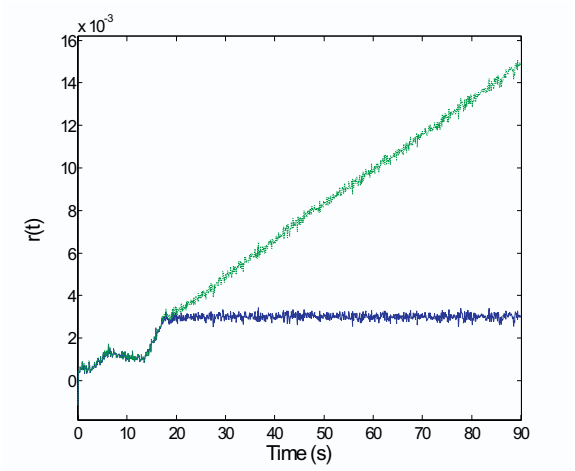

Figure 5.48: KF residuals when a fault $f_s(t)$ *case 1* occurs.

stochastic environment. The table collect the minimal detectable fault on the four output measurements, if residual or innovation values are monitored using a geometrical test and fixed thresholds.

The minimal detectable fault values in Table (5.22) are expressed as percentage of the signal values and are relative to the case in which the occurrence of a fault must be detected as soon as possible.

It is worthy to note how the values of the faults obtained by using geometrical analysis on KF innovations, collected in Table (5.22), are different than the ones reported in the same table and computed in the deterministic environment exploiting classical observers.

Table (5.22) shows also that faults modeled by ramp functions may not be immediately detected, since the delay in the corresponding alarm normally depends on fault mode.

The minimal detectable fault can be found by fixing a detection delay, defined in Fig-

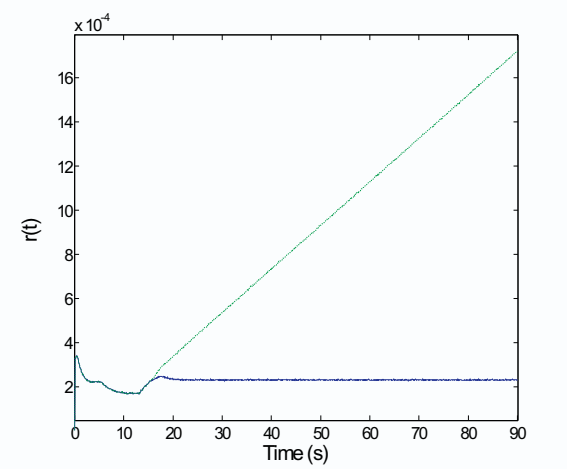

Figure 5.49: KF residuals in case of output *case 2* sensor fault $f_y(t)$ occurrence.

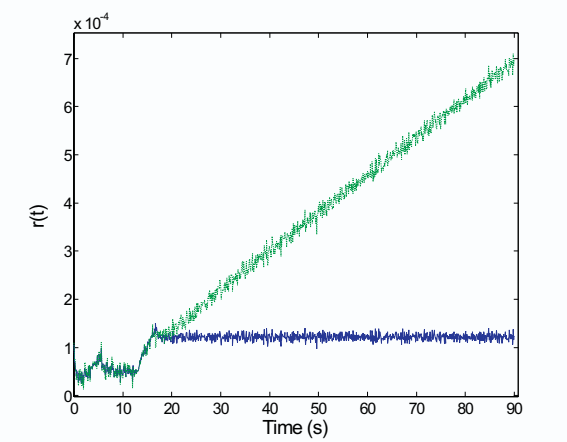

Figure 5.50: Component *case 3* fault $f_s(t)$ and KF residuals.

Fault Case	Noise-free measurements	Noisy measurements	Detection delay
Case 1	0.5%	1.0%	30s
Case 2	10.0%	12.0%	30s
Case 3	5.0%	7.0%	60s
Case 4	1.0%	3.0%	10s

Table 5.22: Minimum detectable faults by monitoring residual and innovation values.

ure (5.52). If a longer delay in detection is tolerable, the amplitude of the minimal detectable fault is lower.

The minimal detectable faults on the various sensors seem to be adequate to the industrial diagnostic applications, by considering also that the minimal detectable faults can be reduced

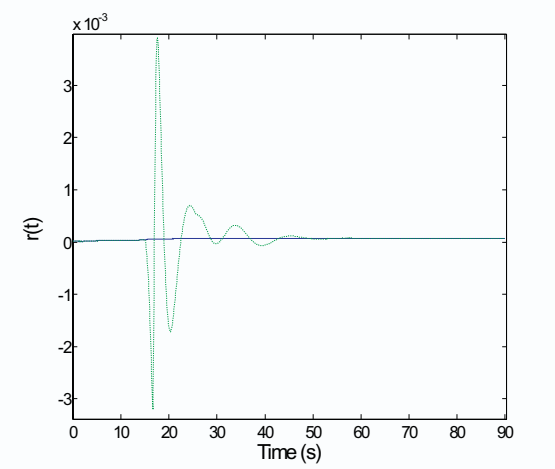

Figure 5.51: Actuator fault $f_u(t)$ and KF residuals *case 4*.

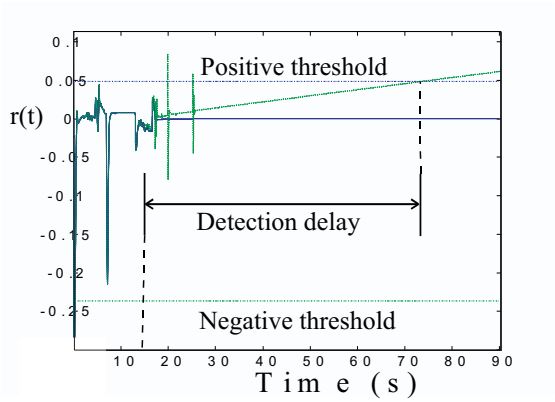

Figure 5.52: Detection delay definition.

if a delay in detection promptness is tolerable.

5.9 Conclusion

In this chapter, several simulated and real examples were presented in order to test the FDI techniques presented in Chapter 4.

Complete design procedures for the detection, isolation and identification of faults concerning actuators, components, input and output sensors of industrial processes were described.

The fault diagnosis was performed by using banks of dynamic observers and UIO or, when the measurement noises are not negligible, banks of KF and UIKF.

Single step and ramp faults on the actuators, components, input and output sensors and multiple faults on the output sensors were considered on the real and simulated processes.

The FDI methods exploited in the chapter do not require any physical knowledge of the processes under observation since the input–output links were obtained by means of identification methods.

Under this assumption, identification techniques recalled in Chapter 3 were applied in order to obtain suitable models of the processes under investigation.

The procedures were applied to different models of industrial gas turbines.

The results obtained by this approach indicate that the minimal detectable faults on the various sensors are of interest for the industrial diagnostic applications.

Chapter 6

Conclusions and Further Research

This thesis concludes by first summarizing the contributions concerning the development of a comprehensive methodology for model-based fault detection, isolation and identification. After the summary, topics for future researches, which come to light during this work are suggested.

6.1 Introduction

The main challenge in model-based FDI is to diagnose incipient and abrupt faults in complex dynamic systems under the assumption that input and output measurements are affected by noises.

The thesis has set the main objective to present and apply model-based diagnostic methodologies for complex and uncertain processes by identifying a reliable model of the system under investigation from noisy input-output time series of data. Moreover, these FDI techniques were demonstrated on real and simulated industrial plants.

This task was developed by means of a number of intermediate stages to be achieved:

1. To present a general framework for model-based FDI methods and give some basic definitions.
2. To show existing strategies for model-based residual generation, such as unknown input observers, dynamic observers and Kalman filters.
3. To develop theory and techniques for identifying a model of the monitored system from noisy input-output data.
4. To present a new method for generating robust residuals using decoupling techniques.
5. To overcome the problem of the difference between theoretical assumptions and practical reality.
6. To demonstrate and apply FDI techniques in real and simulated industrial processes.

The results presented in the previous chapters indicate that these goals have been met and that the overall objective of the thesis has been achieved.

Results arising from the presented researches have been and continue to be published in the open literature.

It is important to note that, the results obtained are of a general nature and are applicable not only to particular systems but to a wide class of linear and nonlinear dynamic systems.

In the following, the main topics and contributions are summarized chapter by chapter.

Chapter 1 presented an introduction to the fault diagnosis problem and outlined the structure of the thesis. Briefly, the international nomenclature concerning the FDI theory was recalled. Moreover, the chapter tried to comment on some developments in the field of fault detection and diagnosis based on papers selected during 1991-1998. Therefore, by going through the literature, the chapter recalled main FDI applications in order to understand the goals of the contributions and to compare the different approaches.

Chapter 2 presented the basic principles and general framework for model-based FDI. The residual generation was identified as the essence of this framework and some basic definition concerning residual properties were given. The distribution of all possible faults in systems was also studied. This chapter has provided comments upon some commonly used residual generation approaches. Examples of their applicability have been discussed and suggestions for the selection of methods have also been given. The problem of disturbances affecting residuals was briefly introduced. The chapter concluded with a discussion on integrating different diagnostic methods for FDI in complex dynamic systems using neural networks and fuzzy models. The contribution of this chapter was to give a general view of main FDI methods.

Chapter 3 investigated the problem of identifying an accurate model of the monitored system in order to apply model-based FDI techniques. In the chapter, different procedures were presented for the identification of both linear and nonlinear dynamic system from data affected by noise. Linear, piecewise affine and fuzzy models were also exploited. For the case of piecewise affine and fuzzy models, the multiple model approach consists in using several local affine submodels each describing a different operating condition of the process. The identification algorithms exploited to estimate parameters and orders of the local affine submodels are based on the well-established Frisch Scheme method for linear systems. For the nonlinear case, in order to obtain a continuous piecewise affine prototype describing the input-output behavior of the process, continuity constraints between local linear dynamic models have to be forced. The most important contribution of this chapter was the proposal of methods for nonlinear system identification by means of piecewise affine dynamic approximators.

Chapter 4 has given a development of unknown input observers for residual generation. This chapter presented the full-order unknown input observer structure, its existence conditions and design procedure. Using its structure, the residuals can be also made to have directional properties. The remaining design freedom can be exploited to satisfy disturbance decoupling conditions. Moreover, the design of classical dynamic observers in deterministic environment, Kalman filters and Kalman filters with unknown inputs, when measurements are affected by noises, was shown and applied for FDI goals. Actuator, component, input and output fault detection, isolation and identification schemes were finally given in this chapter. The main contribution of this chapter was to show how to develop model-based FDI techniques which uses mathematical description of the monitored system obtained by means of identification techniques.

Chapter 5 presented several simulated and real examples in order to test the FDI techniques developed in previous chapter. Complete design procedure for the detection, isolation and identification of faults concerning actuators, components, input and output sensors of industrial processes were described. The fault diagnosis was performed by using unknown input and dynamic observers or, when the measurement noises are not negligible, Kalman filters. Step and ramp faults on the actuators, components, input and output sensors and multiple faults on the output sensors were considered on the real and simulated processes. The FDI methods exploited in the chapter do not require any physical knowledge of the processes under observation since the input-output links are obtained by means of identification methods. The results obtained by this approach indicate that the minimal detectable faults on the processes are of interest for the industrial diagnostic applications.

Chapter 6 recalled how model-based FDI is a very rich research field and that there is a large scope for new contributions. The author has, through collaboration with colleagues, studied different problems in this field. Evidence of this can be clearly seen through the publications referenced at the end of the thesis. Some of the research were conducted by the author beyond the scope of this thesis. To conclude the thesis, some directions for future studies are suggested in the following sections, some of which are already topics being published by the Automatic Control Group of the Department of Engineering at the University of Ferrara.

6.2 Suggestion for Future Research

Model-based FDI has been studied for over 20 years, however is still an open research domain and many problems are awaiting to be solved. The research developed in this thesis has inevitably had to end before all the interesting topics for future FDI research could be explored. In the following, those directions which, in the author's opinion, are the most important topics for future research are therefore listed.

6.3 Frequency Domain Residual Generation

The design of a residual generator in the frequency domain was firstly based on the factorization of the transfer function matrix of the monitored system. The method was later extended and developed by Ding and Frank [20].

In its early development, such an FDI approach offered only an alternative interpretation of the residual generator, depicted in Figure (2.1), and hence it is equivalent to the time-domain design such as observers (see Chapter 4).

The frequency domain FDI design technique really demonstrated its power when was incorporated into the H^∞ optimization method.

As recalled in this thesis, there are many ways for eliminating or minimizing disturbance effects on residuals, such as the unknown input observer, eigenstructure assignment, optimal robust parity equations [24].

While these techniques are different, one feature is common among them, the original framework of these methods was developed for ideal systems or with special uncertainty structure. Furthermore, efforts have been made to include nonideal or more general uncertainties.

In contrast, H^∞ is a design method with the original motivation rooted in the consideration of various uncertainties. H^∞ optimization has been developed from the beginning with the understanding that no design goal of a system can be perfectly achieved without being compromised by an optimization in the presence of uncertainty. Hence, this technique is very suitable to tackle uncertainty issue. After several years of development, it is now playing a leading role in tackling the robustness problem in control systems.

The aim of this research is to maximize the following performance index [24]

$$J = sup_{Q(s)} \frac{\| Q(s)G_f(s) \|_\infty}{\| Q(s)G_d(s) \|_\infty} \tag{6.1}$$

over a frequency range. $Q(s)G_f(s)$ is the transfer matrix between the residual and fault, whilts $Q(s)G_d(s)$ the transfer matrix between the residual and disturbance.

Solutions for this optimization problem were given and revised, in order to obtain robust FDI technique. Unfortunately, it was shown that $\| Q(s)G_f(s) \|_\infty$ may be smaller than $\| Q(s)G_d(s) \|_\infty$ in certain frequency range even their ratio (6.1) has been maximized. This can cause difficulties in fault diagnosis. A new strategy which guarantees the lower bound of $\| Q(s)G_f(s) \|_\infty$ is above the upper bound of $\| Q(s)G_d(s) \|_\infty$ in the required frequency range was suggested to solve robust FDI design problem. This offer a better diagnostic performance in the presence of disturbance.

It should be pointed that the transfer function matrix $G_d(s)$ can only be defined for disturbance, hence the technique presented can only deal with robustness against disturbance. The robust problem with respect to modeling errors has still not been solved. The only solution suggested is to calculate the residual bound and set and adaptive threshold.

Few progresses were made solving the robust FDI problem against modeling errors when μ synthesis with H_∞ optimization is incorporated. Robust FDI design based on H_∞ optimization and μ synthesis is still in its early development, even if some research is still needed. This could be a direction for future research which has great potential.

In connection with frequency domain FDI techniques can exploit a different identification approach from the one presented in Chapter 3.

An identification method based on the frequencial approach for errors-in-variable models and its application to the dynamic Frisch scheme estimation technique in still in development [72, 74].

Such a procedure can provide an accurate estimation of the transfer matrices $Q(s)$, $G_f(s)$ and $G_d(s)$ from input-output measurements affected by white, mutually uncorrelated and correlated noises.

This general method, using the frequencial approach, allows to uniquely determine both the characteristics of the noise affecting the data ($G_d(s)$) as well as the transfer matrices ($Q(s)$ and $G_f(s)$) of the process under investigation. A comparison between time-domain and frequency-domain approach can be found in [73].

6.4 Adaptive Residual Generators

The system dynamics and parameters may vary or to be perturbated during the system operation. A fault diagnosis system designed for system model given at the nominal condition may not perform well when applied to the system with perturbated conditions.

To overcome this problem, instead of using complex nonlinear models, residual generator scheme using adaptive observers were proposed. The idea is to estimate and compensate system parameter variations. Figure (6.1) illustrates the basic principle of this approach. It can be applied to linear systems with parametric variations if stability and convergence conditions are satisfied.

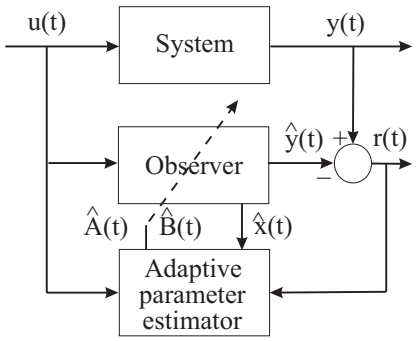

Figure 6.1: Residual generator with adaptive observer.

Adaptive residual generation schemes for both linear and nonlinear uncertain dynamic systems using adaptive observers were proposed in literature [23]. Unfortunately, the disadvantage of this approach is the complexity.

Chen and Patton [24] presented an alternative way to generate adaptive symptoms using a method to estimate the bias term in the residuals due to modeling errors, then compensate it adaptively. This technique decreases the effects of uncertainties on residuals. The approach to estimate such a bias term in residuals rather than computing modeling errors themselves avoids complicated estimation algorithms.

The state $\hat{x}(t)$, and parameters, $\hat{\mathrm{A}}(t)$, $\hat{\mathrm{B}}(t)$ simultaneous estimation algorithms presented in [33, 67] can be also used to generate adaptive residuals. With reference to Figure (6.1), observer parameters are linked by the relations

$$\begin{cases} \hat{\mathbf{x}}(t+1) &= \hat{\mathrm{A}}(t)\hat{\mathbf{x}}(t) + \hat{\mathrm{B}}(t)\mathbf{u}(t) \\ \hat{\mathbf{y}}(t) &= C\hat{\mathbf{x}}(t). \end{cases} \tag{6.2}$$

An adaptive residual generation algorithm normally involves both state and $\hat{x}(t)$ and parameter $\hat{\mathrm{A}}(t), \hat{\mathrm{B}}(t)$ estimation can be considered as a combination observer and identification based FDI approaches. Hence, complementary advantages in both approaches can be gained.

For all adaptive methods, the main problem to be tackled is that fault effects may be compensated as well as the compensation of modeling errors and parameter variations. This makes the detection for incipient faults almost impossible while for abrupt ones can be acceptable. To overcome this problem, the effect of faults can be considered as a slow varying parameter which can be estimated along with parameters. Under the assumption that parameters and faults varying in different speed, two filters with different gains can be used. However, much research effort is still needed in the theory and application of adaptive residual generation methods.

6.5 Integration of Identification, FDD and Control

A conventional feedback control design for complex systems may result in unsatisfactory performance in the event of malfunction in input-output sensors, actuators and system components. A fault tolerant closed-loop control system is very attractive because can tolerate failures maintaining desiderable performances.

The conventional approach to the design of a fault-tolerant control includes different steps and separate modules: modeling or identification of the controlled system, design of controller and FDI scheme, reconfiguration technique. Identification and design of the controller can be performed separately or using combined methods. Hence, FDI and controller are linked through the reconfiguration module. The fundamental problem with such a system lies in the identification stage, in the independent design of the control and FDI modules. Significant interactions occurring among these modules can be neglected. There is therefore a need for a research study into the interactions among system identification, control design, FDI stage and fault tolerant strategy.

6.6 Fault Identification

Fault identification is very important among all fault diagnosis tasks. When a fault is estimated, detection and isolation can be easily achieved since the fault nature can improve the diagnosis process. However, the fault identification problem has not gained enough research attention.

Most fault diagnosis techniques, such as parameter identification, parity space and observer-based methods cannot directly be used to identify faults in sensors and actuators.

Very little research has been done to overcome the fault identification problem. Kalman filter used in connection with statistic tests and fault estimation filters were proposed [23] but they presented very high computation demand.

Recently, fault identification scheme solving a system inversion problem was recently proposed [90, 24, 91]. In the scheme depicted in Figure (6.2) fault identification is performed by estimating the nonlinear relationship between residuals and fault sizes. This is possible because robust residuals should only contain fault information.

Such a nonlinear function approximation and estimation can be performed by using neural networks or an inversion of the transfer matrix between residuals and faults.

6.7 Fault Diagnosis of Nonlinear Dynamic Systems

The central task in model-based fault detection is the residual generation. Most residual generation technique are based on linear system models. For nonlinear systems, the traditional approach is to linearize the model around the system operating point. However, for systems with high nonlinearity and a wide dynamic operating range, the linearized approach fails to give satisfactory results.

One solution is to use a large number of linearized models corresponding to a range of operating points. This means that a large number of FDI schemes corresponding to each operating points is needed.

Hence, it is important to study residual generation techniques which tackle nonlinear dynamic systems directly. There are some research studies on the residual generation of nonlinear dynamic

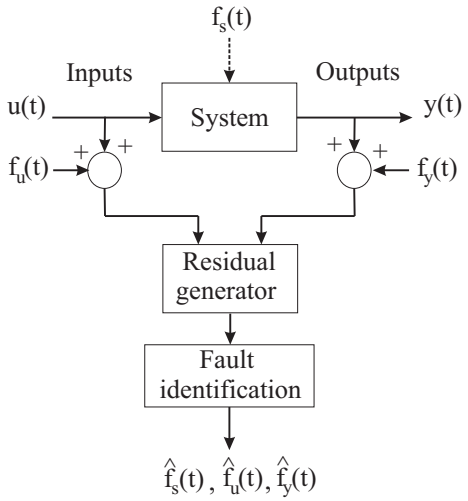

Figure 6.2: Fault estimation scheme.

systems. There have been some attempts to use nonlinear observers to solve nonlinear system FDI problem [24], e.g. nonlinear unknown input observers including, adaptive observers and sliding mode observers. If the class of nonlinearities can be restricted, observers for bilinear systems were also proposed [24].

On the other hand, the analytical models, which the nonlinear observer approaches are based on, are not easy to obtain in practice. Sometimes, it is impossible to model the system using an explicit mathematical models. To overcome this problem, it is desiderable to find a universal approximate model which can be used to represent the real system with an arbitrary degree of accuracy. Different approaches were proposed and they are currently under investigation: neural networks [24, 90, 91], fuzzy models [24, 96, 97, 98, 94] and hybrid models [99, 100, 101].

Neural networks are a powerful tool of handling nonlinear problems. One of the most important advantages of neural networks is their ability to implement nonlinear transformations for functional approximation problems. Therefore, neural networks can be used in a number of ways to tackle fault diagnosis problems for nonlinear dynamic systems. In early publications, they were mainly exploited as fault classifier with steady state processes. Other potential of neural networks have not been fully used. Recently, neural networks have been used as residual generators, as models of nonlinear dynamic systems [24] and as nonlinear function approximators [90, 91, 102].

Fuzzy models can be used to design a novel FDI scheme based on model-based methods. The main idea is to exploit TS models, presented in Section 3.9, to build an FDI scheme based on fuzzy observers. Estimated outputs and residuals are computed as fuzzy fusion of local observer output and residuals. The main problem concerns the stability of the global observer. A linear matrix inequality method was proposed by Patton [24] using Lyapunov theorem. The main problem of such a method regards existence condition fulfillment. Less conservative and more general stability conditions have been currently investigated by the Automatic Control Group of the Department of Engineering at the University of Ferrara and new results are to be published [103].

Hybrid models can describe the behavior of any nonlinear dynamic process if they are described as a composition of several local affine models selected according to the process operating conditions. Instead of exploiting complicated nonlinear models obtained by modeling techniques, it is possible to describe the plant by a collection of affine models. Such a compound system requires the identification of the local models from data. Several works proposed by the author [99, 100, 101] addressed a method for the identification and the optimal selection of the local affine models from a sequence of noisy measurements acquired from the process. The developed techniques were also applied to simulated models. A novel research field applying these models in FDI of nonlinear systems is also under development by the Automatic Control Group [104, 105, 106], but many studies are still to be done.

6.8 Conclusion

This chapter concludes the thesis by first summarizing the contributions concerning the design of tools for model-based detection, isolation and identification of faults on actuators, components and input-output sensors of the system under investigation.

After the summary, topics for future researches, which came to light during this work are suggested.

In particular, the chapter briefly discussed the extension of observer-based approaches for linear systems to nonlinear ones. To tackle with nonlinear systems, techniques which do not critically depend on analytical models are needed. Neural networks, fuzzy and hybrid models were discussed.

Finally, this thesis concerned mainly the development of a comprehensive methodology for FDI of dynamic systems by using a state estimation approach, in conjunction with residual processing schemes The final result consists in a fault FDI strategy based on fault diagnosis schemes to generate redundant residuals.

The suggested method does not require any physical knowledge of the process under observation since, instead of exploiting complicated nonlinear models obtained by modeling techniques, linear models obtained by means of identification schemes using EE and EIV models were exploited.

This thesis regarded mainly the application of the presented FDI techniques to real and simulated power plants, whose linear mathematical description is obtained by using identification procedures. It is very difficult, in fact, to find in literature practical applications of FDI for real nonlinear dynamic system.

Bibliography

[1] R. Isermann and P. Ballé, "Trends in the application of model-based fault detection and diagnosis of technical processes," *Control Engineering Practice*, vol. 5, no. 5, pp. 709–719, 1997.

[2] R. Isermann, "Supervision, fault detection and fault diagnosis methods: an introduction," *Control Engineering Practice*, vol. 5, no. 5, pp. 639–652, 1997.

[3] R. J. Patton, "Preface to the Papers from the 3rd IFAC Symposium SAFEPROCESS'97," *Control Engineering Practice*, vol. 7, no. 1, pp. 201–202, 1999.

[4] R. V. Beard, "Failure accomodation in linear systems through self-reorganisation," Tech. Rep. MVT-71-1, Man Vehicle Lab., Cambridge, Mass, 1971.

[5] H. L. Jones, *Failure detection in linear systems.* PhD thesis, Dept. of Aeronautics, M.I.T., Cambridge, Mass, 1973.

[6] A. S. Willsky, "A survey of desogn methods for failure detection systems," *Automatica*, vol. 12, 1976.

[7] A. Rault, A. Richalet, A. Barbot, and J. P. Sergenton, "Identification and modelling of a jet engine," in *IFAC Symposium od Digital Simulation of Continuous Processes*, (Gejör).

[8] H. Siebert and R. Isermann, "Fault diagnosis via on-line correlation analysis," tech. rep., VDI/VDE Darmstadt, 1976. In German.

[9] D. M. Himmelblau, "Fault detection and diagnosis in chemical and petrochemical processes." Elsevier, 1978. Amsterdam.

[10] R. N. Clark, "Instrument fault detection," *IEEE Trans. on Aerospace and Electronic Systems*, vol. 14, 1978.

[11] H. Hohmann, *Automatic monitoring and failure diagnosis for machine tools.* Dissertation, T. H. Darmstadt, Germany, 1977. in German.

[12] C. Bakiotis, J. Raymond, and A. Rault, "Parameter identification and discriminant analysis for jet engine mechanical state diagnosis," in *IEEE Conference on Decision and Control*, (Fort Lauderdale), 1979.

[13] G. Geiger, "Monitoring of an elecrical driven pump using continuous-time parameter estimation models," in *6th IFAC Symposium on Identification and Parameter Estimation* (O. Pergamon Press, ed.), (Washington), 1982.

[14] D. Filbert and K. Metzger, "Quality test of systems by parameter estimation," in *9th IMEKO Congress*, (Berlin), 1982.

[15] R. Isermann, "Process fault detection based on modelling and estimation methods: A survey," *Automatica*, vol. 20, 1984.

[16] E. Y. Chow and A. S. Willsky, "Analytical redundancy and the design of robust dtection systems," *IEEE Trans. Automatic Control*, vol. 29, no. 7, 1984.

[17] R. J. Patton and J. Chen, "A review of parity space approaches to fault diagnosis," in *Proc. IFAC SAFEPROCESS Symposium '91*, (Baden-Baden), 1991.

[18] J. Gertler, "Analytical redundancy methods in fault detection and isolation," in *Proc. IFAC SAFEPROCESS Symposium '91*, (Baden-Baden), 1991.

[19] T. Höfling and T. Pfeufer, "Detection of additive and multiplicative faults - Parity space vs. parameter estimation," in *Proc. IFAC SAFEPROCESS Symposium '94*, (Espoo, Finland), 1994.

[20] X. Ding and P. M. Frank, "Fault detection via factorization approach," *Syst. Contr. Lett.*, vol. 14, pp. 433–436, 1990.

[21] M. Massoumnia, G. C. Verghese, and A. S. Willsky, "Failure detection and identification," *IEEE Trans. Automat. Contr.*, vol. 34, pp. 316–321, 1989.

[22] L. F. Pau, *Failure diagnosis and Performance monitoring.* New York: Marcel Dekker, 1981.

[23] R. J. Patton, P. M. Frank, and R. N. Clark, *Fault Diagnosis in Dynamic Systems, Theory and Application.* Control Engineering Series, Hertfordshire: New York: Prentice Hall, 1989.

[24] J. Chen and R. J. Patton, *Robust Model-Based Fault Diagnosis for Dynamic Systems.* Kluwer Academic Publisher, 1999.

[25] J. Gertler, *Fault Detection and Diagnosis in Engineering Systems.* New York: Marcel Dekker, 1998.

[26] R. Isermann, *Supervision and fault diagnosis.* Düsseldorf: VDI-Verlag, 1994. In German.

[27] J. Gertler, "Survey of model-based failure detection and isolation in complex plants," *IEEE Control Systems Magazine*, 1988.

[28] P. M. Frank, "Fault diagnosis in dynamic systems using analytical and knowledge-based redundancy: A survey and some new results," *Automatica*, vol. 26, 1990.

[29] R. Isermann, "Integration of fault detection and diagnosis methods," in *Proc. IFAC SAFEPROCESS Symposium '94*, (Espoo, Finland), 1994.

[30] "Reliability, Availability and maintainability Dictionary." ASQC Quality press, 1988. Milwaukee.

[31] IFIP working group 10.4, *Reliable computing and fault tolerance*, (meeting in Como, Italy), 1983.

[32] J. Norton, *An Introduction to Identification*. London: Academic Press, 1986.

[33] T. Söderström and P. Stoica, *System Identification*. Englewood Cliffs, N.J.: Prentice Hall, 1987.

[34] L. Ljung, *System Identification: Theory for the User*. Englewood Cliffs, N.J.: Prentice Hall, second ed., 1999.

[35] G. P. Liu and R. J. Patton, *Eigenstructure Assignment for Control System Design*. England: John Wiley & Sons, 1998.

[36] D. G. Luenberger, *Introduction to Dynamic System: Theory, Models and Application*. New York: John Wiley and Son, 1979.

[37] K. Watanabe and D. M. Himmelblau, "Instrument fault detection in systems with uncertainties," *Int. J. System Sci.*, vol. 13, no. 2, pp. 137–158, 1982.

[38] A. H. Jazwinski, *Stochastic processes and filtering theory*. New York: Academic Press, 1970.

[39] L. Xie, Y. C. Soh, and C. E. de Souza, "Robust Kalman filtering for uncertain discrete-time systems," *IEEE Transaction on Automatic Control*, vol. 39, pp. 1310–1314, 1994.

[40] L. Xie and Y. C. Soh, "Robust Kalman filtering for uncertain systems," *Systems and Control Letters*, vol. 22, pp. 123–129, 1994.

[41] R. Frisch, *Statistical Confluenece Analysis by Means of Complete Regression Systems*. University of Oslo, Economic Institute, publication n. 5 ed., 1934.

[42] R. E. Kalman, "System identification from noisy data," in *Dynamical System II* (A. Bednarek and L. Cesari, eds.), pp. 135–164, New York: Academic Press, 1982.

[43] R. E. Kalman, "Nine lectures on identification," *Lecture Notes on Economics and Mathematical System*, (Springer-Verlag, Berlin, 1990).

[44] S. Beghelli, R. P. Guidorzi, and U. Soverini, "The Frisch scheme in dynamic system identification," *Automatica*, vol. 26, no. 1, pp. 171–176, 1990.

[45] E. Y. Chow and A. S. Willsky, "Issue in the development of a general algorithm for reliable failure detection," in *Proc. of the 19th Conf. on Decision & Control*, (Albuquerque, NM), 1980.

[46] M. Basseville, "Detecting changes in signals and systems: a survey," *Automatica*, vol. 24, no. 3, pp. 309–326, 1988.

[47] R. Isermann and D. Fussel, "Knowledge-based fault detection and diagnosis systems." Tutorial Workshop, Karlsruhe,Germany, September 1999.

[48] R. P. Guidorzi, "Canonical Structures in the Identification," *Automatica*, vol. 11, pp. 361–374, 1975.

[49] J. Gertler, "Diagnosing Parametric Faults: from Parameter Estimation to Parity Relations," in *ACC'95*, (Seatle, Washingtown), pp. 1615–1620, 1995.

[50] G. Delmaire, P. Cassar, M. Staroswiecki, and C. Christophe, "Comparison of multivariable identification and parity space techniques for FDI purpose in M.I.M.O. systems," in *ECC'99*, (Karlsruhe, Germany), 1999.

[51] R. Isermann, "Estimation of physical parameters for dynamic processes with application to an industrial robot," *Int. J. Control*, vol. 55, pp. 1287–1298, 1992.

[52] R. Isermann, "Fault diagnosis of machines via parameter estimation and knowledge processing," *Automatica*, vol. 29, no. 4, pp. 815–835, 1993.

[53] W. H. Chung and J. L. Speyer, "A game theoretic fault detection filter," *IEEE Transaction on Automatic Control*, vol. 43, pp. 143–161, February 1998.

[54] J. L. Speyer, "Residual sensitive fault detection filters," in *MED'99*, June 1999.

[55] X. Lou, A. S. Willsky, and G. C. Verghese, "Optimally robust redundancy relations for failure detection in uncertainty systems," *Automatica*, vol. 22, no. 3, pp. 333–344, 1986.

[56] A. E. Emami-Naeini, M. M. Akhter, and S. M. Rock, "Effect of model uncertainty on failure detection: the threshold selector," *IEEE Trans. Aut. Contrl*, vol. AC-33, no. 2, p. 1988, 1988.

[57] S. H. Rich and V. Venkatasubramanian, "Model-based reasoning in diagnostic expert system for chemical process plant," *Comp. chem. Engng*, vol. 11, pp. 111–122, 1987.

[58] M. A. Kramer, "Malfunction diagnosis using quantitative models with non-boolean reasoning in expert systems," *AIChE*, no. 33, pp. 130–140, 1987.

[59] R. J. Patton and J. Chen, "Observer-based fault detection and isolation: Robustness and applications," *Control Eng. Practice*, vol. 5, no. 5, pp. 671–682, 1997.

[60] I. J. Leonaritis and S. A. Billings, "Input-output parametric models for non-linear systems," *International Journal of Control*, vol. 41, pp. 303–344, 1985.

[61] T. Takagi and M. Sugeno, "Fuzzy identification of systems and its application to modelling and control," in *IEEE Trans. Sys. Man. & Cyber.*, vol. 15, pp. 116–132, 1985.

[62] J. C. Hoskins and D. M. Himmelblau, "Artificial neural network models of knowledge representation in chemical engineering," *Comp. chem. Engng*, vol. 12, pp. 881–890, 1988.

[63] W. E. Dietz, E. L. Kiech, and M. Ali, "Jet and rocket engine fault diagnosis in real time," *J. of Neural Network Computing*, vol. 1, pp. 5–18, 1989.

[64] V. Venkatasubramanian and K. Chan, "A neural network methodology for process fault diagnosis," *AIChE J.*, no. 35, pp. 1993–2002, 1989.

[65] R. J. McDuff and P. K. Simpson, "An adaptive reasonance diagnostic system," *J. of Neural Network Computing*, no. 2, pp. 19–29, 1990.

[66] S. Chen, A. S. Billings, C. F. N. Cowan, and P. M. Grant, "Practical identification of NARMAX models using radial basis function," *Int. J. Control*, vol. 52, pp. 1327–1350, 1990.

[67] L. Ljung, *System Identification: Theory for the User*. Englewood Cliffs, N.J.: Prentice Hall, 1987.

[68] J. Hadamard, *La theorie des equations aus derivees partielles*. Pekin: Editions Scientifiques, 1964.

[69] A. Tikhonov and V. Arsenin, *Solution of Ill-posed Problems*. Washington: Winston and Wiley, 1977.

[70] V. Morozov, *Methods for Solving Incorrectly Posed Problems*. Berlin: Springer, 1984.

[71] S. Beghelli and U. Soverini, "Identification of linear relations from noisy data: Geometrical aspects," *System and Control Letters*, vol. 18, no. 5, pp. 339–346, 1992.

[72] S. Beghelli, P. Castaldi, R. P. Guidorzi, and U. Soverini, "The Frisch identification scheme: properties of the solution in the dynamic case," in *SYSID'94*, vol. 2, (Copenhagen, Denmark), pp. 605–609, 1994.

[73] S. Beghelli, P. Castaldi, and U. Soverini, "Dynamic Frisch scheme identification: time and frequency domain approaches," in *IFAC'94*, 10th IFAC Symposium on System Identification, 1994.

[74] S. Beghelli, P. Castaldi, and U. Soverini, "A frequential approach to the dynamic frisch scheme identification," in *ECC'97*, (Brussels), 4th European Control Conference, July 1997.

[75] S. Beghelli, P. Castaldi, R. P. Guidorzi, and U. Soverini, "A comparison between different model selection criteria in Frisch scheme identification," *Systems Science Journal*, vol. 20, pp. 77–84, Sept. 1994. Wroclaw, Polonia.

[76] R. P. Guidorzi, "Invariants and canonical forms for system structural and parametric identification," *Automatica*, no. 17, pp. 117–133, 1981.

[77] R. Babuska and H. B. Verbruggen, "Identification of composite linear models via fuzzy clustering," in *Proc. 3rd ECC'95*, pp. 1207–1212, 1995.

[78] R. Babuska, J. Keizer, and M. Verhaegen, "Identification of nonlinear dynamic systems as a composition of local linear parametric or state space models," in *Proc. of SYSID'97*, (Fukuoka, Japan), 1997.

[79] R. Babuska, *Fuzzy Modeling for Control*. Kluwer Academic Publishers, 1998.

[80] D. E. Gustafson and W. C. Kessel, "Fuzzy Clustering with a Fuzzy Covariance Matrix," in *Proc. IEEE CDC*, (San Diego, CA, USA), pp. 161–166, 1979.

[81] S. H. Wang, E. J. Davison, and P. Dorato, "Observing the state of of systems with unmeasurable disturbance," *IEEE Trans. Automat. Contr.*, vol. 20, pp. 716–717, 1975.

[82] MathWorks, *MATLAB User's Guide*. MathWorks Inc., 1990. South Natick, MA, U.S.A.

[83] S. K. Chang and P. L. Hsu, "A novel design for the unknown input fault detection observer," *Control Theory and Advanced Technology*, vol. 10, no. 4, 1995.

[84] R. Diversi and R. P. Guidorzi, "Filtering-oriented identification of multivariable errors-in-variables models," in *Proc. of the MNST'98 Symposium* (A. Beghi, L. Finesso, and G. Picci, eds.), (Padova, Italy), pp. 775–778, Il Poligrafo, July 1998.

[85] M. Baseville, "Detecting changes in signal and systems: A survey," *Automatica*, vol. 24, pp. 309–326, 1988.

[86] P. Castaldi and U. Soverini, "Identification of errors-in-variables models and optimal output reconstruction," in *Proc. of the MNST'98 Symposium* (A. Beghi, L. Finesso, and G. Picci, eds.), (Padova, Italy), pp. 727–730, Il Poligrafo, July 1998.

[87] S. Simani, C. Fantuzzi, and S. Beghelli, "Diagnosis techniques for sensor faults of indistrial processes," *IEEE Transactions on Control Systems Technology*, 1999. (Accepted).

[88] S. Simani, P. R. Spina, S. Beghelli, R. Bettocchi, and C. Fantuzzi, "Fault detection and isolation based on dynamic observers applied to gas turbine control sensors," in *ASME TURBO EXPO LAND, SEA & AIR '98*, (Stockholm, Sweden), The 43rd ASME Gas Turbine and Aeroengine Congress, Exposition and Users Symposium, STOCKHOLM INTERNATIONAL FAIR, June, Tuesday, 2 - Friday, 5 1998.

[89] S. Simani and P. R. Spina, "Kalman filtering to enhance the gas turbine control sensor fault detection," in *6th IEEE Med '98*, (Alghero, Sardinia, Italy), The 6th IEEE Mediterranean Conference on Control and Automation, June, 9-11 1998.

[90] S. Simani, C. Fantuzzi, and P. R. Spina, "Application of a neural network in gas turbine control sensor fault detection," in *CCA'98*, (Trieste, Italy), 1998 IEEE Conference on Control Applications, September, 1-4 1998.

[91] S. Simani, F. Marangon, and C. Fantuzzi, "Fault diagnosis in a power plant using artificial neural networks: analysis and comparison," in *ECC'99*, (Karlsruhe, Germany), European Control Conference 1999, 31. August - 3. September 1999.

[92] S. Simani, "Sensor fault diagnosis of a power plant: an approach based on state estimation techniques," in *IMACS-IEEE'99* (N. E. Mastorakis, ed.), vol. Recent Advances in Signal Processing and Communications, (Athens.), pp. 274–281, International Conference on Computer Engineering in System Applications, World Scientific Engineering Society, July 4-8 1999.

[93] S. Simani, C. Fantuzzi, and S. Beghelli, "Improved observer for sensor fault diagnosis of a power plant," in *MED99. The 7th IEEE Mediterranean Conference on Control & Automation*, (Haifa, Israel), pp. 826–834, 28-30, June 1999.

[94] S. Simani, "Fuzzy multiple inference identification and its application to fault diagnosis of industrial processes," in *ISAS'99/SCI'99*, vol. 7, (Orlando, FL, USA), pp. 185–191, The Fifth Conference of the ISAS (Information Systems Analysis and Synthesis)/ The Third Conference of the SCI (Systemics, Cybernetics and Informatics), 1999.

[95] S. Simani and R. J. Patton, "Identification and fault diagnosis of a simulated model of an industrial gas turbine," Tech. Rep. 1, Department of Electronic Engineering at the University of Hull, Hull, U.K., April 1999.

[96] S. Simani, C. Fantuzzi, R. Rovatti, and S. Beghelli, "Noise rejection in parameters identification for piecewise linear fuzzy models," in *WCCI'98, FUZZ-IEEE'98*, (Ancorage, Alaska), 1998 IEEE International Conference on Fuzzy Systems, May, 5-9 1998.

[97] C. Fantuzzi, R. Rovatti, S. Simani, and S. Beghelli, "Fuzzy modeling with noisy data," in *EUFIT'98*, (Aachen, Germany), The 6th European Congress on Intelligent Techniques and Soft Computing, September, 7-10 1998.

[98] R. Rovatti, C. Fantuzzi, S. Simani, and S. Beghelli, "A geometrical approach to noise-rejection in piecewise-linear fuzzy systems," *Signal Processing Journal*, July 1999. (Accepted).

[99] R. Rovatti, C. Fantuzzi, S. Simani, and S. Beghelli, "Parameter Identification for Piecewise Linear Model with Weakly Varying Noise," in *CDC'98*, (Tampa, Florida), 1998 IEEE Conference on Decision and Control, December, 16-18 1998.

[100] S. Simani, C. Fantuzzi, R. Rovatti, and S. Beghelli, "Parameter identification for piecewise linear fuzzy models in noisy environment," *International Journal of Approximate Reasoning*, July 1999. (Accepted).

[101] S. Simani, C. Fantuzzi, R. Rovatti, and S. Beghelli, "Nonlinear algebraic system identification via piecewise affine models in stochastic environment," in *CDC'99*, (Phoenix, AZ, U.S.A.), 1999 IEEE Conference on Decision and Control, December, 7-10 1999.

[102] S. Simani, "Fault Diagnosis of a Power Plant at Different Operating Points using Neural Networks," in *SAFEPROCESS2000*, (Budapest, Hungary), 4th Symposium on Fault Detection Supervision and Safety for Technical Processes, 14-16 June 2000. Invited session. (Submitted).

[103] S. Simani, "Multi Model Based Fault Diagnosis of a Sugar Cane Crushing Process," in *SAFEPROCESS2000*, (Budapest, Hungary), 4th Symposium on Fault Detection Supervision and Safety for Technical Processes, 14-16 June 2000. (Submitted).

[104] S. Simani and R. J. Patton, "Fault diagnosis of a simulated model of an industrial gas turbine prototype using identification techniques," in *SAFEPROCESS2000*, (Budapest, Hungary), 4th Symposium on Fault Detection Supervision and Safety for Technical Processes, 14-16 June 2000. (Submitted).

[105] S. Simani, C. Fantuzzi, R. Rovatti, and S. Beghelli, "Nonlinear dynamic system modelling in noisy environment using multiple model approach," in *ACC'00*, (Chicago, Illinois, USA), American Control Conference, June, 28-30 2000. (Submitted).

[106] S. Simani, C. Fantuzzi, S. Beghelli, and R. Rovatti, "Identification of hybrid model in noisy environment," *International Journal of Control*, 2000. (Submitted).